



# University of HUDDERSFIELD

## University of Huddersfield Repository

Alabied, Samir

Enhancement of Condition Monitoring Information from the Control Data of Electrical Motors Based on Machine Learning Techniques

### Original Citation

Alabied, Samir (2020) Enhancement of Condition Monitoring Information from the Control Data of Electrical Motors Based on Machine Learning Techniques. Doctoral thesis, University of Huddersfield.

This version is available at <http://eprints.hud.ac.uk/id/eprint/35263/>

The University Repository is a digital collection of the research output of the University, available on Open Access. Copyright and Moral Rights for the items on this site are retained by the individual author and/or other copyright owners. Users may access full items free of charge; copies of full text items generally can be reproduced, displayed or performed and given to third parties in any format or medium for personal research or study, educational or not-for-profit purposes without prior permission or charge, provided:

- The authors, title and full bibliographic details is credited in any copy;
- A hyperlink and/or URL is included for the original metadata page; and
- The content is not changed in any way.

For more information, including our policy and submission procedure, please contact the Repository Team at: [E.mailbox@hud.ac.uk](mailto:E.mailbox@hud.ac.uk).

<http://eprints.hud.ac.uk/>

# **ENHANCEMENT OF CONDITION MONITORING INFORMATION FROM THE CONTROL DATA OF ELECTRICAL MOTORS BASED ON MACHINE LEARNING TECHNIQUES**

**Samir Alabied**

This Thesis is submitted to the School of Computing and Engineering,  
University of Huddersfield, in partial fulfilment of the requirements for the  
degree of Doctor of Philosophy

September 2020

# COPYRIGHT

## Copyright statement

- i. The author of this thesis (including any appendices and/or schedules to this thesis) owns any copyright in it (the "Copyright") and s/he has given The University of Huddersfield the right to use such copyright for any administrative, promotional, educational and/or teaching purposes.
- ii. Copies of this thesis, either in full or in extracts, may be made only in accordance with the regulations of the University Library. Details of these regulations may be obtained from the Librarian. This page must form part of any such copies made.
- iii. The ownership of any patents, designs, trademarks and any and all other intellectual property rights except for the Copyright (the "Intellectual Property Rights") and any reproductions of copyright works, for example graphs and tables ("Reproductions"), which may be described in this thesis, may not be owned by the author and may be owned by third parties. Such Intellectual Property Rights and Reproductions cannot and must not be made available for use without the prior written permission of the owner(s) of the relevant Intellectual Property Rights and/or Reproductions.

## **Abstract**

Centrifugal pumps are widely used in many manufacturing processes, including power plants, petrochemical industries, and water supplies. Failures in centrifugal pumps not only cause significant production interruptions but can be responsible for a large proportion of the maintenance budget. Early detection of such problems would provide timely information to take appropriate preventive actions.

Currently, the motor current signature analysis (MCSA) is regarded to be a promising cost-effective condition monitoring technique for centrifugal pumps. However, conventional data analysis methods such as statistical and spectra parameters often fail to detect damage under different operating conditions, which can be attributed to the present, limited understandings of the fluctuations in current signals arising from the many different possible faults. These include the fluctuations due to changes in operating pressure and flow rate, electromagnetic interference, control accuracy and the measured signals themselves. These combine to make it difficult for conventional data analyses methods such as Fourier based analysis to accurately capture the necessary information to achieve high-performance diagnostics.

Therefore, this study focuses on the improvement of data analysis through machine learning (ML) paradigms for promoting the performance of centrifugal pump monitoring. Within the paradigms, data characterisation methods such as empirical mode decomposition (EMD) and the intrinsic time-scale decomposition (ITD) reveal features based purely on the data, rather than finding pre-specified similarities to basic functions. With this data-driven approach, subtle changes are more likely to be captured and provide more effective and accurate fault detection and diagnosis.

This study reports the application of two of the above data-driven approaches, using MCSA for a centrifugal pump operated under normal and abnormal conditions to detect faults seeded into the pump. The research study has shown that the use of the ITD and EMD signatures combined with envelope spectra of the current signals proved to be competent in detecting the presence of the centrifugal pump fault conditions under different flow rates. The successful analysis was able to produce a more accurate analysis

of these abnormal conditions compared to conventional analytical methods. The effectiveness of these approaches is mainly due to the inclusion of high-frequency information, which is largely ignored by conventional MCSA.

Finally, a comprehensive diagnostic approach is suggested based on the support vector machine (SVM) as a diagnosing method for three seeded centrifugal pump defects (two bearing defects and compound defect outer race fault with impeller blockage) under different flow rates. It is confirmed that this novel data-driven paradigm is effective for pump diagnostics. The proposed method based on a combined ITD and SVM technique for extracting meaningful features and distinguishing between seeded faults is significantly more effective and accurate for fault detection and diagnosis when compared with the results obtained from other means, such as envelope, EMD and discrete wavelet transform (DWT) based features.

## **Declaration**

This dissertation is submitted for the degree of Doctor of Philosophy at the University of Huddersfield. I hereby declare that the work in this dissertation was carried out in accordance with the Regulations of the University of Huddersfield.

This work is original except where acknowledgement and references are made to the previous work. Neither this nor any substantially similar dissertation has been or is being submitted for a degree, diploma or other qualification at any other university.

Samir Alabied

## **Acknowledgements**

First and foremost. I would like to thank God Almighty for giving me the power, Knowledge and ability to undertake this research study. Without his blessings, this achievement would not have been done. I would like to express my special appreciation and thanks to my supervisors Prof. Fengshou Gu and Prof. Andrew Ball. For the guidance, encouragement and motivation throughout my study. Without their guidance and constant feedback, this thesis would not have been achievable. I am extremely grateful for their assistance, advice and comments have been invaluable.

I would like to thank all colleagues and friends at the Centre for Efficiency and Performance Engineering (CEPE) research group for their support and advice. I would like to thank the technical team who have given their support and assistance. Also, I would like to thank my friend Usama Haba for valuable assistance and continuous encouraging me throughout my research study. A special thanks and deepest appreciation to my family. Words cannot express how grateful I am to my mother and father for all of the sacrifices that you have made on my behalf. My wife, for her invaluable support and encouragement me during my study. My brothers and sisters for supporting me throughout my study.

Finally, I would like to thank my government (the government of Libya) for their financial support.

## List of Publications

1. **S. Alabied**, O. Hamomd, A. Daraz, F. Gu and A. D. Ball. (2017). Fault diagnosis of centrifugal pumps based on the intrinsic time-scale decomposition of motor current signals. 2017 23rd International Conference on Automation and Computing (ICAC), IEEE.

The author suggested main storylines, conducted the test, data analysis and composed the first draft. The main contribution of this paper was the successful implementation of a data-driven technique (ITD) to analyse the motor current signals for condition monitoring of the centrifugal pump.

2. O, Hamomd, **S. Alabied**, Y. Xu, A. Daraz, F. Gu and A. D. Ball. (2017). Vibration-based centrifugal pump fault diagnosis based on modulation signal bispectrum analysis. 2017 23rd International Conference on Automation and Computing (ICAC), IEEE.

In this paper, the author was responsible for obtaining the vibration data and then participated in analysing the data using the proposed method.

3. Daraz, **S. Alabied**, A. Smith, F. Gu and A. D. Ball. (2018). Detection and diagnosis of centrifugal pump bearing faults based on the envelope analysis of airborne sound signals. 2018 24th International Conference on Automation and Computing (ICAC), IEEE.

In this paper, the author was responsible with the main author for data acquisition and analysis and then participated in the writing of the paper.

4. **S. Alabied**, U. Haba, A. Daraz, F. Gu and A. D. Ball. (2018). Empirical mode decomposition of motor current signatures for centrifugal pump diagnostics. 2018 24th International Conference on Automation and Computing (ICAC), IEEE.

I was the main author, developing the storyline, producing key results and writing the manuscript. The main contribution of this paper was to investigate the use of EMD for analysing current signature for monitoring the health condition of a centrifugal pump.

5. Haba. U, K. Brethee, **S. Alabied**, D. Mondal, F. Gu and A. D. Ball. (2018). Modelling and simulation of a two-stage reciprocating compressor for condition monitoring based on the motor current signature analysis. 2018 31st International Congress on Condition Monitoring and Diagnostic Engineering Management (COMADEM).

In this paper, I participated in the preliminary analysis of the motor current signals and literature gathering.

6. **S. Alabied**, A. Daraz, K. Rabeyee, I. Alqatawneh, F. Gu and A. D. Ball. (2019). Motor current signal analysis based on machine learning for centrifugal pump fault diagnosis. 2019 25th International Conference on Automation and Computing (ICAC), IEEE.

I was the main author, generating key results and preparing the manuscript. The main contribution of this paper was using a SVM algorithm to classify centrifugal pump faults based on motor current data.

7. Daraz, **S. Alabied**, F. Gu and A. D. Ball. (2019). Modulation signal bispectrum analysis of acoustic signals for the impeller wear detection of centrifugal pumps. 2019 25th International Conference on Automation and Computing (ICAC), IEEE.

The contribution to this paper was to undertake the experimental tasks and data collection.

8. Khalid Rabeyee, Yuandong Xu, **Samir Alabied**, Fengshou Gu, A. D. Ball. (2019). Extraction of Information from Vibration Data using Double Density Discrete Wavelet Analysis for Condition Monitoring. Accepted In Proceedings of Sixteenth International Conference on Condition Monitoring and Asset Management, 25th - 27th June 2019, Glasgow, UK.

I worked closely with the main author monitoring the health condition of roller bearings based on analysis of vibration data using Double Density Discrete Wavelet Analysis for feature extraction and selection.

9. Alashter . A, Y. Cao, K. Rabeyee, **S. Alabied**, F. Gu, and A. D. Ball. (2019). Bond Graph Modelling for Condition Monitoring of Induction Motors. 32nd

International Congress on Condition Monitoring and Diagnostic Engineering Management (COMADEM).

The author contributed in the preliminary analysis of the simulated motor current datasets and relative literature review.

# Table of Contents

<b>COPYRIGHT</b> .....	<b>2</b>
<b>Abstract</b> .....	<b>3</b>
<b>Declaration</b> .....	<b>5</b>
<b>Acknowledgements</b> .....	<b>6</b>
<b>List of Publications</b> .....	<b>7</b>
<b>Table of Contents</b> .....	<b>10</b>
<b>List of Figures</b> .....	<b>17</b>
<b>List of Tables</b> .....	<b>22</b>
<b>List of Abbreviations</b> .....	<b>23</b>
<b>List of Nomenclatures</b> .....	<b>25</b>
<b>Chapter 1 Introduction</b> .....	<b>26</b>
<i>1.1 Background</i> .....	<i>27</i>
<i>1.2 Research Application and Motivation</i> .....	<i>28</i>
<i>1.3 The Aim and Objectives of the Research</i> .....	<i>30</i>
<i>1.4 Thesis Organisation</i> .....	<i>31</i>
<b>Chapter 2 Condition Monitoring</b> .....	<b>34</b>
<i>2.1 Introduction</i> .....	<i>35</i>
<i>2.2 Condition Monitoring Overview</i> .....	<i>35</i>
<i>2.3 Condition Monitoring System</i> .....	<i>36</i>
<i>2.4 Maintenance Strategies</i> .....	<i>37</i>
<i>2.4.1 Run to Break Maintenance</i> .....	<i>37</i>
<i>2.4.2 Preventive Maintenance</i> .....	<i>37</i>
<i>2.4.3 Predictive Maintenance</i> .....	<i>38</i>

2.5	<i>Condition Based Maintenance</i> .....	38
2.6	<i>Condition Monitoring Techniques</i> .....	38
2.6.1	<i>Thermal Monitoring</i> .....	38
2.6.2	<i>Vibration Monitoring</i> .....	39
2.6.3	<i>Acoustic Emission Monitoring</i> .....	40
2.6.4	<i>Electrical Signature Analysis (Current Monitoring)</i> .....	40
2.7	<i>Key Findings</i> .....	44
<b>Chapter 3 Fundamentals of Centrifugal Pump, Types and Common Failures ....</b>		<b>45</b>
3.1	<i>Introduction</i> .....	46
3.2	<i>Basic Concept of Centrifugal Pump</i> .....	47
3.3	<i>Classification of Centrifugal Pump</i> .....	48
3.3.1	<i>Radial Flow Centrifugal Pump</i> .....	48
3.3.2	<i>Axial Flow Pump</i> .....	49
3.3.3	<i>Mixed Flow Pump</i> .....	49
3.4	<i>The Construction of Centrifugal Pump</i> .....	50
3.4.1	<i>Pump Impeller</i> .....	50
3.4.2	<i>Shaft of Pump</i> .....	52
3.4.3	<i>Volute</i> .....	52
3.4.4	<i>Seales</i> .....	52
3.4.5	<i>Pump Bearings</i> .....	53
3.4.6	<i>Other Parts</i> .....	54

3.5	<i>Centrifugal Pump Performance Characteristics</i> .....	54
3.5.1	<i>Net Positive Suction Head (NPSH)</i> .....	56
3.6	<i>Common Fault Modes in Centrifugal Pumps</i> .....	57
3.6.1	<i>Impeller Faults</i> .....	58
3.6.2	<i>Bearing Faults</i> .....	58
3.6.3	<i>Seal Faults</i> .....	59
3.7	<i>Induction Motor</i> .....	60
3.7.1	<i>Construction of Induction Motors</i> .....	61
3.8	<i>The Effect of Pump Condition on the Signature of the Electrical Motor Current.</i> .....	61
3.8.1	<i>Current Responses for Normal operating of the pump</i> .....	63
3.8.2	<i>Current Responses for Abnormal operating of the pump</i> .....	64
3.9	<i>Key Findings</i> .....	66
<b>Chapter 4 Techniques for Extracting Condition Monitoring Information</b> .....		<b>67</b>
4.1	<i>Introduction</i> .....	68
4.2	<i>Time Domain Analysis</i> .....	68
4.2.1	<i>Root Mean Square</i> .....	69
4.2.2	<i>Kurtosis</i> .....	70
4.2.3	<i>Crest Factor</i> .....	70
4.3	<i>Frequency Domain Analysis</i> .....	71
4.4	<i>Time-Frequency Domain</i> .....	72
4.4.1	<i>Short Time Fourier Transform</i> .....	72

4.4.2	<i>Wavelet Transform</i> .....	73
4.5	<i>Envelope Analysis</i> .....	74
4.6	<i>Empirical Mode Decomposition</i> .....	74
4.6.1	<i>Empirical Mode Decomposition Algorithm</i> .....	75
4.7	<i>Intrinsic Time-Scale Decomposition (ITD)</i> .....	80
4.7.1	<i>Intrinsic Time-Scale Decomposition Algorithm</i> .....	80
4.8	<i>Key Findings</i> .....	84
<b>Chapter 5</b>	<b>Machine Learning for Fault Detection and Diagnosis</b> .....	<b>85</b>
5.1	<i>Introduction</i> .....	86
5.2	<i>Types of Machine Learning</i> .....	86
5.3	<i>Support Vector Machine</i> .....	88
5.3.1	<i>Theory of SVM</i> .....	89
5.4	<i>Feature Extraction</i> .....	95
5.5	<i>Key Findings</i> .....	96
<b>Chapter 6</b>	<b>Experimental Test Facility Setup and Fault Simulation</b> .....	<b>97</b>
6.1	<i>Introduction</i> .....	98
6.2	<i>Test Rig Construction</i> .....	98
6.3	<i>Test Rig Facility</i> .....	100
6.4	<i>Instrumentations</i> .....	102
6.4.1	<i>Power Supply Analyser (Electrical Power Measurement)</i> .....	102
6.4.2	<i>Flow-Rate Transducer</i> .....	103
6.4.3	<i>Pressure Transducers</i> .....	105

6.4.4	<i>Speed Controller</i> .....	106
6.4.5	<i>Shaft Encoder</i> .....	108
6.4.6	<i>Vibration Measurement (Accelerometer)</i> .....	109
6.5	<i>Data Acquisition System</i> .....	111
6.6	<i>Centrifugal Pump Performance</i> .....	112
6.7	<i>Fault Simulation</i> .....	113
6.7.1	<i>Bearing Defect</i> .....	113
6.7.2	<i>Impeller Defect</i> .....	115
6.8	<i>Experimental Procedure</i> .....	116
6.9	<i>Key Findings</i> .....	117
<b>Chapter 7 Detection and Diagnosis of Centrifugal Pump Faults using Conventional Current Signal Analysis Technique</b> .....		<b>118</b>
7.1	<i>Introduction</i> .....	119
7.2	<i>Time Domain Analysis (waveform)</i> .....	119
7.3	<i>Frequency Domain (Spectrum)</i> .....	122
7.4	<i>Key Findings</i> .....	129
<b>Chapter 8 Empirical Mode Decomposition of Motor Current Signal for Centrifugal Pump Diagnostics</b> .....		<b>130</b>
8.1	<i>Introduction</i> .....	131
8.2	<i>The Performance of EMD on Numerical Simulation Signal</i> .....	132
8.3	<i>The Performance of EMD on Experimental Current Signal</i> .....	134
8.4	<i>Spectrum of IMFs</i> .....	137
8.5	<i>Envelope Spectrum of IMFs</i> .....	138

8.6	<i>Key Findings</i> .....	140
<b>Chapter 9 Intrinsic Time Scale Decomposition for Fault Detection and Diagnosis of Centrifugal Pump</b> .....142		
9.1	<i>Introduction</i> .....	143
9.2	<i>The Performance of ITD on Experimental Current Data</i> .....	143
9.3	<i>Diagnosis Approach based on Motor Current RMS</i> .....	146
9.4	<i>Key Findings</i> .....	148
<b>Chapter 10 Support Vector Machine for Enhance Detection and Diagnosis of Centrifugal Pump Faults</b> .....150		
10.1	<i>Introduction</i> .....	151
10.2	<i>Centrifugal Pump Diagnostic Approach based on SVM</i> .....	151
10.3	<i>SVM classifier based on ITD features</i> .....	152
10.4	<i>SVM classifier based on EMD features</i> .....	155
10.5	<i>SVM classifier based on DWT features:</i> .....	157
10.6	<i>SVM classifier based on Envelope features:</i> .....	159
10.7	<i>Comparison of the diagnostic approach with different methods:</i> .....	161
10.8	<i>Key Findings</i> .....	164
<b>Chapter 11 Conclusions and Suggestions for Future Work</b> .....165		
11.1	<i>Review of the Aims, Objectives and Achievements</i> .....	166
11.2	<i>Conclusion</i> .....	169
11.3	<i>Contributions to the Knowledge</i> .....	170
11.4	<i>Recommendations for Future Work</i> .....	171
<b>References</b> .....		<b>173</b>

**Appendix A.....195**

## List of Figures

<i>Figure 1-1 Research methodology scheme flowchart.....</i>	<i>33</i>
<i>Figure 2-1 Condition monitoring process, schematic diagram.....</i>	<i>36</i>
<i>Figure 3-1 Types of pumps [62] .....</i>	<i>46</i>
<i>Figure 3-2 Types of centrifugal pumps [62].....</i>	<i>47</i>
<i>Figure 3-3 Cross-section and flow path of a centrifugal pump [68] .....</i>	<i>48</i>
<i>Figure 3-4 Radial flow centrifugal pump [71] .....</i>	<i>48</i>
<i>Figure 3-5 Diagram of axial flow pump [72].....</i>	<i>49</i>
<i>Figure 3-6 Diagram of a mixed flow pump [74] .....</i>	<i>50</i>
<i>Figure 3-7 Main components of a centrifugal pump [75].....</i>	<i>50</i>
<i>Figure 3-8 Centrifugal pump impeller types: (a) open, (b) semi-open, (c) closed [73]...51</i>	
<i>Figure 3-9 Construction of mechanical seal [88] .....</i>	<i>53</i>
<i>Figure 3-10 Ball bearing components [89].....</i>	<i>54</i>
<i>Figure 3-11 Performance characteristics of a centrifugal pump [95].....</i>	<i>56</i>
<i>Figure 3-12 Three-phase induction motor construction [117] .....</i>	<i>60</i>
<i>Figure 4-1 Time domain current signal for flow rate 350 l/min .....</i>	<i>69</i>
<i>Figure 4-2 Envelope Analysis Method [150]. .....</i>	<i>74</i>
<i>Figure 4-3 Flowchart of the EMD algorithm [156].....</i>	<i>76</i>
<i>Figure 4-4 Illustration of the EMD method [157].....</i>	<i>78</i>
<i>Figure 4-5 Illustration of standard ITD method, decomposing <math>x(t)</math> into <math>L_t</math> and <math>H_t</math> [167] 80</i>	
<i>Figure 4-6 Flow chart of ITD algorithm .....</i>	<i>81</i>

<i>Figure 5-1 The supervised learning framework [182]</i> .....	87
<i>Figure 5-2 A hyperplane separating and classifying two classes (a) small margin and (b) large margin [190]</i> .....	89
<i>Figure 5-3 The One-Against-All approach of multi-class SVM [196].</i> .....	93
<i>Figure 5-4 The One-Against-One approach of multi-class SVM [196].</i> .....	93
<i>Figure 5-5 SVM with a Directed Acyclic Graph for a multi-classification problem [198].</i> .....	94
<i>Figure 6-1 The test-rig facility</i> .....	99
<i>Figure 6-2 The centrifugal pump used in this work (Pedrollo Model F32/200)</i> .....	100
<i>Figure 6-3 A schematic diagram of the test facility.</i> .....	101
<i>Figure 6-4 The current measurement unit</i> .....	102
<i>Figure 6-5 The output of the HTC</i> .....	103
<i>Figure 6-6 Schematic of GEMS RFO electronic flow sensor</i> .....	103
<i>Figure 6-7 Electronic flow sensor in the pipeline</i> .....	104
<i>Figure 6-8 Raw data from the GEMS RFO flow rate sensor</i> .....	104
<i>Figure 6-9 Pressure transducers installed at the pump inlet and outlet</i> .....	106
<i>Figure 6-10 Omron speed controller, external and internal views</i> .....	107
<i>Figure 6-11 Mounted Hengstler shaft encoder</i> .....	108
<i>Figure 6-12 Raw data of Shaft encoder</i> .....	108
<i>Figure 6-13 Vibration transducer mounted on the pump</i> .....	109
<i>Figure 6-14 Output signal of the accelerometer</i> .....	110
<i>Figure 6-15 YE6232B Data Acquisition System (DAS)</i> .....	111

<i>Figure 6-16 The performance of the centrifugal pump .....</i>	<i>112</i>
<i>Figure 6-17 (a) Inner race defect (b) Outer race defect .....</i>	<i>114</i>
<i>Figure 6-18 Pump head vs Flow rate for (i) healthy pump (baseline), (ii) pump with inner race fault and (iii) pump with outer race fault .....</i>	<i>114</i>
<i>Figure 6-19 Blockage impeller.....</i>	<i>115</i>
<i>Figure 6-20 Pump head vs Flow rate for (i) healthy pump (baseline), and (ii) pump with outer race fault and impeller blockage.....</i>	<i>115</i>
<i>Figure 7-1 Time-domain waveforms for baseline, inner race, outer race and combined fault (outer race and impeller blockage) under different flow rates .....</i>	<i>120</i>
<i>Figure 7-2 Motor current RMS values for a healthy pump, and faulty conditions at different flow rates.....</i>	<i>121</i>
<i>Figure 7-3 Kurtosis values for the current signal for four pump conditions under different flow rates .....</i>	<i>122</i>
<i>Figure 7-4 Vibration envelope spectral analysis for baseline and inner-race fault under different flow rates.....</i>	<i>123</i>
<i>Figure 7-5 Vibration envelope spectral analysis for baseline and outer race fault under different flow rates.....</i>	<i>124</i>
<i>Figure 7-6 Current spectrum for baseline and inner race fault at three flow rates.....</i>	<i>125</i>
<i>Figure 7-7 Current spectrum for baseline and outer race fault at three flow rates.....</i>	<i>125</i>
<i>Figure 7-8 Current spectrum for baseline and combined fault (outer race and impeller blockage) for three flow rates.....</i>	<i>126</i>
<i>Figure 7-9 Peak value of fundamental supply frequency for the healthy pump and pump with seeded faults under different flow rates .....</i>	<i>126</i>
<i>Figure 7-10 Envelope spectrum of current signal for baseline and inner race fault under different flow rates.....</i>	<i>127</i>

<i>Figure 7-11 Envelope Spectrum Analysis of current signal for baseline and outer race fault under different flow rates .....</i>	<i>128</i>
<i>Figure 8-1 Simulated AM signal and its frequency spectrum: (a) a portion of the raw signal and (b) frequency spectrum. ....</i>	<i>133</i>
<i>Figure 8-2 EMD results of simulated AM signal.....</i>	<i>133</i>
<i>Figure 8-3 EMD decomposition results of Baseline at 250 l/min .....</i>	<i>134</i>
<i>Figure 8-4 EMD decomposition results for the outer race fault at 250 l/min.....</i>	<i>135</i>
<i>Figure 8-5 EMD decomposition results for the inner race at 250 l/min.....</i>	<i>135</i>
<i>Figure 8-6 EMD decomposition results for the combined fault at 250 l/min.....</i>	<i>136</i>
<i>Figure 8-7 Current spectra of the first 3 IMFs for all cases at 250 l/min.....</i>	<i>137</i>
<i>Figure 8-8 Peak values at <math>f_s</math> from the current spectrums of IMF1 and IMF2 .....</i>	<i>138</i>
<i>Figure 8-9 Envelope spectrum of IMF1, IMF2 and IMF3 for all cases at 250 l/min. ...</i>	<i>139</i>
<i>Figure 8-10 Peak value of <math>f_s</math> from the envelope spectrum for IMF1 and IMF2 .....</i>	<i>140</i>
<i>Figure 9-1 ITD decomposition result for the healthy pump at 350 l/min.....</i>	<i>144</i>
<i>Figure 9-2 ITD decomposition results for inner race bearing fault at 350 l/min. ....</i>	<i>144</i>
<i>Figure 9-3 ITD decomposition results for outer race bearing fault at 350 l/min. ....</i>	<i>145</i>
<i>Figure 9-4 ITD decomposition results for the combined fault of impeller blockage and outer race defect, at 350 l/min.....</i>	<i>145</i>
<i>Figure 9-5 RMS of current signals at different flow rates (a) raw data, (b) first PRC..</i>	<i>147</i>
<i>Figure 9-6 Figure 9-7 Fault separation based on static and dynamic features of the current signal.....</i>	<i>148</i>
<i>Figure 10-1 An adaptive diagnostic approach for a centrifugal pump based on data analysis and SVM. ....</i>	<i>152</i>

<i>Figure 10-2 Confusion matrix of multi-class SVM based on ITD features .....</i>	<i>154</i>
<i>Figure 10-3 Multi-class SVM classification results using ITD features .....</i>	<i>155</i>
<i>Figure 10-4 Confusion matrix of multi-class SVM based on EMD features .....</i>	<i>156</i>
<i>Figure 10-5 Multi-class SVM classification results using EMD features .....</i>	<i>157</i>
<i>Figure 10-6 SVM Confusion matrix of multi-class SVM based on DWT features .....</i>	<i>158</i>
<i>Figure 10-7 Multi-class SVM classification results using DWT features .....</i>	<i>159</i>
<i>Figure 10-8 SVM Confusion matrix of multi-class SVM based on envelope features....</i>	<i>160</i>
<i>Figure 10-9 multi-class SVM classification results using envelope features .....</i>	<i>161</i>
<i>Figure 10-10 Comparison between different feature extraction techniques .....</i>	<i>162</i>

## List of Tables

<i>Table 6-1 Specification of the centrifugal pump</i> .....	100
<i>Table 6-2 Specification of the three-phase HTC unit</i> .....	102
<i>Table 6-3 Specifications of GEMS RFO flow rate sensor</i> .....	105
<i>Table 6-4 Specifications of the pressure transducer</i> .....	106
<i>Table 6-5 Speed controller specifications</i> .....	107
<i>Table 6-6 Specifications of the shaft encoder</i> .....	109
<i>Table 6-7 Specifications of the accelerometer</i> .....	110
<i>Table 6-8 Technical specification of the data acquisition</i> .....	112
<i>Table 6-9 Characteristics of the bearing</i> .....	113
<i>Table 10-1 Data set of statistical features (experimental data)</i> .....	153
<i>Table 10-2 Multiclass SVM class names</i> .....	153
<i>Table 10-3 Comparison of diagnostic results obtained using the different techniques for all cases</i> .....	161
<i>Table 10-4 Comparison of the current work with the comparable work reported in the literature</i> .....	163

## List of Abbreviations

MCSA	Motor current signature analysis
ESA	Electrical signal analysis
MSS	Motor supply signals
CM	Condition monitoring
ITD	Intrinsic time scale decomposition
EMD	Empirical mode decomposition
SVM	Support vector machine
CBM	Condition-based maintenance
ORNL	Oak Ridge National Laboratory
FFT	Fast Fourier transform
DWT	Discrete wavelet transform
WPD	Wavelet packet decomposing
CWT	Continuous wavelet transformation
SWT	Stationary wavelet transform
HHT	Hilbert-Huang transform
MSB	Modulation signal bispectrum
BEP	Best efficiency point
NPSH	Net positive suction head
NPSHr	Net positive suction head required
NPSHa	Net positive suction head available
RMS	Root mean square
EMF	Electromagnetic force
CT	Current transducer
CF	Crest factor
SC	Spectral centroid
SS	Spectral spread
SF	Spectral Flux
STFT	Short time Fourier transform
WT	Wavelet transform
IMF	Intrinsic mode function

ICA	Independent component analysis
ANN	Artificial neural network
PRC	Proper rotation component
RVM	Relevant vector machine
ML	Maximum likelihood
OAA	One-against-the all
OA0	One-against-one
DAG	Directed acyclic graph
DAS	Data acquisition system
IAS	Instantaneous angular speed
AM	Amplitude-modulating
BL	Baseline
RBF	Radial basis function
K-CV	K-fold cross-validation

## List of Nomenclatures

Symbol	Description
$H_v$	Velocity Head
$H_s$	Static head
$H_f$	Friction head
$Q$	Pump capacity
$E_f$	Efficiency of pump
$E_f$	Efficiency of pump
$P_w$	Hydraulic power
$P_s$	shaft power
$h_a$	Head suction
$h_{vp}$	Vapour pressure
$h_f$	Friction losses
$\varphi$	Linkage flux
$f_s$	Fundamental frequency
T	Torque
J	Motor inertia
$\phi$	Angular displacement
P	Number of pole pairs
$x(t)$	Time domain signal
$\psi(t)$	The wavelet function

## Chapter 1 **Introduction**

*The chapter provides a brief introduction to the research presented in this thesis. It outlines the study background, research applications, and provides the motivation for this study. Also, the main aim and objectives are presented. Finally, the contents of the thesis chapters are listed.*

## 1.1 Background

Condition monitoring (CM) is a vital requirement for evaluating the condition of rotating machines. It has been used for identifying faults, preserving machine efficiency, reducing unexpected damage, and lowering maintenance cost [1]. CM plays a significant role by monitoring parameters such as vibration and current amplitudes that indicate changes in the mechanical and/or the electrical condition of the machine while in operation. Routine preventive maintenance can also protect against catastrophic failure, provided the time intervals between inspections is short enough. In industry, these periods are often the result of experience and advice from the manufacturer's of the machines. By monitoring physical parameters that enable the condition of the machine to be determined, developing faults can be identified and the remaining working life can be predicted [2, 3]. It is now generally accepted that CM should be implemented as the best way for reducing downtime and maintenance costs, preventing machine failure and enhancing operational uptime [4, 5].

CM methods can be classified into two types: intrusive monitoring techniques, such as vibration monitoring, where installation of sensors on the machine is necessary to acquire the necessary data. The other type is non-intrusive monitoring, which includes electric signal monitoring, and which it does not require sensors to be installed on the machine [6]. While each method has its limitations, electric signal monitoring is a desirable technique for those industrial applications where external sensors are difficult to install because of, for example, insufficient space or harsh environmental conditions. The latter has the advantage of relatively easy installation and can begin monitoring the machine's condition without any interruption to its operation [7]. Therefore, CM based on electrical signal analysis should be examined for developing and applying advanced signal analysis techniques to detect machine defects. While it is essential to avoid catastrophic failures by using robust CM techniques, detection of faults at an early stage would be highly advantageous but will require highly accurate diagnostic techniques [8, 9].

CM normally includes three main steps: acquiring data, processing the data and interpretation of the data [10]. An essential part of CM is to reliably acquire accurate data about the machine's condition to determine whether the operating condition is normal or not. Also, essential is the use of suitable techniques for analysing the acquired data and capturing useful information for determining the machine's condition and identifying any

developing fault. This information should be sufficient for diagnostic and prediction purposes. This will assist the maintenance team in determining appropriate action.

Electrical signal analysis (ESA) is a powerful CM method used to detect and diagnose damage in machine systems. However, the current signal is invariably contaminated by a variety of noise, most of which will be produced by non-linear processes. Thus, it is usually difficult to capture accurately diagnostic features with conventional data analysis methods.

This research focuses on investigating current data obtained from an electrical control system and investigates the motor signals based on data-driven techniques to enhance the CM of a rotating machine, a centrifugal pump.

## **1.2 Research Application and Motivation**

Because of their simplicity of design and flexibility in use, centrifugal pumps are widely used in numerous manufacturing processes and applications, for example, agricultural irrigation, chemical plants, oil and gas industry [11, 12]. The components of a centrifugal pump may fail during operation due to excessive stress on, and reduced strength of, its component parts. These failures occur in ways that affect the efficiency of the pump, and may interrupt the manufacturing process, causing cessation of production [13].

It would be very useful to have detection and precise diagnosis, of faults developing in centrifugal pumps. This would help maximise production by allowing efficient long-term maintenance scheduling and avoidance of unexpected shutdowns. A CM system that is reliable and low-cost is highly desirable, and an exciting area of research is to improve the long-term performance of centrifugal pumps.

However, the monitoring of centrifugal pumps is still challenging because of the limited access to many pumps and the consequent difficulty in installing or accessing in-situ sensors such as accelerometers. Such sites would include the very important nuclear and off-shore oil and gas industries [14]. It would be extremely useful for these, and many other, industries to have available enhanced CM methods, including diagnostic techniques for analysing the data acquired from a pump's electrical control system, where the current signal is easy to obtain at any appropriate location without any interruption of the machine. Hence, there has developed a trend for employing techniques that require less equipment and non-intrusive sensors for collecting CM data.

Using Motor Current Signal Analysis (MCSA) for monitoring the condition of the pump is thus a potentially powerful and useful tool [14]. It has been shown to be a reliable and beneficial method for monitoring rotating machinery [15]. Thus, monitoring the condition of a centrifugal pump based on the current signature of the driving motor is considered an interesting topic for research: to demonstrate that it is possible to thoroughly investigate pump characteristics using data analysis techniques based MCSA.

However, the motor current is subjected to noise interference which is a function of the given operating conditions, and will invariably be a complicated non-linear, and non-stationary process. Therefore, advanced data analysis techniques are necessary for detection of a fault before a complete breakdown of the pump operation.

Machine Learning (ML) paradigms and data-driven methods are adopted in this research to analyse non-stationary current signals for different pump conditions. With these methods, such as empirical mode decomposition (EMD) and intrinsic time-scale decomposition (ITD), the decomposed signals provide a baseline which is determined from the signals themselves, rather than finding the similarity to specified basis functions, such as in wavelet transformations. The diagnostic features can be seen, and the underlying trends on the signals can be captured, providing meaningful information for more effective and accurate fault identification. However, the author believes that no reports were found in the literature where ITD was used for analysing pump motor current signals. It is this specific application that is one of the novel features of this project. Later classification method based on the support vector machine (SVM) algorithm will be used for distinguishing centrifugal pump faults (simulated faults).

Thus, the motivation for this research is to produce a robust method for extracting useful information that will accurately identify diagnostic features using data-driven techniques in a platform and overcome the serious limitations of conventional data analysis techniques [16]. In particular, the platform will be used to investigate modulating frequencies contained in the current signals to accomplish high-performance diagnostics of rotating machines.

### 1.3 The Aim and Objectives of the Research

The aim of this research project is to produce a platform using advanced ML paradigms capable of analysing the motor current signals of centrifugal pumps to detect developing faults and produce an accurate diagnosis.

The specific objectives of this thesis can be summarized as follows.

- Objective 1.** To review CM methods and maintenance strategies and explain the most common techniques used for fault detection of centrifugal pumps.
- Objective 2.** To refine the existing test facility and use it for monitoring the condition of a centrifugal pump with different simulated pump faults under various flow rates.
- Objective 3.** To examine the ability of motor current data obtained from the electrical control system for detecting various mechanical faults of the pump by examining the current signature using various signal process techniques.
- Objective 4.** To explore the current signal under different operating conditions using conventional data analysis methods to identify and obtain the most critical fault defining feature, that will be used for comparison with those obtained from the data-driven techniques.
- Objective 5.** To explore and apply data-driven techniques for extraction of the weak nonlinear characteristics of the current signals that are affected by, for example, fluctuations in pump operating pressures and flow rate, and various electromagnetic noises interfering with the measured signals.
- Objective 6.** To examine supervised machine learning techniques such as SVM, for enhancement of CM performances based on the electrical data from the motor.
- Objective 7.** To investigate and evaluate the use of ITD combined with SVM classification algorithm to detect and diagnose the seeded faults. Also, to compare the results of the proposed method with those adopted using a combination of the SVM algorithm with EMD, with DWT and with envelope analysis. The results will also be compared with those of other researchers in this area.
- Objective 8.** To provide meaningful recommendations for future research in this particular subject.

## 1.4 Thesis Organisation

The thesis is divided into eleven chapters, including the current chapter that contains background, research application and motivation, and the research aim and objectives. An outline of each subsequent chapter is presented below:

**Chapter 2** starts by introducing CM, and the importance of a maintenance strategy for manufacturing processes, also it provides a brief introduction to commonly used CM techniques for detecting and diagnosing of rotating machinery faults. Finally, the chapter addresses the motor current signal analysis, which is the main subject of this research.

**Chapter 3** describes the common configurations of the centrifugal pump and its mechanical construction. It also explains the driver induction motor, following by the pump failure modes. Finally, the impacts of centrifugal pump operation under different conditions on the current signature of the electrical motor are presented.

**Chapter 4** presents a literature overview of data analyses methods for extracting monitoring information. It demonstrates the advantages of the data analyses based on data-driven methods for detection and identification of machine faults. This chapter mainly focuses on the MCSA method relevant to detecting and diagnosing different centrifugal pump faults.

**Chapter 5** presents an overview of machine learning paradigms used for machine fault diagnosis. It explains the supervised learning framework. Details of the SVM technique and feature extraction method are provided to classify the centrifugal pump faults.

**Chapter 6** describes the experimental facilities used in this study. It explains the construction of the centrifugal pump test rig, describes all components and control systems that are used to carry out the investigation, with the motor current measurement system. Finally, simulated faults are described and illustrated, and the experimental procedure is presented.

**Chapter 7** presents the investigation of the centrifugal pump fault detection under different operating conditions based on analysing the motor current signal with conventional signal analysis methods. Time domain and frequency domain techniques are used to examine the changes in the current signature related to the pump operation; the

waveform representation shows the modulation effect on the current signal. Finally, common statistical parameters are presented.

**Chapter 8** shows the detection of the impeller and bearing faults based on the Empirical Mode Decomposition (EMD) technique for extracting features of the current motor signature. The envelope technique is also used for demodulating the current signal and detecting abnormal conditions in the centrifugal pump.

**Chapter 9** investigates a data-driven technique for analysing and decomposing the motor current signal, and its application for detecting the centrifugal pump faults. Intrinsic Time Scale Decomposition (ITD) is used to examine the condition of the centrifugal pump. Root mean square of ITD is shown to have the capability for detecting and characterizing the pump fault.

**Chapter 10** investigates the efficiency of using a machine learning method for classifying the faults in the centrifugal pump based on current signals. SVM classifiers are constructed using statistical parameters. In addition, this chapter introduces the diagnostic approach based on the proposed method (ITD and SVM), a comparison of effective features for diagnostic faults is carried out using other methods (Envelope, EMD and DWT) in order to evaluate the performance of the proposed method.

**Chapter 11** concludes the thesis, it presents the conclusions, reviews the achievements against the objectives, and describes contributions to knowledge and novel aspects; finally, the chapter proposes some topics for future work

The summaries of the general structure of the research work and the scheme developed showed in Figure 1-1.

The flowchart explains the main steps for achieving the objectives of this study. The process starts with the current signals being gathered from the centrifugal pump test rig. In the second stage, the current signals are analysed to extract statistical features by using the proposed method ITD and by other signal processing techniques (Envelope, ITD and DWT), then a machine learning algorithm (SVM) is employed for generating the classifiers based on these features, and used for diagnosing the particular centrifugal pump faults.

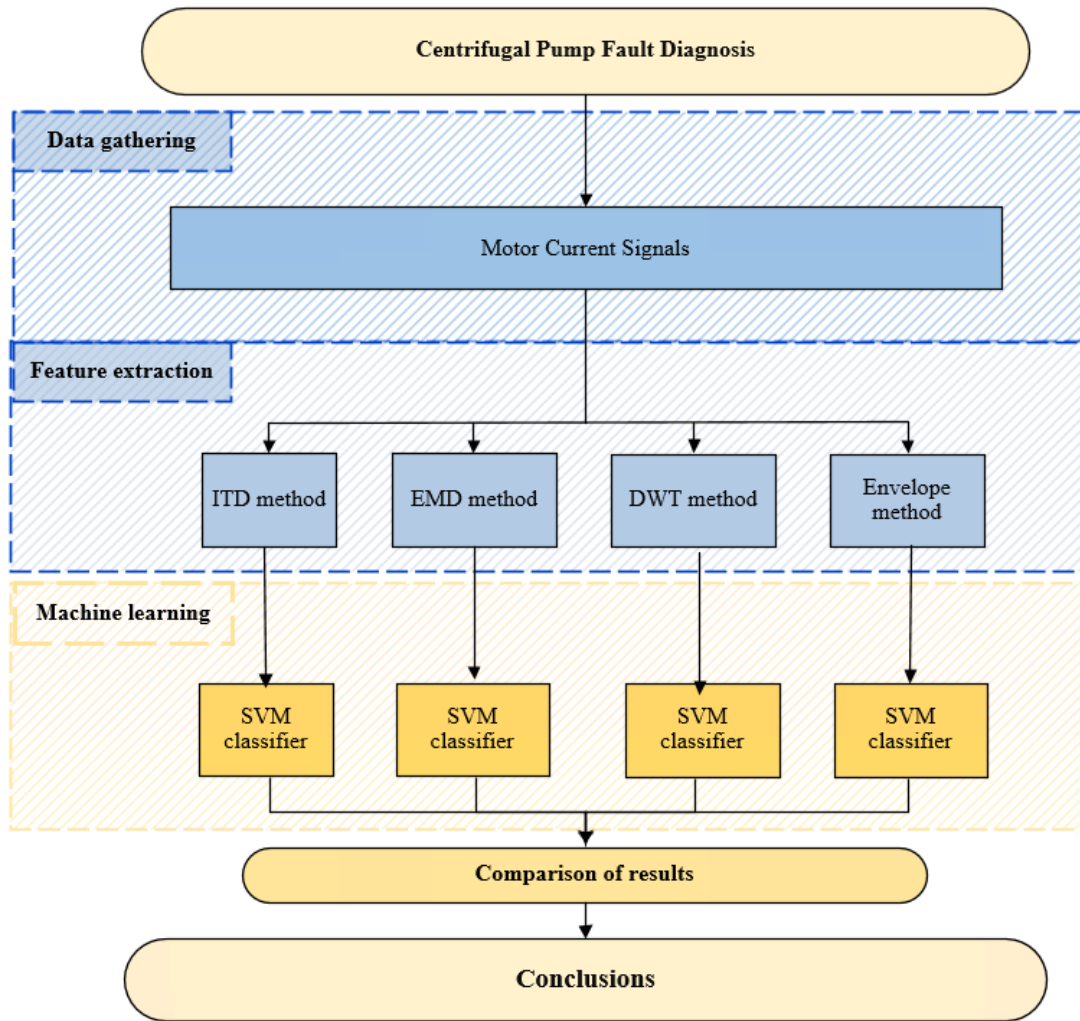


Figure 1-1 Research methodology scheme flowchart

## Chapter 2 **Condition Monitoring**

*This chapter begins by presenting basic Condition Monitoring (CM) techniques. It explains the main CM methods and essential maintenance strategies. It then describes various CM techniques used for the detection of common machinery faults, which includes critical comments on each of the techniques in order to gain sufficient understanding of them and subsequently identify the potential of applying emerging signal processing techniques for improving the performance of CM systems.*

## **2.1 Introduction**

Rotating machines are extensively employed in commercial systems and industrial plant. They require regular monitoring to assess their condition to take an appropriate decision for maintenance work. Early stage faults, if undetected may grow to adversely affect the efficiency of the plant or cause a catastrophic failure. Monitoring of downstream mechanical systems can provide accurate and prompt fault detection and adequate information for the task of decision-making. Therefore, fault detection and isolation of rotating machines such as gearbox boxes, wind turbines, and centrifugal pumps are essential to provide stability of performance and to minimise operating costs.

## **2.2 Condition Monitoring Overview**

CM is the procedure for determining the condition of the rotating machine by monitoring associated parameters with the machine working; it is used to decrease the maintenance cost, ensure machine efficiency and even extend the working life of the machine. It has been widely used to examine and develop techniques for early detection of initial faults [17]. CM is an essential tool for fault detection and diagnosis, it provides continuous assessment of machines, provides an early warning of the expected failures and makes it possible to reschedule future maintenance. It reduces downtime and ensures the reliability of scheduled maintenance [18]. There are many goals of using CM in industry, such as [19]:

- Improve machine reliability and availability.
- Decrease maintenance expenses.
- Enhance safety performance.
- Predict equipment failure.
- Increase the accuracy of fault prognosis.
- Promote the reliability of machine components.
- Enhance equipment performance.
- Eliminate unscheduled downtime.

CM has attracted attention in many branches of research, especially determining the most appropriate monitoring technique for fault detection and identification in specific appliances such as pumps.

The CM process is based on analysing the data gained from the machine to assess the condition of the machine.

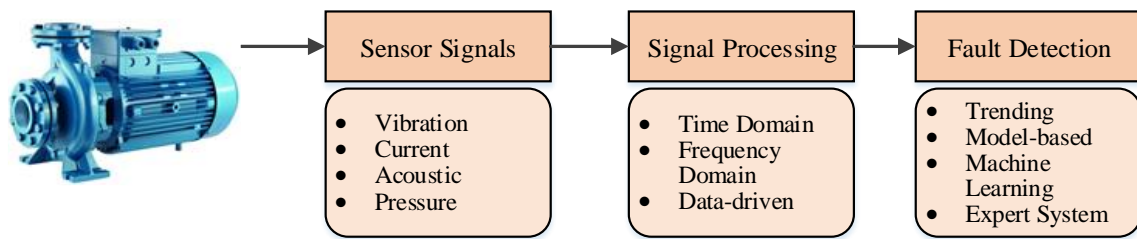


Figure 2-1 Condition monitoring process, schematic diagram

Figure 2-1 shows a schematic diagram of this process. The procedure starts from the left, the machine requiring monitoring is presented. Then various sensors can be utilised to collect data from the machine. Data analysis methods can be applied for extracting precise information, for analysing the signal and detecting and diagnosing defects. The obtained information helps make a precise decision about the condition of the machine [20].

### 2.3 Condition Monitoring System

The chosen CM system is designed to provide the operators and engineers with meaningful information about machinery condition and performance. It is important to adopt a reliable and integrated monitoring system to achieve high performance of the pump throughout its life [21]. For an effective CM system, the selection procedure should include the following [22]:

**Detection:** the basic information of a fault condition that occurs in the machine, detection is essential for taking appropriate action to avoid the sudden shutdown of the system.

**Diagnosis:** for determining the type of the fault and its precise location also the severity of the defect.

**Prognosis:** this procedure is focused on the prediction of the remaining working life of the pump before breakdown or failure. It is essential for CM to provide the most effective action or strategy for dealing with the faults detected.

**Maintenance:** repairs or replacements of any faulty parts of the pump to keep the machine properly functional.

## **2.4 Maintenance Strategies**

There are three types of maintenance strategies, one is based on breakdown maintenance, and the other types are based on predicting and preventive maintenance, Selection of the most appropriate maintenance approach depends on the machine to be assessed and the experience of the maintenance team. Run-to-breakdown allows the machinery to run-to-failure while preventive and predictive maintenance represents early remedial actions to avoid equipment breakdowns, the main purposes of maintenance strategy are [23]:

- To develop and preserve productivity.
- To ensure a high quality of products.
- To increase the lifetime of the machine.
- To decrease the number of repairs and replacement procedures.

### **2.4.1 Run to Break Maintenance**

This type of maintenance is considered as the traditional maintenance method, the machine is operated until breakdown happens. This method allows the machine to keep operating until shutdown, but failure can be catastrophic and result in severe damage. In this strategy, the maintenance is performed only after the machine breaks down. Run to breakdown is still used in some industries where production is not, or only a little, affected by losing one machine for a short time. These industries tend to have a high number of small machines in operation [2].

### **2.4.2 Preventive Maintenance**

This strategy is based on a certain period of time between scheduled maintenance visits; it is more appropriate where the time to failure can be sensibly predicted. It aims to extend the working life of the machine and prevent breakdowns. It involves activities such as monitoring without intervention. In this strategy, a predetermined monitoring routine is performed on a particular machine to evaluate its operation and system health to decide which equipment or parts need more investigation or even replacement. During this latter process, the system may require a shutdown, a good plan allows scheduling of the best time for system-shutdown for repairing and maintaining the machines [24].

### **2.4.3 Predictive Maintenance**

This approach is based on precise measurements in real-time operation. It requires a reliable CM technique; the maintenance events can be scheduled in advance depending on the particular criteria used for making any necessary predictions. It gives the management team a time limit for purchasing necessary parts for repair rather than having a big inventory of replacement parts. Predictive maintenance can extend the period between preventive maintenance actions, and as it detects the faults in an early time, predictive maintenance prevents catastrophic failures [25].

### **2.5 Condition Based Maintenance**

Condition based maintenance (CBM) is a technique that monitors the machine and recommends maintenance decisions using the meaningful information obtained from the machine being monitored. Generally, CBM involves three essential stages: data gathering, data analysis, and maintenance decision making. CBM is capable of providing a robust technique for reducing maintenance costs and ensuring the efficacy of the machine. It is employed to avoid unnecessary maintenance tasks by helping to reduce the number of unessential scheduled preventive activities, hence, reducing the maintenance cost of the machine [10].

### **2.6 Condition Monitoring Techniques**

There are many techniques used for monitoring rotating machinery CM is processes to monitor parameters or condition such as vibration, temperature, pressure and current signal in the system, that involves observing the components of the machine to detect changes in operation that can be indicative of developing failures [26]. Selecting an appropriate technique depends on its capabilities and limitations for detecting early changes in the parameters and trends. CM is used as a part of the condition monitoring system to prevent unplanned breakdown and reduces the maintenance cost. The following methods are generally utilised for detecting and diagnosing machine faults:

#### **2.6.1 Thermal Monitoring**

It is one of common indicator of the machine condition. Worn machinery parts and damaged material components can lead to abnormal temperature distribution. The friction

is the one cause of temperature overloading. Temperature overloading is recognised as one of the major cause of machine failure. This monitoring technique is based on measuring the local temperature of the machine. Thermal monitoring employed to protect the machines from overheating, also, to ensure the better usage of the machine under different operating conditions [27]. Different sensors can be used to monitor the machine temperature. Such as infrared camera [28], the obvious benefits of thermal imaging are that it is a non-contact procedure, and can offer monitoring of a relatively large area. Its disadvantages are its cost, it measures surface temperatures and changes in the local environmental temperature will influence the measurements made. Other temperature measuring devices such as thermistors [29], and thermocouples [30] are usually used in CM to detect the presence of a fault through excessive temperatures, but it is difficult to use them for identifying particular faults.

One of the drawbacks of thermal monitoring is that the observation must be given to the external heat sources, such as the change of the environmental temperature will influence the reliability and accuracy of the measurements of this technique [31].

### **2.6.2 Vibration Monitoring**

Vibration monitoring is widely used for fault detection and diagnosis of rotating machines. In the working environment, vibration generated by machines can be acquired using special sensors, usually accelerometers. The vibration signals have a direct association with the mechanical condition of the machine and the movements of the machine's components [32]. Vibration can be described in terms of three features: amplitude, velocity and acceleration, a variety of transducers are used for measuring and recording these features depending on the vibration to be monitored [33]. Each component of the rotating machine has a distinct vibration signature, and this signature may change if parts are failing. It is important to measure the baseline behaviour of the machine components as these will generate some vibration even with no faults. Thus abnormalities can be detected by comparison of the two vibration signatures to identify damaged components. [22].

Vibration signals are appropriate for monitoring centrifugal pump faults. Vibration monitoring fundamentally depends on the data collected by transducers. These sensors must have an appropriate frequency range and be placed in a suitable position on the machine in order to monitor and detect the failures [34].

The main drawback of vibration monitoring is that the vibration transducers are not always easy to install, such as on inaccessible machines [35].

### **2.6.3 Acoustic Emission Monitoring**

The acoustic emission (AE) technique works in a comparable manner to the vibration technique. Acoustic emission is a non-directional method, so it can use one sensor for measuring the signal compared with the vibration technique that may require up to three axes for gathering the necessary data. AE is a sensitive technique that can give good results when used for CM of machines and detection of faults. AE detects high-frequency signals, typically in the range 20 kHz to 1 MHz [36].

AE is defined as high-frequency stress waves generated by the interaction between two surfaces in relative movement [37] and any change of acoustic signature generated by the rotating machine may indicate damage of one or more machine parts [38].

AE is a non-intrusive method for the CM of the rotary machine, and can offer useful information about the machine's condition [39].

Baydar and Ball [40] have applied the wavelet transform on the acoustic signal for detection of faults in a gearbox, and claim that results achieved by AE analysis are more effective than those obtained by vibration analysis. Alfayez and Mba [41] have investigated the usage of AE for detecting incipient cavitation in a centrifugal pump. Their analysis showed that there is an increase in the AE level when cavitation first appears in the operation of the pump. AE has received very little attention compared to vibration monitoring because the acquired signals are more difficult to process, interpret and classify [38].

### **2.6.4 Electrical Signature Analysis (Current Monitoring)**

MCSA is a monitoring technique developed at the Oak Ridge National Laboratory [42]. As an appropriate method for CM in a varied range of applications. MCSA is based on the induction motor driving a mechanical load being regarded as a permanently available transducer sensing changes in the mechanical load, and converting them into variations in the induced current generated in the motor windings. These changes in motor current are carried in the electrical cables connecting the motor and can be extracted at any appropriate

location without any interruption of the machine. Only a single transducer is required [43]. It is a non-intrusive method [44], where faults in downstream equipment driven by induction motors can be indirectly detected by monitoring the motor current signal [45].

MCSA is based on stator current monitoring, which contains frequency components related to numerous defects that occur in the machine. Any defect in the rotating machine operated by an induction motor like a gearbox or pump will produce a change in the load torque on the rotor of the motor. Thus a magnetic force will be induced in the stator coils. Consequently, the current signal will be modulated and sidebands around the supply frequency will be generated and can be detected [45]. MCSA is a robust technique for determining defects in mechanical systems that are otherwise inaccessible for condition monitoring by vibration analysis such as submersible pumps, where the current data of the pump are just required to access the supply lines carrying the current [46]. Therefore, current monitoring can be applied without any extra devices. It is an effective method for fault detection of the electrical and mechanical equipment.

MCSA can be implemented economically and effectively to analyse and evaluate the electrical and mechanical condition of a machine, for avoiding catastrophic failures and saving on maintenance cost [47].

It has been widely used in monitoring various rotating machines, including gearboxes, centrifugal pumps, and reciprocating compressors. Luo, et al., [48] employed a sensorless monitoring method based on MCSA using FFT analysis for identifying the occurrence of cavitation in a centrifugal pump. Results showed that characteristics of the current spectrum such as the harmonics and vane pass frequency components exhibited characteristics related to the cavitation stage, these changed as the cavitation progressed.

Singh, et al., [49] have used MCSA for bearing fault detection in a mechanical system, they explained that the defects in a bearing mounted in a bearing house can be detected through the change in the magnitude of the motor current harmonics, and sidebands appear around the shaft frequency. A continuous wavelet transform (CWT) was applied to detect an outer race fault.

Popaleny, et al., [50] have examined the effect of mechanical and electrical defects in the current of electrical submersible pumps and their reflection in the dynamic current

spectrum. Different defects such as broken rotor bars, mass unbalance and process issues such as cavitation were investigated using MCSA and power spectral density plots. Results showed that the MSCA was able to identify the defects that occurred.

Martin, et al., [51] have investigated the influence of broken rotor bar faults in an induction motor. Traditional MCSA was used for detecting these faults. For more efficient monitoring of the system, MSCA can be combined with other techniques. For example, Magdaleno, et al., [52], have proposed method based on MCSA with a neural network algorithm for detecting broken rotor bar faults.

However, the classical MCSA based method has certain drawbacks. When the pump is operated under continuous load variations or in the case of ‘pulsating load torque’, its speed is not constant, which might be misinterpreted in the Fourier spectrum of the currents and can lead to an incorrect diagnosis of failure [53]. Niu et al. [54] applied the discrete wavelet transform (DWT) to a transient stator current signal for diagnosing faults in an induction motor. For the classification task, their study used a decision-level fusion model. Inaki, et al., [55] used MCSA for assessing the condition of a gearbox operating under different speeds. The acquired current data were analysed by both DWT and dual-level time asynchronous techniques. This approach allowed the differentiation of healthy gearboxes from faulty cases. MSCA with wavelet packet transform (WPT) was applied for detection of outer bearing fault [56]. Kar and Mohanty studied MCSA for monitoring transmission gearboxes and investigated two defects; one tooth broken, and two teeth broken. The study compared the performance of DWT relative to CWT and found that gearbox defects could be identified more effectively using DWT for analysing the current signals, than CWT [57].

Kompella, et al., [58] applied the MCSA to detect bearing faults utilising frequency spectral subtraction based on different wavelet transforms such as DWT and the stationary wavelet transform (SWT). These techniques were implemented and compared based on a number of indexing fault parameters. The results showed that the proposed method was suitable and effective for differentiating the bearing faults.

Nevertheless, analysing signals by wavelet transforms is not easy, as choosing predefined mother wavelet is itself difficult. Meaning some characteristics of important frequencies

may not be captured by the selected wavelet base, which could lead to loss of useful information for diagnosing faults.

Sun, et al., [59] investigated centrifugal pump operation under different conditions. Both current and vibration data were collected under normal and cavitation conditions. Then the signals were interrogated using the Hilbert-Huang Transform (HHT). The results showed that an unstable flow rate due to cavitation in the pump would produce an energy variation, and the time-frequency characteristics of the signal, such as RMS, extracted from the results of the HHT process can be used to detect pump operating conditions. Amirat et al., [60] have proposed a diagnostic method based on ensemble EMD of the motor phase current for bearing faults detection. Three defects were investigated: cage defect, ball defect, and inner race defect. The closest intrinsic mode function (IMF) based on a Pearson correlation was removed from the original signal, after that standard deviation as fault criterion was calculated and used to specify the condition of the induction motor, where the faulty conditions have higher values than the healthy case. However, this study did not investigate how to distinguish between different fault cases.

Tian, et al., [7] utilized a modulation signal bispectrum (MSB) technique for extracting nonlinear characteristics of the current signal acquired from the motor driving a centrifugal pump system under different impeller faults. Results showed that this method was capable of effectively detecting impeller faults. MSB was found to be capable of capturing the sidebands around the vane pass frequency from the current spectrum.

MCSA is a powerful technique for determining faults in mechanical systems where the machine is inaccessible, or more traditional sensors are difficult to install or access [45]. However, MSCA requires more investigation to assess how to extract more meaningful information, which is usually hidden by noise, from the acquired signal. An advanced signal processing technique is necessary for analysing nonstationary and nonlinear signals, to extract and reveal features from the acquired current signal. Here the study focuses on using the data-driven techniques with machine learning as these can offer more effective and accurate for fault detection and diagnosis.

## **2.7 Key Findings**

The basic concepts and scope of CM technologies have been presented, which was explained in association with the main elements of a maintenance strategy. The most important CM methods such as vibration, acoustics and thermal imaging have been described in this literature overview. Although these methods are of proven worth, they generally have one or more deficiencies in their use, e.g., inconvenient setup, expensive hardware and complex computations.

Moreover, the literature review demonstrated that MCSA can provide a robust diagnostic tool for CM, which is safe and efficient and needs less hardware investment. These key merits of MCSA provide the essential bases for developing more cost-effective CM for pump systems.

However, more investigation is desirable in order to improve the capabilities of MCSA in terms of signal noise reduction and enhanced monitoring of weak signal components. It is proposed to do this by utilizing data analysis techniques based on ML approaches, to capture the most effective features for enhanced CM of rotating machines. The study will focus on the detection and diagnosis of faults seeded into a centrifugal pump. The principal components of such pumps, their types and common failures will be described in the next chapter.

## **Chapter 3 Fundamentals of Centrifugal Pump, Types and Common Failures**

*This chapter presents an overview of centrifugal pumps. It explains the construction of the centrifugal pump and the pump's performances characteristics in detail. Then, an overview of the most common failure modes in centrifugal pumps is given with a critical analysis of their causes and effects. Finally, the motor current signals under pump defects are presented at the end of this chapter with analysis and explanation of the interactions between torque load and motor torque.*

### 3.1 Introduction

The main task of any pump is to transfer fluid or gas from one point to another. It is a mechanical device that can be used to move fluid from low-pressure to higher pressure areas using a rotating impeller to accelerate the liquid by converting electrical energy into kinetic energy of the fluid [61]. In general, pumps are categorized in terms of the fundamental operation of the pump; positive displacement pumps and kinetic pumps, as shown in Figure 3-1.

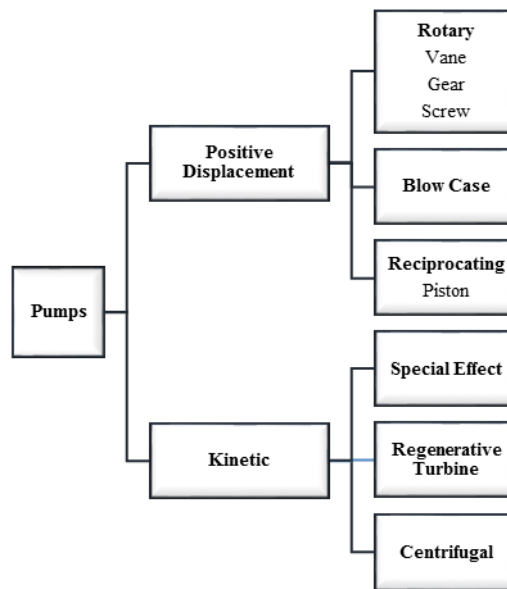


Figure 3-1 Types of pumps [62]

Positive displacement pumps move a fixed amount of fluid during each discharge stroke. They have a fixed displacement volume, and the flow rates directly correspond to their speed. They are typically used for highly viscous fluids under high pressure and low flow operation. Reciprocating pumps such as a piston are common types of the positive displacement pump, where the fluid is delivered as a pulsing flow [63].

The second category of pumps is kinetic pumps, where pumping the fluid is achieved by imparting velocity to the fluid passing through the pump, and subsequently, converting the velocity into pressure. Centrifugal pump is popular and commonly used for the transfer of fluids. Figure 3-2 presents the types of centrifugal pumps [64].

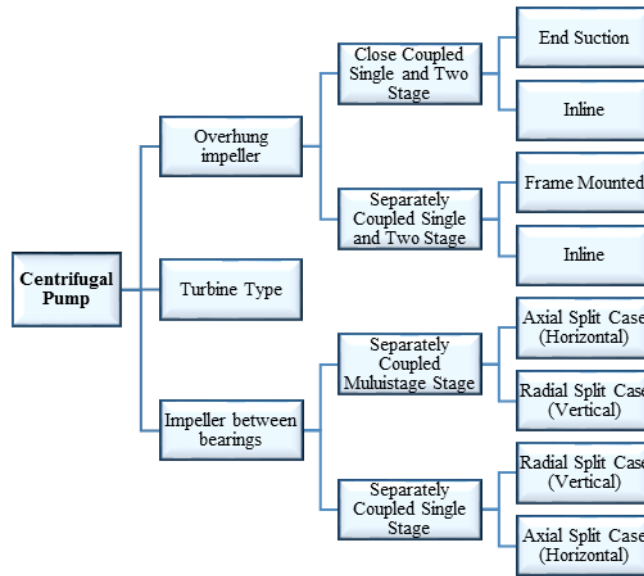


Figure 3-2 Types of centrifugal pumps [62]

In this research, only the centrifugal pump is considered as it widely used in industry, offers high capability, a wide range of capacity and is simple and safe to operate [65].

### 3.2 Basic Concept of Centrifugal Pump

A centrifugal pump is a type of a roto-dynamic pump that is extensively used in manufacturing, agriculture, petroleum, and chemical industries. Typically, it is used for systems requiring larger volume flow rates. It is used to transport liquid via a rotating impeller at high speed [66]. The main purpose of centrifugal pumps is to transfer fluids by lifting a specific volume flow to a specific required level. The transfer operation of the pump is based on well understood hydrodynamic processes [67].

A centrifugal pump operates as follows: the rotation of the impeller moves the liquid outwards, generating a low pressure region at its centre which “draws in” fluid at the pump inlet. The kinetic energy of rotation of the impeller is transformed into pressure by the relative movement between the impeller and volute. The fluid pressure is further increased as the fluid passes through the expansion area. Finally, the high-pressure fluid is discharged via the discharge nozzle. Figure 3-3 depicts a cross-section of a centrifugal pump and shows the motion of the fluid [68].

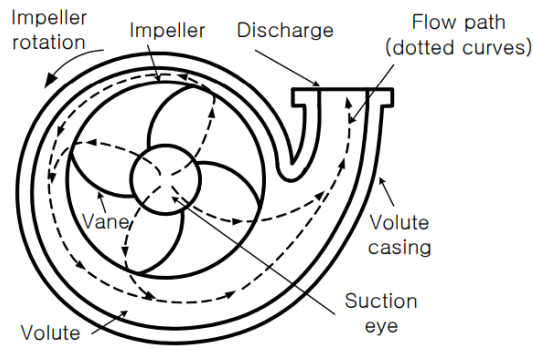


Figure 3-3 Cross-section and flow path of a centrifugal pump [68]

### 3.3 Classification of Centrifugal Pump

Centrifugal pumps can be categorized based on the pattern of the fluid movement through the pump, the fluid discharge direction, and the point to which the liquid needs to be moved. In general, there are three types of centrifugal pumps, which are introduced below.

#### 3.3.1 Radial Flow Centrifugal Pump

In a radial flow pump, the direction of the flow is radial, at right angles to the axis of rotation. The impeller in this type has a large outlet diameter compared to the inlet diameter. The liquid enters at the centre of the casing and then passes through the impeller, and is subsequently moved outwards, gaining angular velocity from the rotating shaft. The blades of radial flow pumps are longer than those of mixed flow pumps [69]. Figure 3-4 shows a typical radial flow centrifugal pump. Radial flow pumps have higher power due to a large amount of fluid flowing inside the impeller. Furthermore, radial flow pumps provide higher head pressure compared with the other pumps, but the flow capacity is smaller [70].

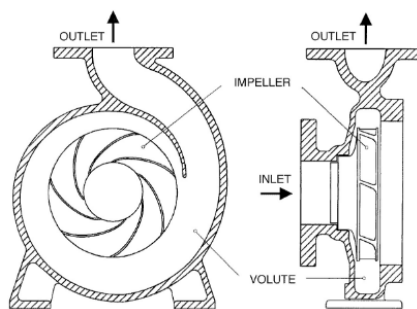


Figure 3-4 Radial flow centrifugal pump [71]

### 3.3.2 Axial Flow Pump

Axial-flow pumps generate less head pressure than radial flow centrifugal pumps but a higher flow rate. They have a simple design and are available in a wide range of capacities. In an axial-flow pump, the direction of the liquid flow is parallel to the axis of the pump. Thus, the fluid flows along the shaft of the pump, and the fluid is discharged from the impeller nearly axially [65]. Figure 3-5 presents a diagram of such a pump, which has a high proportional flow rate with the low head at the entrance, and can be driven by an electric motor or a steam turbine. The pump casing can be divided either horizontally or vertically to provide full access to the fan, and the pitch of the pump can be amended to improve its efficiency. This pump is used when large amounts of fluid at low pressure are required, and it is useful in treating sewage from industrial plants and commercial sites [72].

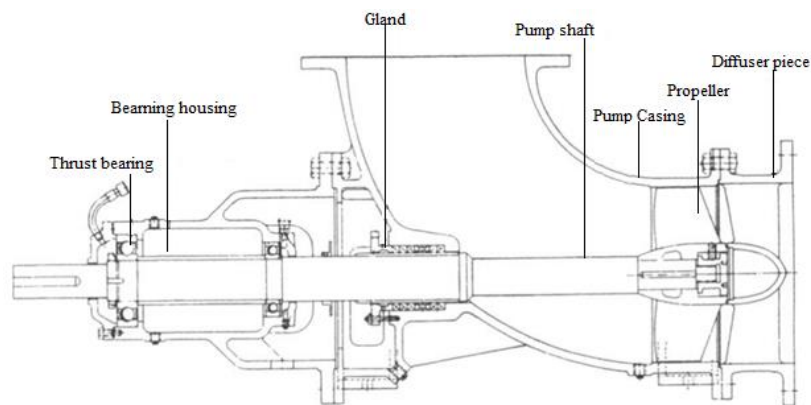


Figure 3-5 Diagram of axial flow pump [72]

### 3.3.3 Mixed Flow Pump

A mixed flow pump has mixed characteristics of both radial flow and axial flow pumps, as shown in Figure 3-6. It is also called a semi-axial flow pump. The fluid generally moves by centrifugal force, where the rotating blades of the fan transfer energy of movement to the flowing liquid, which is then discharged from the pump at an angle less than 90 degrees to the axial direction of the impeller and the casing design [73].

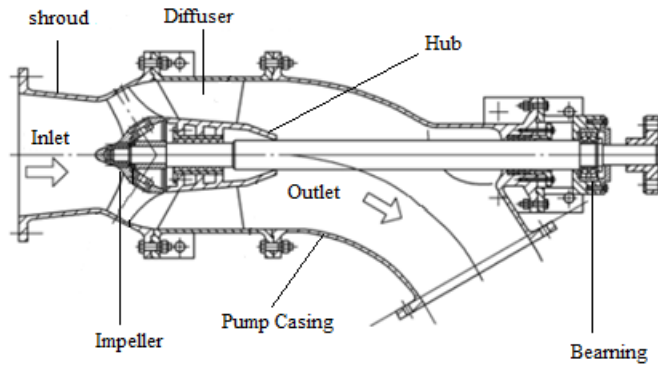


Figure 3-6 Diagram of a mixed flow pump [74]

### 3.4 The Construction of Centrifugal Pump

Pumps are available in different designs and body sizes. Typical centrifugal pump components are shown in Figure 3-7. Such pumps consist of a casing (volute), an impeller, a shaft and bearing, and an electric motor to provide the torque via a shaft into the impeller. A brief explanation of these components is provided below.

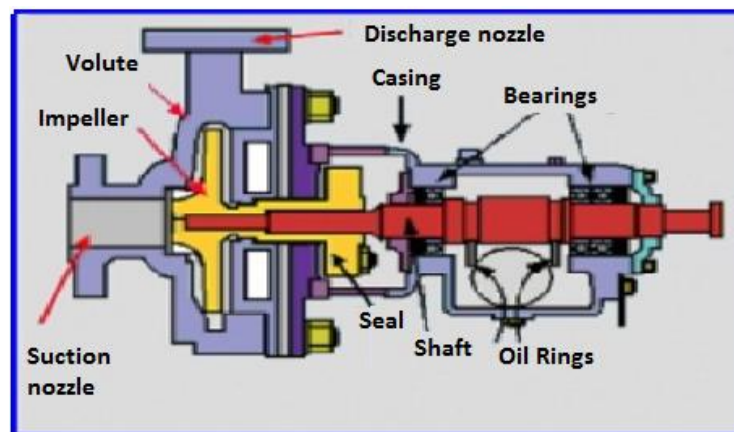


Figure 3-7 Main components of a centrifugal pump [75]

#### 3.4.1 Pump Impeller

The impeller is the fundamental component of a centrifugal pump, which is the key part that generates the centrifugal power which, in turn, moves the liquid to the outside wall of the casing. It consists of a set of curved vanes and has a number of channels determined by the blades that rotate within the casing (the volute) and create a spiral-shaped flow. Various materials can be used to manufacture the impeller, including steel, aluminium, bronze, or plastic. The impeller can be designed in several forms to deliver the requirement

of a specific pump efficiency [76]. In a centrifugal pump, a single impeller is usually sufficient. However, some applications, such as water pumps in firefighting systems, require higher pressures. A pump with multiple impellers is required where a massive lift is needed [77]. The impeller can be categorised based on impeller shape and operating characteristics into open, semi-open, or enclosed impellers.

An open impeller is the simplest impeller design, where the vanes are visible at least from one side of the impeller. Such an impeller involves only a set of blades attached to the shaft, as shown in Figure 3-8 (a). To obtain the best pump efficiency throughout its life, a close tolerance is required between the rotating blades and the casing wall. In general, this type of impeller is selected, particularly when the required fluid includes hung solids [78]. It offers less efficiency compared with a closed impeller, while it has the advantage of a high capacity to discharge the fluid, which can help prevent blockage of the pump by any impurities [70].

Impellers without a front shroud are referred to as semi-open impellers. In a semi-open impeller, shown in Figure 3-8 (b) the shroud makes the impeller structurally stronger. The semi-open impeller offers higher efficiency compared with the open impeller, and are used in small pumps that deal with fluids that include suspended solids [79].

Figure 3-8 (c) shows a diagram of a closed-impeller, which has circular plates attached to both sides of the blades. The design of a closed impeller is more effective with less leakage than either open or semi-open impellers. This is due to the fact that the close clearance between the casing and the end of impeller blades is easier to manufacture accurately, while the adjustment of the clearance is more complicated for other impeller types. Closed-impellers are widely used for centrifugal pumps handling clear liquid [80].

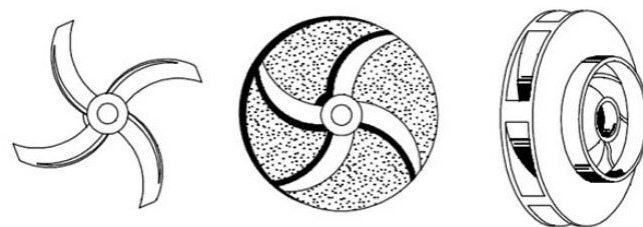


Figure 3-8 Centrifugal pump impeller types: (a) open, (b) semi-open, (c) closed [73]

### **3.4.2 Shaft of Pump**

The main function of the pump shaft is to transmit the mechanical force from the prime motor to drive the pump impeller [81]. The shaft should be strong enough to support all of the forces acting on the impeller, no matter what their direction, longitudinal, lateral, rotational, etc. Since the shaft is subjected to tension and torsions throughout the life-cycle of the pump, it is essential that the pump shaft is used in a manner that does not exceed the endurance limits of the shaft material under any operation conditions [82].

### **3.4.3 Volute**

The pump impeller is positioned inside the volute, which has a curved funnel-like shape, see Figure 3-4. The volute is the portion of the pump casing where the liquid is collected and guided to the discharge nozzle. It helps in transforming the velocity energy of the fluid into pressure energy before the discharge. The form of the volute can determine the direction of rotation of the centrifugal pump and the flow route [83].

There are several different volute designs that are commonly used, such as the single volute and double volute. A double volute involves two single volutes being combined in an opposed arrangement. The double volute casing is designed to minimise or reduce the radial forces imparted on the impeller shaft [84].

### **3.4.4 Seales**

Pump seals are required to provide leak-proof isolation. Seals prevent liquid leaking from the pump or entering into the pump from the side clearance around the pump shaft under operating condition [85]. Mechanical seals are devices designed to protect the rotary and stationary parts of the pump from any damage caused by leakage. The seals must prevent the leakage between the faces of the seals, and between stationary elements and the seal housing, as well as between the rotating component and the shaft of the pump [83]. Generally, mechanical seals are categorized into two groups, stationary seals and rotating (or conventional) seals. In stationary seals, the seal, such as the spring face, does not rotate, while in rotating seals (shaft seals), the seal rotates as a part of the pump shaft [86]. As shown in Figure 3-9, the components of the typical mechanical seal are [87]:

- A mating ring, which consists of the stationary sealing ring and the primary sealing ring mounted on the shaft.
- Secondary seals for the rotating ring mount, which include O-rings.
- A spring and a retainer to ensure good contact between the seal faces.
- A collar linked to the shaft to support the spring.

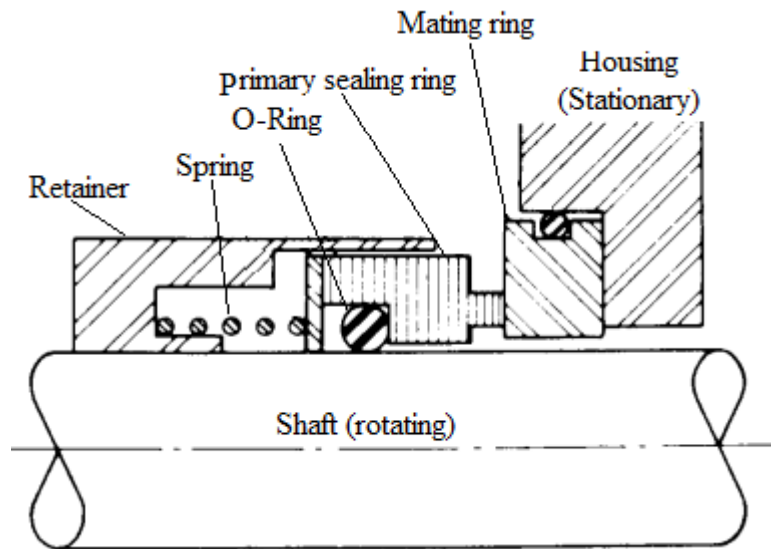


Figure 3-9 Construction of mechanical seal [88]

### 3.4.5 Pump Bearings

Pump bearings are employed to support the pump shaft and absorb all forces that impact on the shaft. They carry the hydraulic loads and forces on the impeller. In centrifugal pumps, the essential purpose of the bearing is to keep the shaft correctly aligned and positioned with respect to the stationary parts. Furthermore, to enhance the pump capability, the bearings should allow the shaft to spin with little friction [76]. Ball bearings have the advantages of being capable of operating at high speed with low friction. Thus they are widely used in small and medium centrifugal pumps where high speed is required [86]. For some pumps, the bearings are mounted in a housing attached to the pump casing because such a setup has proved more protective of the bearing. In general, ball bearings consist of four main parts, which are a set of ball elements, an inner and outer race, and a cage, as shown in Figure 3-10. The balls are placed between the inner and outer ring and distributed by a separator cage to reduce friction. The outer race is mounted in the housing, and the inner race is fixed on the shaft [76].

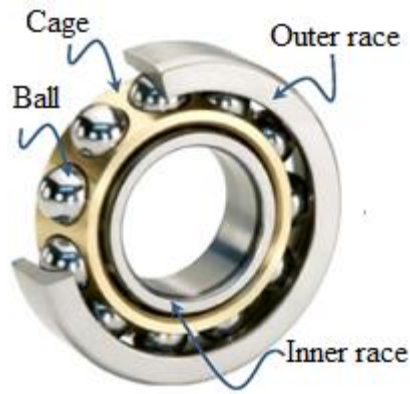


Figure 3-10 Ball bearing components [89]

### 3.4.6 Other Parts

The pump also has some other important parts such as a cooling fan, which is placed at the non-drive end of the motor to prevent overheating for both the stator and rotor parts [90].

### 3.5 Centrifugal Pump Performance Characteristics

Generally, the parameters used to measure pump performance include; head, efficiency, flow, and power.

**The Head:** is the height to which the liquid can be raised by the pump. In other words, it is the vertical distance between the discharge of the pump and the highest point at which the fluid can be delivered. The total head consists of three parameters: static head, velocity head, and friction head.

**Velocity Head ( $H_v$ ):** is the kinetic energy of the fluid at any point in the flow. It is given by;

$$H_v = \frac{V^2}{2g} \quad (3-1)$$

where  $V$  is the liquid velocity, and  $g$  is the local acceleration due to gravity [91].

**Static Head ( $H_s$ ):** is the actual head to which the fluid needs to be raised. It is the vertical distance between the height of the fluid level in the supply tank and the elevation of the fluid discharge level [92].

**Friction Head ( $H_f$ ):** is the pump head required to overcome the frictional forces opposing flow that exists in the pipes.  $H_f$  is affected by the fluid itself, and the material and size of the pipe [91].

**Pump Capacity ( $Q$ ):** is the maximum flow rate through the pump, which depends on the design of the pump. It is the amount of flow that travels through the pump in a specific time, measured in litres per minute at a particular pressure. The centrifugal pump is designed to operate around the rated capacity. In the case of operating the pump below its capacity, cavitation will arise in the pump case and will affect the productivity of the pump and damage the impeller [93].

**Pump Efficiency ( $E_f$ ):** is the ratio of the liquid (output) power generated by the pump to the shaft (input) power. It can be calculated using the equation;

$$E_f = \frac{P_w}{P_s} \quad (3-2)$$

where  $P_w$  is the hydraulic power supplied by the pump which is defined as flow multiplied by pressure, and  $P_s$  is the shaft power [87].

Generally, the performance curve of the centrifugal pump is determined by plotting the head versus the flow rate. Figure 3-11 shows an example of the graphic representation of the relationship between pump performance characteristics. The figure includes the head pump curve, the efficiency curve, the system curves, and the net positive suction required curve. The efficiency of the pump can be identified under different operating conditions [94].

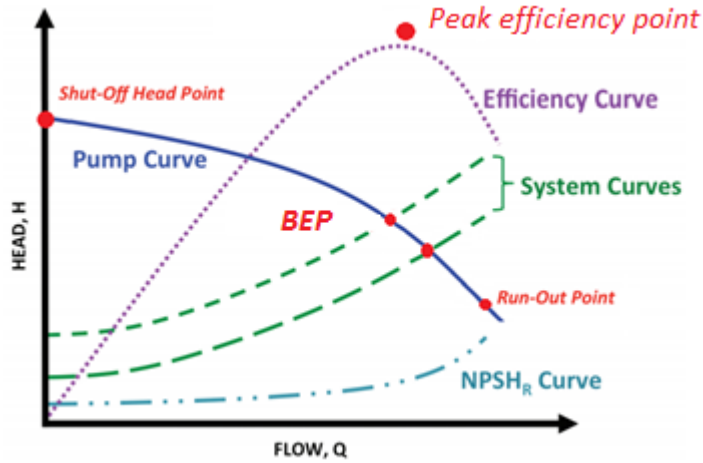


Figure 3-11 Performance characteristics of a centrifugal pump [95].

From this figure, it is clear that when the head decreases, the flow rate increases. The system curve can be defined as the relationship between the total head versus the liquid flow rate. A pump has more than one system curve, which can be determined for different pressures. From the figure above, it is desirable to operate the pump close to where the head curve intersects with the system curve. In addition, to enhance and preserve the efficiency of pump operation, the pump should not be run at the shut-off head point or the run-out point.

Furthermore, running the pump without taking into account the specific range of the system curves can have a negative effect on the operation of the pump or an insufficient supply from the pump [95]. The best efficiency point (BEP) is the flow when the pump operates at the optimum efficiency based on the impeller diameter. The pump performance characteristics depend on the geometry of the impeller, size of the casing, and the operating speed of the pump [94].

### 3.5.1 Net Positive Suction Head (NPSH)

NPSH measures the absolute pressure of the fluid at the inlet section of the impeller. The NPSH value is an essential parameter in pumping system design, as it provides a useful sign of when cavitation will occur. NPSH in a centrifugal pump is represented in two ways [96]:

### 3.5.1.1 Net Positive Suction Head Required (NPSHr)

NPSHr is the minimum head suction pressure required from the pump to function under normal conditions without cavitation. Several factors affect the NPSHr such as the pump speed, the form of the suction nozzle, and the frame of the impeller [61].

### 3.5.1.2 Net Positive Suction Head Available (NPSHa)

NPSHa is the real energy of the liquid in the inlet section of the pump impeller. Generally, a minimum value of NPSHa is required to reduce the likelihood of cavitation and associated damage. An adequate NPSHa is essential to operate the pump so as to decrease the hydraulic forces inside it. NPSHa is influenced by the characteristics of the pump and the suction line, and is calculated by the equation:

$$NPSHa = h_s + h_a - h_{vp} - h_f \quad (3-3)$$

where  $h_s$  is the static head close to the impeller,  $h_a$  the head on the surface of the fluid supply,  $h_{vp}$  is the vapour pressure of the fluid,  $h_f$  is the friction loss in the suction piping. In general, the head suction available must be greater than the head suction pressure required to prevent cavitation [97].

## 3.6 Common Fault Modes in Centrifugal Pumps

Centrifugal pumps can fail during their operation due to failures in one or more components which will decrease pump efficiency, and may cause catastrophic failure. Bearing, seal and impeller defects are common failures in centrifugal pumps. These faults commonly occur at the surface locations and are more likely to happen than other defects such as wear, fatigue and distortion. In many fault conditions, as shown below, periodic oscillations in the torque can be caused by the radial vibrations produced by mechanical defects. This phenomenon leads to the modulation of the current signal at specific frequencies [98].

### **3.6.1 Impeller Faults**

With abnormal pump operation, the impeller will wear, and that reduces flow rate and hydraulic performance [70]. The size and shape of the impeller are vital elements for determining the performance of the pump. Moreover, design errors of asymmetric impeller geometry or an incorrect installation inside the casing can lead to the deformation of the impeller. Such faults can affect the liquid flow, cause noise, generate vibrations, and reduce pump efficiency [99]. Pump performance is also influenced by the number and the design shape of vanes in the impeller, and any change in impeller form caused by, e.g., cavitation or blockages will reduce pump efficiency [61].

Blockage problems in centrifugal pumps come from debris, dirt, or other material caught by the impeller blades that causes a blockage in the impeller [100]. This will cause mechanical imbalance and produce large vibration loads. Such imbalances can affect other parts, such as the bearing. Over time, corrosive and abrasive liquid passing through a centrifugal pump may induce wear of the impeller and casing. To attain the original pump efficiency, replacements of impeller and/or casing are necessary [101].

### **3.6.2 Bearing Faults**

Two rolling bearings located at both ends of the rotor are used to assist the rotation of the shaft system. Pump bearing failure occurs as a result of the contamination of the bearing lubrication by water, or from overloading during pump operation. Lack of proper maintenance can also lead to bearing failures [33] which account for around 40% of all machine failures [102]. These faults can occur at any parts of the bearing, and detecting the damage can help in avoiding machine disruption [103]. Bearing damage can be categorised into distributed or localised. Distributed defects, such as surface roughness, are usually caused by manufacturing errors. Localised defects like cracks and pits tend to be caused by fatigue damage on the rolling surfaces, and can be classified according to the affected element; outer race, inner race, ball and cage defects [102, 104]. The present research will focus only on localised inner race and outer race defects in the centrifugal pump bearings.

When a bearing rotates, each type of bearing defect will produce a specific and characteristic frequency of vibration. These characteristic frequencies are determined by

the bearing geometry, and the shaft frequency of the pump,  $f_r$ . The fundamental defect frequencies are given as [105, 106]:

$$f_o = \frac{N_b}{2} f_r \left(1 - \frac{D_b}{D_p} \cos \beta\right) \quad (3-4)$$

$$f_i = \frac{N_b}{2} f_r \left(1 + \frac{D_b}{D_p} \cos \beta\right) \quad (3-5)$$

where  $f_o$  is the outer race fault frequency,  $f_i$  is the inner race fault frequency,  $N_b$  is the number of balls,  $D_b$  is the ball diameter,  $D_p$  is the pitch diameter, and  $\beta$  is the contact angle.

The relationship between stator current spectrum and bearing vibration results from the fact that any air gap eccentricity in the electric motor driving the system produces corresponding anomalies in the air gap flux [107]. Consequently, the characteristic bearing-fault frequencies in vibration can be present in the motor current as sidebands around the fundamental frequency. The current frequencies for bearing faults,  $f_{ber}$ , are predicted by [108]:

$$f_{ber} = |f_s \pm m f_v| \quad (3-6)$$

where  $f_s$  is the electrical supply frequency,  $m=1,2,3,\dots$ , and  $f_v$  represents either the outer race or inner race vibration fault frequency defined by Equations (3-4) and (3-5) and  $f_{ber}$  is the bearing fault frequency components reflected in the motor current.

However, the modulating components of the bearing fault have a very small amplitude that is buried in noise which can swamp the bearing fault frequencies when the fault is just beginning [109, 110]. It is necessary to use advanced signal processing techniques to extract efficiently the diagnostic features of the bearing fault from the current signals under these conditions.

### 3.6.3 Seal Faults

The main function of the seal is to prevent any leakage of the pumped fluid. Therefore, the seal to be capable of performing as required, must be installed correctly, and proper lubrication must be used to avoid seal failure [111]. Seal failures commonly result from lack of lubrication film, abrasive material in the pumped liquid, both of which produce

abrasion and high wear of the seal, which will invariably be followed by an excessive leakage or breakdown of the pump. Wear of the seal faces is also influenced by the velocity of the shaft, the temperature of the pump, and operating in fluids containing solids [112].

Types of mechanical damages of seal faces can arise include sliding wear, chipping, fractions, disfigurement, and abrasion. The operating conditions of a centrifugal pump have a significant effect on seal behaviour and may lead to damage of the seal in cases where strong vibrations exist in other parts of the pump or from cavitation. Another condition that can damage the seal is excessive driving torque, which can break or split the carbon rings forming the primary sealing surfaces at the end-face of the mechanical seal. This damage is usually due to inadequate lubrication conditions or the liquid being too viscous. The range of seal defects vary widely, from small wear of the seal's surface to extensive damage resulting in a broken seal [113].

### 3.7 Induction Motor

Induction motors are used as a prime mover for most industrial equipment, such as reciprocating compressors and pumps. The main function of an induction motor is to convert electrical energy into mechanical energy [114]. Induction motors are extensively used in numerous manufacturing and domestic applications because of their simplicity, reasonable size, low cost, ease of operation, and readily available power supply [115]. However, induction motors are affected by both electrical and mechanical stresses, which can cause failures in some components. Faults can take the form of either mechanical or electrical damage, and, for instance, an unbalanced shaft or a stator fault could lead to a decline in the productivity of the machine and possibly lead to a catastrophic failure [116]. Figure 3-12 presents a dissected view of the three-phase induction motor.

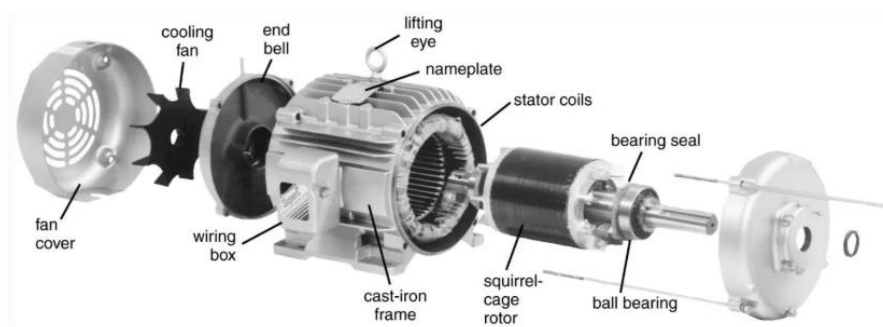


Figure 3-12 Three-phase induction motor construction [117]

### **3.7.1 Construction of Induction Motors**

Fundamentally, the induction motor consists of two main components: a stationary part (the stator) and a rotating part (the rotor). The stator is separated from the rotor by a small air gap.

#### **3.7.1.1 Stator**

The stator is the fixed part of the motor. It contains a cylindrical frame, stator winding and stator core, the frame used to support and protect the stator, and the bearings supporting the rotating shaft [118]. The stator core is usually composed of a set of steel lamination pressed together, and forming the main magnetic flux circuit of the motor. The stator winding contains a set of coils connected in a certain way according to specific conditions. It is covered to reduce eddy current losses and heating. The function of the stator winding is to produce a magnetic field, which helps to achieve the final conversion of energy.

#### **3.7.1.2 Rotor**

The rotating part in the motor is the rotor. It is fixed to the shaft, which is located inside the stator. The core task of the rotor is to convert electrical energy to mechanical energy. The rotor comprises a stack of steel laminations with spaced slots around the circumference. There are two types of rotors used in asynchronous motors, wound rotors and squirrel cage rotors. The wound rotor has a three-phase insulated winding comparable to those on the stator. The ends of the winding are connected to three designed slip rings attached on the shaft [119]. In the squirrel cage rotor type, there is no winding, as it consists of a set of short-circuited bars that are made from copper or aluminium, with two end-rings [118]. Induction motors also consist of other parts such as the frame, bearing, shaft, and fan.

### **3.8 The Effect of Pump Condition on the Signature of the Electrical Motor Current**

As stated above, centrifugal pumps are driven by induction motors, where the current signal can be affected by the pump's operational condition, which means that any faults in the pump will cause a modulation of the current signal. To show the feasibility of using the motor current signature for diagnosing pump faults, the relation between the motor

torque and the pump torque is explained below where the mechanical model of the pump is expressed by the following equation [7, 120] :

$$J_m \frac{d\omega}{dt} = T_e - T_l - T_\xi \quad (3-7)$$

where  $J_m$  represents the moment of the inertia of the mechanical system,  $\omega$  is the angular velocity,  $T_e$  is the electromagnetic torque produced by the motor,  $T_l$  is the passive load torque introduced by the pump and  $T_\xi$  is the viscous torque. It shows any changes in load torque  $T_l$ , due to any disturbance such as flow variation, external and internal abnormalities, would need a corresponding change of the motor torque  $T_e$  in order to maintain the desired speed. In addition, the change of the motor torque would require a change of motor current because the motor torque is proportional to the current as [7]:

$$T_e = \left(\frac{3}{2}\right) \left(\frac{p}{2}\right) L_m (i'_{dr} i_{qs} - i'_{qr} i_{ds}) \quad (3-8)$$

where the motor parameters  $L_m, p, i'_{dr}, i_{qs}, i'_{qr}, i_{ds}$ , denote the mutual inductance, number of poles of the motor, d-axis rotor current, q-axis stator current, q-axis rotor current and d-axis stator current respectively. For a given pump system where the mechanical parameters are fixed, a change in the load will influence the current either dynamically or statically depending on the characteristics of the load variation. To understand the load characteristic in a centrifugal pump, Equation (3-8) presents the load torque due to flow effects [120, 121]:

$$T_l = a_{t1} Q_i - a_{t2} Q_i^2 + a_{t0} \omega^2 + J_{M_v} \frac{d\omega}{dt} - K_Q \frac{dQ_i}{dt} \quad (3-9)$$

where

$$a_{t2} = \left( \frac{r_2 \cot(\beta_2)}{A_2} - \frac{r_2 \cot(\beta_1)}{A_1} \right), \quad a_{t1} = \rho (r_2^2 - r_1^2), \quad a_{t0} = K_n.$$

$Q_i$  is the volume flow,  $r_1, r_2$  are the inner and outlet diameters of the impeller,  $A_1, A_2$  the inlet and the outlet areas of the impeller,  $\rho$  is the density of the liquid in the system,  $\beta_1, \beta_2$  inlet and outlet angles at the vane,  $K_n$  is the casing loss. These terms are constant with a steady flow. The other terms relating to the dynamic load which changes with changes in speed and flow rate.  $J_{M_v}$  is the moment of inertia of the water inside the impeller, and  $K_Q$  represent the effects of changes in impeller torque.

The equation above shows that abnormalities or defects on the impeller due to cavitation, erosion or blockage will cause changes in pressure, flow rates and corresponding oscillations, which in turn lead to changes in both static motor torque and dynamic motor torque. These will affect both the static and dynamic elements of the motor current data. This implies that both static and the dynamic current components could be valuable for fault detection and diagnosis of these faults.

Thus the motor current signature could be valuable for detection and diagnosis of pump faults. In addition, the flow rate will be adjusted by vanes inside each vane exhibits impulsive behaviour, and these will be reflected into the current signature through the load torque. Therefore, investigating these changes in the motor current signals will allow the monitoring of the pump condition.

### 3.8.1 Current Responses for Normal operating of the pump

For simplicity and a better understanding, the electromagnetic operation of the electrical motor (healthy condition) one phase of the three phases of a power supply system is considered. The current signal in this phase, phase A, for the healthy motor can be represented as [122, 123].

$$i_A = \sqrt{2}I \cos(2\pi f_s t - \alpha_I) \quad (3-10)$$

The magnetic flux in the motor stator is

$$\varphi_A = \sqrt{2}\varphi \cos(2\pi f_s t - \alpha_\varphi) \quad (3-11)$$

The electrical, magnetic torque produced by the interaction between the current and the flux, it can be presented as:

$$T = 3P\varphi I \sin(\alpha_I - \alpha_\varphi) \quad (3-12)$$

where  $P$  is the number of pole pairs of the phase, and  $I$  is the RMS amplitude of the stator fundamental current and  $\varphi$  is RMS of the linkage flux, while  $\alpha_I$  is the phase of the current and  $\alpha_\varphi$  is the flux phase, and  $f_s$  is the fundamental frequency of the motor.

### 3.8.2 Current Responses for Abnormal operating of the pump

As explained above the occurrence of any defects in the rotational components, such as the impeller and bearings will lead to extra torque component oscillations around the torque of the motor. Given the additional torque is of amplitude  $\Delta T$ , and is sinusoidal with a frequency,  $f_k$ , it follows that the current amplitude  $I_k$  and phase  $\alpha_k$ , resulting from the oscillatory torque can be obtained from Equation (3-13) [124, 125]:

$$\Delta T = 3P\phi I_k \sin[2\pi f_k t - (\alpha_l - \alpha_\phi) - \alpha_k] \quad (3-13)$$

The change of the torque will cause a fluctuation in the angular speed given by;

$$\Delta\omega = \frac{P}{J} \int \Delta T dt = -\frac{3P^2\phi I_k}{2\pi f_k J} \cos[2\pi f_k t - (\alpha_l - \alpha_\phi) - \alpha_k] \quad (3-14)$$

where  $J$  is the inertia of the system.

This change in angular speed results in phase modulation of the linkage flux and Equation (3-11) becomes;

$$\phi_A^k = \sqrt{2} \phi \cos\{2\pi f_k t - \alpha_\phi - \Delta\phi \sin[2\pi f_k t - (\alpha_l - \alpha_\phi) - \alpha_k]\} \quad (3-15)$$

where  $\Delta\phi = \frac{3P^2\phi I_k}{4\pi^2 f_k^2 J}$ .

This demonstrates that the flux has a nonlinear effect due to the defect in the rotor system. An electromagnetic force (EMF) will be generated by the nonlinear interaction of flux, and therefore, a nonlinear current signal will be induced in the stator.

For a very small  $\Delta\alpha_k$  we have  $\cos(\Delta\alpha_k) \approx 1$  and  $\sin(\Delta\alpha_k) \approx \Delta\alpha_k$ , and the linkage flux can be expressed as:

$$\begin{aligned}
\varphi_A^k &\approx \sqrt{2}\varphi \cos(2\pi f_s t - \alpha_\varphi) + \sqrt{2}\varphi\Delta\alpha_k \sin(2\pi f_s t - \alpha_\varphi) \\
&= \sqrt{2}\varphi \cos(2\pi f_s t - \alpha_\varphi) \\
&\quad + \sqrt{2}\varphi\Delta\varphi_k \cos[2\pi(f_s - f_k)t - \alpha_\varphi - \alpha_k] \\
&\quad - \sqrt{2}\varphi\Delta\varphi_k \cos[2\pi(f_s + f_k)t - 2\alpha_\varphi + \alpha_\varphi - \alpha_k]
\end{aligned} \tag{3-16}$$

From equation (3-16), the flux comprises both the fundamental and sidebands around  $f_s$ . The current can be then be derived from the motor equivalent circuit:

$$\begin{aligned}
i_A^k &= \sqrt{2}I \cos(2\pi f_s t - \alpha_i) \\
&\quad + \sqrt{2}I_l \cos[2\pi(f_s - f_k)t - \alpha_i - \alpha_k - \phi] \\
&\quad - \sqrt{2}I_u \cos[2\pi(f_s + f_k)t - 2\alpha_\varphi + \alpha_\varphi - \alpha_k - \phi]
\end{aligned} \tag{3-17}$$

where  $\varphi$  is the angular displacement at supply frequency,  $I_l$  and  $I_u$  are the RMS amplitudes of the resulting sidebands (lower and upper) around the current produced by the healthy motor, which are induced by the back-EMF voltages produced by the flux variations at frequencies of  $f_s - f_k$  and  $f_s + f_k$ .

This basic expression shows that, in principle, the current signal in the driving motor can be used to detect the presence of a downstream mechanical fault, and has been widely used for CM. However, the equations are based on an idealised motor, and certain simplifying assumptions, and serve as a guide. Equations are an approximation of the real situation when actual faults are present. The equations show that changes are to be expected, and the faults can be detected. This can be based on tracking the characteristic fault frequency or calculating the variation content in the current energy in particular frequency ranges to determine the presence of mechanical defects.[126]. However, other characteristic features may also be present in the signal.

Thus, an advanced signal processing technique is required to analyse and demodulate the motor current signal for detection of mechanical defects. It is hypothesised that data-driven techniques could form a more robust tool to link fault and signal, to increase the effectiveness of MCSA for extracting the weak current signatures generated by faults from the motor current signals in order to yield superior detection and diagnosis of faults. Such

an approach could provide the benefit of enabling us to identify links which do not necessarily correspond to the above analysis, e.g., structural changes in one component could be related to functional changes in another.

### **3.9 Key Findings**

Due to their simplicity of structure and use, and capability of operating at high speed with a steady output flow for long periods, centrifugal pumps are widely used in numerous process industries such as petrochemical, agriculture, and chemical, as well as in water purification plants. Such pumps are often deployed in critical areas, where any defects that occur will not only reduce plant efficiency but could lead to a production breakdown. To preserve pump efficiency and reliability, and to ensure optimum operating conditions, it is crucial to monitor the pump's condition and detect faults at the earliest, so that appropriate actions can be taken in good time to facilitate pump maintenance.

During pump operation, the interaction between the flow and torsional and rotational oscillations of the drive shaft will generate changes in the air-gap's magnetic field. This means that the motor current responds to any mechanical defects during the pump operation. Thus, the MCSA provides a reasonable and attractive technique for monitoring the condition of the pump. The literature review revealed that the most common defects in centrifugal pumps are bearing faults and impeller blockage [100, 102]. Thus these were the faults chosen for investigation in this study. The next chapter explains the data analysis methods in more details.

## Chapter 4 **Techniques for Extracting Condition Monitoring Information**

*This chapter provides a review of the literature on methods used for extracting and analysing diagnostic information for machine CM. It presents the data analytic methods that are widely used for detecting faults in machines; it discusses their algorithms, strengths and limitations. The chapter focuses mainly on relevant MCSA methods in order to obtain effective features to detect and diagnose different centrifugal pump faults. These explanations are introduced to help understand the techniques that will be used in the succeeding chapters of this thesis.*

## **4.1 Introduction**

To achieve reliable condition monitoring and fault diagnosis results, appropriate methods for analysing and assessing the abnormal condition of the rotating machine are required. Several signal processing techniques have been used to analyse and interpret waveform data to extract useful information for a further diagnostic purpose[127].

The current signal acquired from the machine is often contaminated by noise and affected by machine operating condition. Thus, they require suitable and more reliable techniques for extracting features related to the machine condition. Typically, there are three different ways to look into the signal: time domain analysis, frequency domain and time-frequency domain. In this research, advanced data analysis techniques have been used to improve the diagnostic method for various centrifugal pump defects based on the motor current signature analysis.

## **4.2 Time Domain Analysis**

The most basic analysis of a signal is based on its time domain waveform. It is a series of discrete values sampled over a period of time, invariably at regular intervals which are at a frequency at least twice as fast as the highest frequency of interest. In this technique, characteristic features can be extracted based on the amplitude of the signals; these features include root mean square, mean, peak values, standard deviation, and so on. These features provide a means of evaluating a machine's condition [10].

Figure 4-1 shows the time domain waveform of the current of a motor driving a centrifugal pump for different pump conditions with a fixed flow rate. The two signals are for the baseline (healthy) pump condition and the pump with a seeded fault introduced into the inner ball race of the pump bearing. It is clear that the waveforms show changes in the peak amplitudes according to the different pump conditions. It can be seen from the figure that the signals exhibit amplitude modulation.

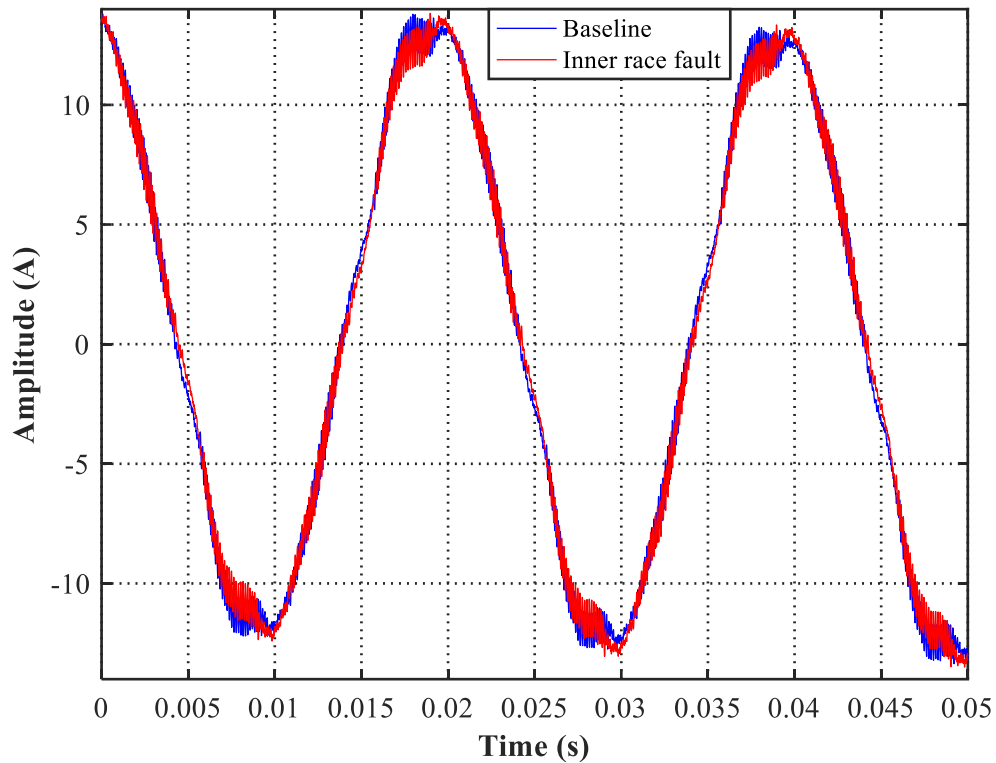


Figure 4-1 Time domain current signal for flow rate 350 l/min

However, it is hard to assess the condition of the centrifugal pump from the signal waveform alone, especially when the pump works under abnormal operation. Thus, there is a need for calculating some of statistical parameters based on the time domain information for assessing the real condition and behaviour of the pump. Statistical parameters such as root mean square, crest vector, and kurtosis [128] are used for diagnosing pump faults. It has been shown that there exists a correlation between the amplitude of these statistical parameters, and the damage occurred in particular components of the machine [129]. Some common statistical features are described in the next sub-section:

#### 4.2.1 Root Mean Square

Root mean square (RMS) represents the overall energy content of the signal. RMS is the most common feature in the time domain of the signal and is also an effective parameter for detecting faults in machines [130]. It can be calculated by the formula [131]:

$$RMS = \sqrt{\frac{1}{N} \sum_{n=1}^N ((x(n) - \bar{x}))^2}$$

where  $N$  is the total number of sampled points in the signal,  $x(n)$  is the amplitude of the signal, and  $\bar{x}$  is the mean value of of the signal amplitude.

Generally, the RMS of the signal is used for tracking the change of the signals [132], and this is considered to be very capable of evaluating the condition of rotary machines [133].

#### 4.2.2 Kurtosis

Kurtosis is a statistical parameter, it is the fourth moment of distribution of the collected data. It used to illustrate the distribution of the signal in the time domain, and it indicates whether the data contains individual peaks or is evenly distributed, and is often compared to the normal distribution [134]. It can be calculated by the following equation:

$$kurtosis = \frac{\frac{1}{N} \sum_{n=1}^N (x(n) - \mu)^4}{\left[ \frac{1}{N} \sum_{i=1}^N (x(n) - \mu)^2 \right]^2} \quad (4-1)$$

where  $N$  is the total number of sampled points in the signal,  $x(n)$  is the discrete time domain, and  $\mu$  is the mean value of the signal amplitude.

That means kurtosis is sensitive to impulses in the signal, so the higher the magnitude and number of impulses, the larger the kurtosis. This can be used as a CM tool to detect faults according to changes in the value of the kurtosis [135].

#### 4.2.3 Crest Factor

Crest Factor is the ratio between the maximum positive values of the signal to its RMS value. The Crest Factor is capable of detecting incipient defects; normally, the fault produces impacts that will increase the peak level [136, 137]. The crest factor is defined by the following formula:

$$\text{Crest factor} = \frac{x_{\max}}{x_{\text{rms}}} \quad (4-2)$$

where  $x_{\max}$  the absolute maximum value of the acquired signal,  $x_{\text{rms}}$  is the RMS value.

From the above equation, the crest factor has a direct relationship with peak value and an inverse relationship with the RMS value. When peak value increases the value of the crest factor also increases. Therefore, the crest factor is an effective indicator primarily when the signal is “impulsive” [137].

### 4.3 Frequency Domain Analysis

In this analysis, the time domain signal is transformed to the frequency domain. The frequency content of the signal (spectrum analysis) is very important for analysing and assessing the acquired signals. Frequency domain analysis identifies precise frequency components in the frequency spectrum or in a specific frequency range. The most commonly used method for transforming time domain samples to the frequency domain is the Discrete Fast Fourier Transform (DFFT) [10, 138].

Let  $x(t)$  be the continuous signal for  $N$  samples:  $x(0), x(1) \dots x(N-1)$

$$\text{The DFFT} = \sum_{x=0}^{x=N-1} x(n) e^{-2j\pi ft}$$

According to the Nyquist theorem, the sampling frequency must be at least twice the highest frequency of interest [139].

All components related to the machine’s operation can be seen in the frequency domain. The characteristic features or patterns present in the frequency domain are very useful for identifying the characteristics and behaviour of the system [140]. It has been found that the most defects generate modulation sidebands around the fundamental frequency of a rotating machine. Also, some faults are associated with particular defect frequencies (and their harmonics), the magnitude of these specific frequencies and sidebands will often afford meaningful information on the condition of the machine [122, 141].

However, FFT has limitations as it suffers from frequency leakage, which makes it difficult to distinguish the signal of a healthy condition from a faulty one. The DFFT is based on samples of short duration, whereas the original signal is likely to have extended over a

considerably longer time. So, for the DFFT to produce representative results, it is assumed the original signal is stationary. The inevitable consequence is that information is lost when transforming a time domain signal into a frequency-domain signal. To minimise, but not eliminate, the error, a windowing function is used which can itself introduce further error. Nevertheless, the DFFT has proved to be an immensely successful and useful tool in the CM of rotating machinery.

Another limitation of this method is its frequency resolution, the total time of signal acquisition has a major effect on the resolution. To overcome this particular limitation, data of sufficient length should be captured [142]. Thus, it is preferable to utilize advanced signal processing techniques such as wavelets and other adaptive methods for more in-depth analysis of the signal [143].

#### **4.4 Time-Frequency Domain**

Both time domain and frequency domain analysis are useful for analysing and extracting meaningful information to evaluate the condition of some rotating machines that generate stationary signals. However, they are limited when analysing non-stationary signals and cannot explain the change of the signal over time, particularly when the signal is subject to frequency modulation [144].

In order to overcome these drawbacks, methods have been developed based on joint time-frequency analysis whereby nonstationary and non-linear signals can be analysed.

As the current signal from the centrifugal pump with a seeded fault will be nonstationary in behaviour, it is worth examining this signal using time-frequency analysis. There are many techniques based on the time-frequency domain, such as:

##### **4.4.1 Short Time Fourier Transform**

Short Time Fourier Transform (STFT) is based on the idea of using a moving window over the time domain data to get the stationary component from the nonstationary signal. The process involves dividing the entire time domain data into a set of segments, then applying the Fourier Transform to each short signal segment one by one [145]. The process of the STFT can be defined by a localised function:

$$STFT(t, f) = \int_{-\infty}^{\infty} x(t)w(t - \tau)e^{-j2\pi ft} dt \quad (4-3)$$

where  $x(t)$  is the original signal,  $w(t)$  is the window function and  $\tau$  is the time-shift parameter.

The main drawback of this transform method is the limit imposed by high redundancy. Another limitation is that the time-frequency resolution is seriously affected by the size of the window. In the STFT method, even though the method can analyse nonstationary signal more effectively than the traditional FFT technique, it still suffers from frequency resolution issues. Analysing the signal by STFT is limited by the constraint of having to use a window of fixed duration. The difficulty is to choose the best window length for a signal that contains both low and high frequencies at the same time since, if a long window is used, there will be better frequency resolution, but poorer time resolution and vice versa [146]. For that reason, STFT is more appropriate for analysing quasi-stationary signals rather than real-life non-stationary signals

#### 4.4.2 Wavelet Transform

The wavelet transform (WT) decomposes the signal utilising a variable length window. The WT uses a mathematical function, called a wavelet function to replicate the signal [147]. Unlike the STFT, it is a robust localisation method as it provides a multi-resolution window that depends mainly on the frequency components of the signal [146]. Mathematically, it can be defined as follows [148]:

$$\psi_{s,\tau}(a, \varphi) = \frac{1}{\sqrt{a}} \int_{-\infty}^{\infty} f(t)\psi^* \left( \frac{t - \varphi}{a} \right) dt \quad (4-4)$$

where  $a$  is the scale parameter,  $\varphi$  the shift parameter, and ‘\*’ represents the complex conjugation operation, and  $\psi(t)$  is the wavelet function.

Formula (4-4) is also called the continuous WT, as it employs a continuous range for both parameters of scale and shift. Moreover, it has the ability to analyse nonstationary signals, whereas the Fourier transform is unable to do so. Unlike Fourier analysis where the window is of constant length, in the WT, the size of the window depends on the scale and the shift parameter [149].

## 4.5 Envelope Analysis

Envelope analysis or the method of demodulation is based on the extraction of low-frequency components from the signal, which is modulated by a high carrier signal. This method has been employed for detecting faults such as bearing defects and cavitation in pumps [150]. It is used for demodulating the signals following the process explained in Figure 4-2. The envelope of an analytic signal is determined by the equation [151]:

$$e(t)=\sqrt{x(t)^2 + H[x(t)]^2} \quad (4-5)$$

where  $H[x(t)]$  it is the Hilbert transformation of the given signal  $x(t)$ .

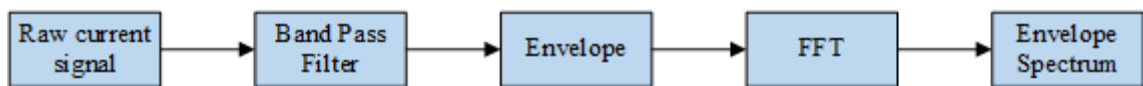


Figure 4-2 Envelope Analysis Method [150].

The process starts with filtering the raw data of the current signal by means of a bandpass filter to specify the frequency range of interest. The next step uses the Hilbert Transform to rectify the signal. Then the FFT is applied to obtain the envelope spectrum [150]. The envelope contributes significantly to reduce the noise and helps to maximise the signal to noise ratio. Also, the amplitude values of the signal become more apparent in the envelope spectrum, which is not evident in the results for the FFT [152].

## 4.6 Empirical Mode Decomposition

Empirical Mode Decomposition (EMD) is an adaptive approach used to analyse the signals based on their local characteristics. EMD is a data-driven and robust decomposition method for analysing nonstationary and non-linear signals. Huang, et al., introduced it in 1998[153]. The fundamental concept of the EMD is decomposing complicated signal iteratively into a number of narrowband components of intrinsic mode functions (IMFs) which remain in the time domain, and are of the same duration as the original signal, which means information related to the frequency content of the signal is retained [74].

Unlike STFT and WT, data-driven EMD is a robust technique. Compared with the STFT, the WT is more appropriate for analysing non-stationary signals, by means of dilation and translation, it utilizes a variable length window that depends on both the scale and the

shifting processes. The wavelet has the major disadvantage that the analysis results depend on the *a priori* choice of an appropriate wavelet function, known as the ‘mother wavelet’. The challenge here lies in choosing a suitable function to capture the required characteristics of the data [154].

The limitations mentioned above regarding analysis of non-stationary signals using a STFT can be overcome by using EMD, as it is a data-driven technique. EMD is an appropriate tool for analysing non-linear and non-stationary signals because the foundation functions are determined from the data itself [74, 155]. In EMD, because there is no need to select a basis function for the decomposition procedure. This method can obtain the characteristics of the signals more precisely than the traditional FFT and WT methods.

#### **4.6.1 Empirical Mode Decomposition Algorithm**

The main function of the EMD decomposes the given signal  $x(t)$  into several modes of oscillation. There are two essential conditions to be satisfied by an intrinsic mode function (IMF):

- (i) In the complete data series, the total number of extrema points and the zero crossings must be equal, or at most differ by 1.
- (ii) The mean constructed from the envelopes must be symmetric in nature [153].

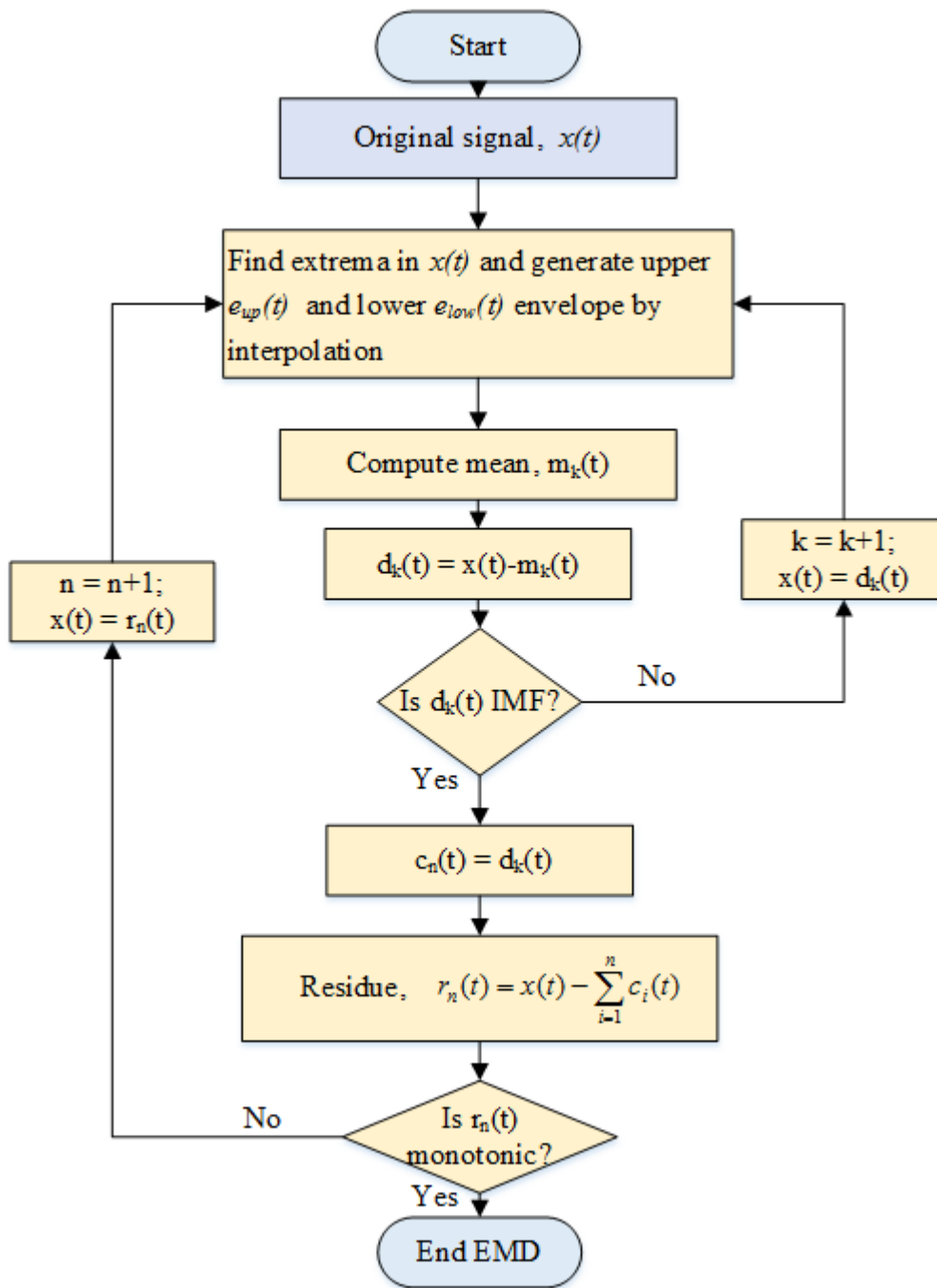


Figure 4-3 Flowchart of the EMD algorithm [156].

Figure 4-3 presents the algorithm of the EMD, which can be explained as follows [155]:

1. Identify both the local extrema (maxima and minima) of the original signal  $x(t)$ .
2. Determine the upper  $e_{up}(t)$  and lower  $e_{low}(t)$  envelopes using a cubic spline interpolation by connecting all recognized maxima and minima points.
3. Calculate the mean,  $m_i(t)$  of the envelopes.

$$m_i(t) = \frac{e_{up}(t) + e_{low}(t)}{2} \quad (4-6)$$

4. Subtract the mean from the original signal.

$$d_i(t) = x(t) - m_i(t) \quad (4-7)$$

where  $i$  is the iteration indicator.

5. If the difference  $d_i(t)$  meets the IMF criterion, then  $d_i(t)$  is treated as the first IMF denoted as  $c_i(t)$  otherwise repeat steps one to four.
6. Obtain the residue function.

$$r_n(t) = x(t) - c_i(t) \quad (4-8)$$

Treat the residue as the original signal for the next step.

7. Iterate the above steps ‘ $n$ ’ number of times to extract the remaining IMFs from the signal  $x(t)$  until the residue function becomes monotonic.

Consequently, the original signal can be reconstructed according to Formula (4-9):

$$x(t) = \sum_{i=1}^n c_i(t) + r_n(t) \quad (4-9)$$

where  $c_i(t)$  is the  $i^{\text{th}}$  IMF,  $r_n(t)$  is the  $n^{\text{th}}$  residue and  $n$  is the empirical mode. The next figure explains the algorithm of EMD.

Figure 4-4 illustrates the working of the EMD algorithm. The first panel (a), contains the original signal, which, here, is a simple signal consisting of two superimposed sine waves. In panel (b), the upper and the lower envelopes are calculated (red lines) using the cubic spline interpolation to connect all maxima and minima. Next, the mean values are calculated and are shown in panel (b) as the dotted blue line. Panel (c) shows the first IMF obtained from the process. The first residual  $r_1(t)$  is shown in panel (d)

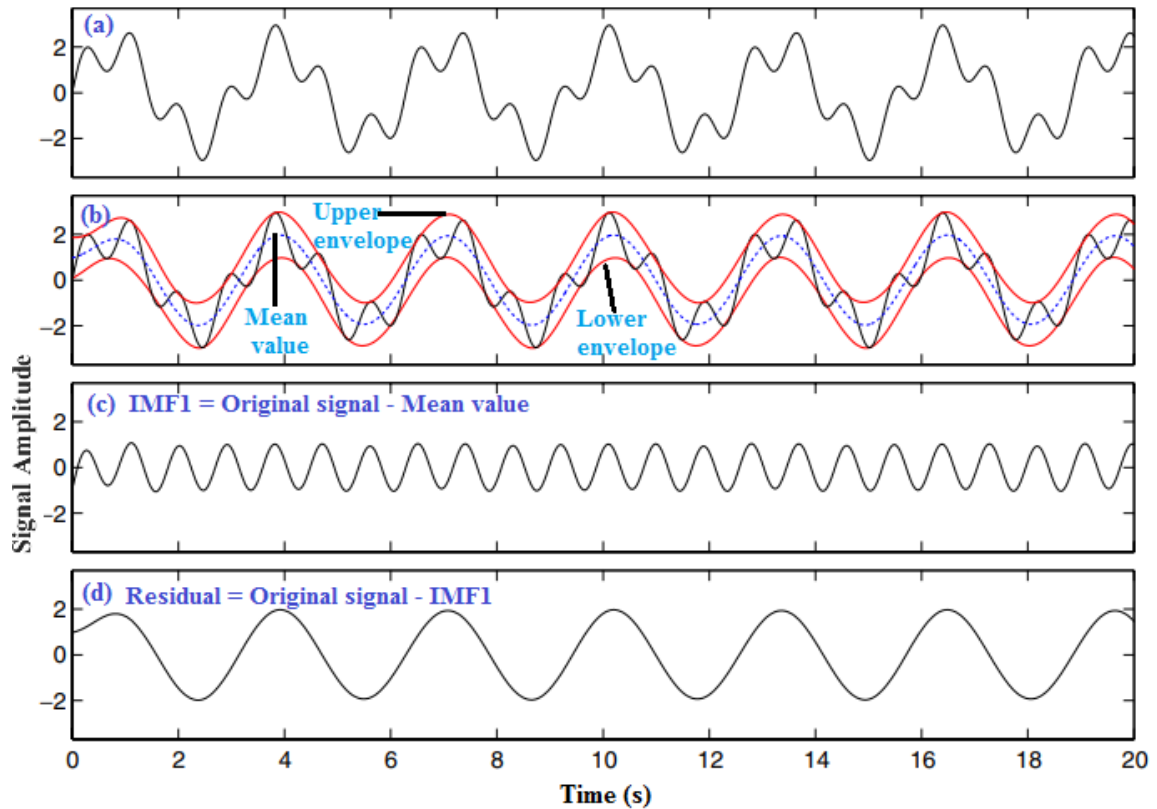


Figure 4-4 Illustration of the EMD method [157].

EMD has been employed to examine the signal behaviour for identifying the defects in rotating machine parts such as rolling bearings, gears, stators and rotors. Lin, et al., [158] extracted IMFs from the vibration signal in order to diagnose the condition of a driving shaft. Miao, et al., [159] utilized independent component analysis combined with EMD to diagnose bearing defects from acquired vibration data. The set of IMFs was chosen depending on the energy content of the frequency spectrum, followed by independent component analysis whereby the fault signatures of both inner and outer races were identified. Georgoulas, et al., [160] introduced a diagnostic approach by combining EMD and pattern recognition methods for the detection of broken-bar faults in an electric motor, where the complex IMF was converted into a discrete time series, then classification was achieved using hidden Markov models.

Sun et al. [59] investigated pump cavitation using the EMD-based Hilbert-Huang transform for analysing vibration and current data. The analysis showed that the unsteady flow responsible for the torque oscillations due to the cavitation process can contribute to variations in the energy of the vibration and current signals, and the RMS of the IMF was

capable of detecting and diagnosing the presence of the pump cavitation. Yunlong and Peng [161] utilised EMD for decomposing the vibration signals of a centrifugal pump in different states of health, and later a support vector machine (SVM) was employed to distinguish the different cases and diagnose the faults.

Ali et al. [162] have applied an automated fault diagnosis technique for bearings based on an artificial neural network (ANN) and EMD, where statistical parameters from the time domain were evaluated and successfully employed to train the ANN technique to classify bearing faults. The analysis results proved its reliability and effectiveness in categorising the bearing defects. Bin, et al., [163] proposed wavelet packet decomposition using EMD combined with an ANN; a set of feature frequencies were extracted from the vibration signal for detection of a crack in rotating machinery. The results show that the proposed method can effectively extract features for diagnosing the early fault of rotating machinery. Liu, et al., [164] applied EMD and Hilbert spectrum to analyse the vibration data for localised gearbox fault diagnosis and found that EMD algorithms have superior performance compared to the continuous WT for enhancing the transients induced by a gear tooth crack.

The EMD method is appropriate for diagnosing the condition of a machine where the faults impose amplitude modulation on the frequency signal from the rotating machine components[165].

With centrifugal pump operation, the modulation of the current signal becomes more noticeable as the flow rate increases. Also, the current signal is invariably contaminated by a variety of noise, and most of which will be generated by non-linear processes. As EMD has the advantage of being able to handle nonlinear and nonstationary signals, it allows the modulated signals to be decomposed into different simple intrinsic modes of oscillation, so that the characteristics of the signal could be revealed clearly and noise components are filtered. Thus, the EMD method is deemed suitable to be used in this research for decomposing the modulated current signals into mono-components that highlight the periodic components of interest-specific frequencies, and extract useful features for more accurate fault detection.

## 4.7 Intrinsic Time-Scale Decomposition (ITD)

Intrinsic Time-Scale Decomposition (ITD) is a new data-driven technique, self-adaptive, and capable of time-frequency analysis, developed by Frei and Osorio [16]. ITD decomposes a complex signal into “a sum of proper rotation components” (PRCs) and a residual or “baseline signature”. This technique was developed to analyse nonstationary and non-linear signals with more efficient decomposition and better high-frequency resolution.

Figure 4-5 shows the ITD operation for a time domain discrete signal  $x(t)$ . The baseline-extracting operator  $L$  separates out the baseline signal, whereby the instantaneous mean curve of the signal as denoted by  $LX_t$ , which is reduced to  $L_t$ . Note  $\tau_k$  is the time corresponding to the original signal.

The signal can be decomposed to  $X_t = L_r + H_r$ ; where, as shown on the figure,  $H_r = X_r - L_r$  and defines the proper rotation component [16, 166].

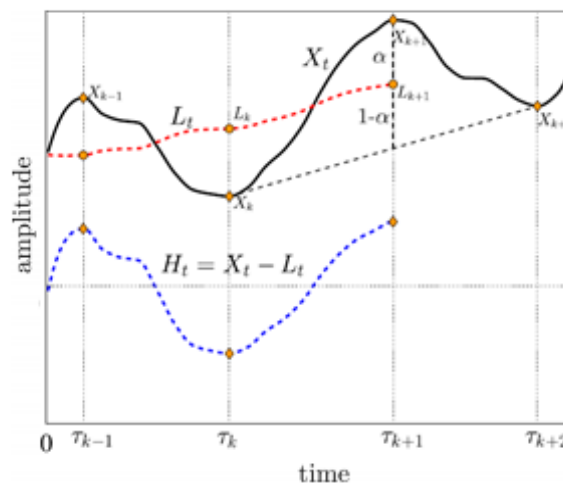


Figure 4-5 Illustration of standard ITD method, decomposing  $x(t)$  into  $L_t$  and  $H_t$  [167]

### 4.7.1 Intrinsic Time-Scale Decomposition Algorithm

Figure 4-6 shows the flow chart for the ITD algorithm, which is described below [168-170]:

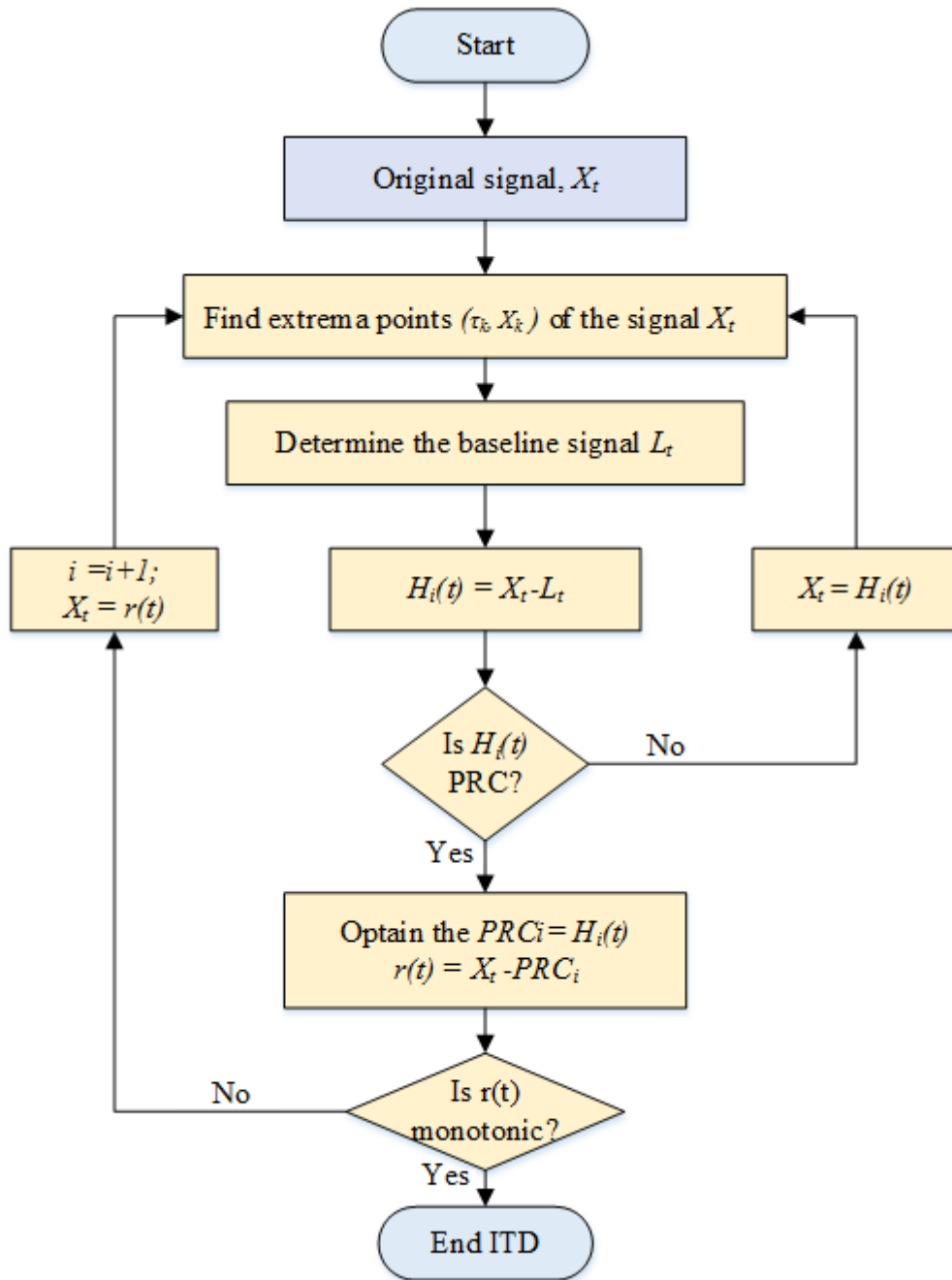


Figure 4-6 Flow chart of ITD algorithm

1. The process starts with calculating the extreme points  $(\tau_k, X_k)$  for the given signal  $X(t)$  that needs to be decomposed.  $X_t$  is the amplitude value of the untreated points, and  $k = 0, 1, 2, \dots$
2. The baseline signal is then obtained based on the extreme points, and the baseline signal is separated from the original signal with the help of baseline-extracting operators  $L_t$  and  $H_t$  determined over the time interval  $[0, \tau_k]$ , where the signal  $X_t$  exists

in the interval  $[0, \tau_{k+2}]$ . Then for the range of  $(\tau_k, \tau_{k+1}]$ , define the baseline-extracting operator  $L_t$  which is a piecewise linear function, realized from Equation (4-10):

$$LX_t = L_t = L_k + \left( \frac{L_{k+1} - L_k}{X_{k+1} - X_k} \right) (X_t - X_k), t \in (\tau_k, \tau_{k+1}] \quad (4-10)$$

where

$$L_{k+1} = \alpha \left[ X_k + \left( \frac{\tau_{k+1} - \tau_k}{\tau_{k+2} - \tau_k} \right) (X_{k+2} - X_k) \right] + (1 - \alpha) X_{k+1} \quad (4-11)$$

and  $0 < \alpha < 1$ . Usually  $\alpha$  is around 0.5.

3. Obtain the baseline signal  $L_t$  in order to maintain the monotonicity of  $X_t$  between the extrema points.
4. For extracting the PRC of the signal, the operator  $H_t$  determined as:

$$H_t = X_t - L_t \quad (4-12)$$

5. Then repeat the previous steps by adopting  $H_t$  as  $X_t$  until  $H_t$  is accepted as  $PRC_1(t)$ .
6. Compute the residual signal,  $r(t)$ , by subtracting  $PRC_1(t)$  from  $X(t)$ .

$$r(t) = X(t) - PRC_1(t) \quad (4-13)$$

Now treat the residual as the given signal.

7. Considering  $r(t)$  as  $X(t)$  the previous steps are repeated until the base signal becomes a monotonic function, or when the signal contains less than three extrema points, the decomposition end, and the set of PRCs with a residual will enable the original signal to be reconstructed as:

$$X_t = \sum_{i=1}^p PRC_i(t) + r_p \quad (4-14)$$

where the  $p$  is the number of the obtained PRCs.

ITD has the ability to overcome some of the limitations of wavelet transformations, where aspects of the signal characteristics may be lost. With WTs, it is hard to obtain a detailed description of the signal because WTs are based on the use of a predefined mother wavelet which is not self-adapting [171].

The ITD method can utilize more local characteristic information of the signal as the process of construct the baseline signal depends on the linear interpolation rather than cubic spline interpolation that used in EMD. Therefore, ITD has evident advantages in the end effects and envelope, thus, the PRC retain almost all extrema information of the original signal [172].

ITD has been used for processing non-linear signals for CM. Feng, et al., [168] have used ITD to decompose the vibration signals from a planetary gearbox into a set of mono-components for demodulation and further analysis. An, et al.,[173] applied ITD for fault diagnosis of wind turbine bearings using measured vibration signals. These researchers applied the ITD to extract the frequency centres of the first PRC as a fault features vector and applied the nearest neighbour algorithm to classify the operational condition of these bearings.

Aijun et al. [174] have diagnosed wind turbine gearbox faults by combining ensemble ITD, with WT to analyse vibration signals, and then adopting correlation to identify the working conditions and fault types. The vibration data were acquired from accelerometers placed on the drive shaft of the gear. Liu, et al., [175] applied ITD to analyse the vibration data from a diesel engine for fault diagnosis. A set of features was extracted from the time and frequency domains for the first several PRCs, and then a multistage relevant vector machine (RVM) model was constructed and employed to diagnose diesel engine faults. Jianbo and Haiqiang [172] applied a combined method based on the ITD and sparse coding shrinkage to extract a weak fault feature contaminated by background noise from bearing vibration signals.

Lin, et al., [176] introduced an approach for detecting rolling element bearing faults based on the ITD method. First, the spectral kurtosis was used to investigate the vibration data. Then ITD was used to decompose the filtered signal by kurtogram, and then envelope analysis was carried out to demodulate the decomposed signals and extract the characteristics of the fault.

Although ITD has been shown to be an effective way of processing vibration signals for machine fault detection and diagnosis, it is noted that very few studies have been carried out using ITD for monitoring pump condition.

There is no significant evidence has been found in the literature of the use of ITD for MCSA for such applications. This research will focus on detecting and diagnosing common centrifugal pump faults using ITD.

#### **4.8 Key Findings**

For assessing the machine condition different detection and diagnosis techniques can be applied to extract useful information, the simplest way from signal processing is time-domain analysis, that present the raw data as a function of time, also spectrum analysis is most widely used for analysing and assessing the acquired signals, it is limited when analysing the non-stationary and non-linear signals for fault diagnosis. As most of the machine faults typically generate non-stationary components in the signals, which contain critical information about machinery condition. Data-driven techniques such as EMD and ITD allow multiple-components of signal to be decomposed into different simple intrinsic components where the effective features can be extracted and used for detecting and diagnosing the faults.

## Chapter 5 **Machine Learning for Fault Detection and Diagnosis**

*This chapter presents a review of Machine Learning in the context of this research. It starts with an introduction to key machine learning algorithms and provides a comprehensive approach on how a supervised classification method can be constructed. The SVM algorithm is examined in more detail as it will be used as a tool in this study for classification and to differentiate different types of centrifugal pump faults. Finally, the chapter describes multi-class support vector machines.*

## 5.1 Introduction

Machine Learning (ML) can be defined as a group of computational techniques that focus on learning from past experiences to make a prediction for the future. The main goals of ML are (i) to construct an accurate model that can be used to make predictions for new data [177], and (ii) to design robust algorithms to achieve this prediction when dealing with large data set [178].

Various ML have methods emerged from the efforts of psychologists developing theories and models for animal and human learning. ML is capable of learning from experience, and analysis of acquired data, which gives it the ability to improve itself. Therefore, by using ML, the efficiency and effectiveness of systems can be improved [3]. ML has been utilized in numerous tasks including, for instance, regression, clustering and classification.

Classification is one of the best-known implementations of ML. It is a method for determining a class label for new input data, where the class label is designated as one of a known set of classes using a model based on ML algorithms [179]. In this study, the classification task is used to distinguish faults based on SVM algorithm.

## 5.2 Types of Machine Learning

In general, ML can be classified into three types: supervised learning, unsupervised learning, and semi-supervised learning [180]. A brief description of these types is provided below:

**Supervised learning:** The primary goal of supervised machine learning is constructing and training the model based on a labelled dataset. The labelled dataset comprises of input and output parameters. The model is used to predict or assign class labels to new data for which the class label is unknown [181]. The broad purpose of supervised learning is as a classification task, where acquired data will be classified in accordance with the training model, as shown in Figure 5-1.

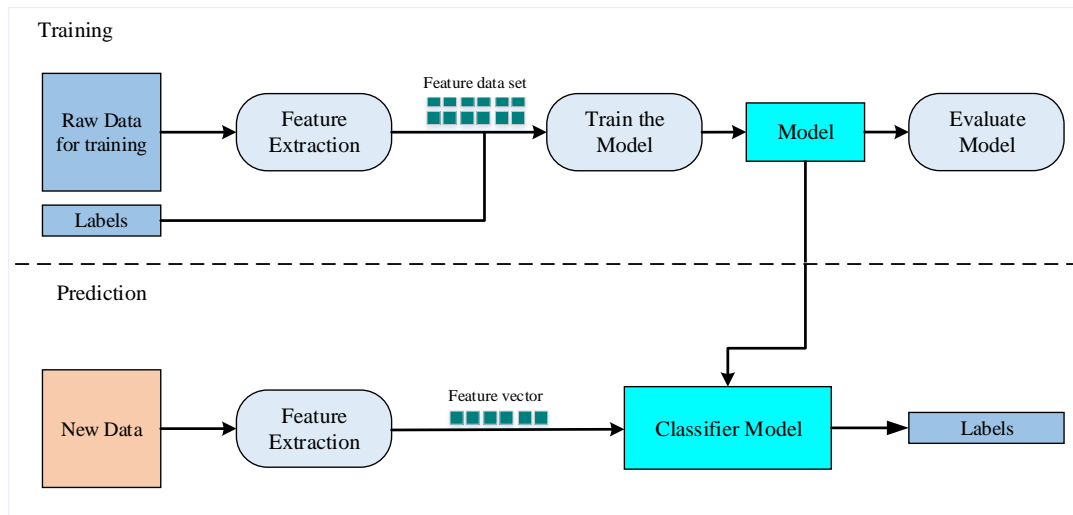


Figure 5-1 The supervised learning framework [182]

The above figure explains the basic framework of the supervised learning model, where the process has two main stages: training the model, and the prediction or classification task. In the first stage, the model is generated using a ML algorithm, such as a SVM. Representative features are extracted from the raw data and associated with known labels and used to teach and construct the model. It is worth noting that it is important to conduct an evaluation of the model before using it for classification. The second stage involves utilizing the generated model for classifying new input data where the target label is unknown. The features contained in the new data should be obtained in an identical way to the previous stage, then, the assignment of a label is achieved by applying the classifier model.

**Unsupervised learning:** This method deals with unlabelled data (i.e. unknown class label), where the model attempts to determine the distributing belonging to the data in order to find out more from it. Algorithms are usually utilized to discover the similarity of the instances based on maximum likelihood density estimation methods such as the clustering based on the k- means method [183].

**Semi-supervised learning:** This method is a particular form of ML, where extensive data is available, but only some data are labelled. In some problems, labelled instances are difficult, time-consuming, and expensive to acquire. To solve these problems and find and recognise the pattern for these data, semi-supervised learning can build a model that is

useful for large sets of combined unlabelled and labelled data. This method sits between supervised and unsupervised learning in terms of applicability [184].

Recently, several machine-learning algorithms have been utilized in the field of CM, such as decision trees, neural networks, naive Bayes, and so on. The main goal of intelligent diagnostic methods is to analyse the gathered data and automatically provide an accurate diagnosis. Such a process has become a new trend in the field of CM [185]. It used to help diagnose the condition of rotating machines, providing a more automatic and intelligent method in which the accuracy of the CM procedure will increase. In this context, many algorithms have been shown to yield effective results for fault detection and diagnosis.

The utilisation of ML for detecting and diagnosing the defects of pumps has become a more popular technique in comparison to conventional methods for signal processing, and a more attractive area for researchers, in particular where it can be merged with advanced data analysis techniques for enhancing the CM of rotating machines [3, 186].

However, the successful employment of ML methods for detecting and diagnostic machine faults depend on such factors as the characteristics of the acquired raw data, the quality of processed datasets, and the extraction of suitable diagnostic features. Specifically, it is critical to extract and select reliable and appropriate features to be used for training the classification model, features which can accurately describe the pattern of the current signal so that the output of the learning model will enhance the overall CM process.

### **5.3 Support Vector Machine**

The Support Vector Machine (SVM) is a machine-learning algorithm used for both classification and regression tasks. This method is founded on the theory of statistical learning and was introduced in 1995 by Cortes and Vapnik [187]. SVM defines an optimal separating hyperplane (decision boundary) that classifies data into separate classes. The principle of building the SVM model is mapping the data into a higher dimensional space and constructing an optimal separating hyperplane in this space. It is suitable for analysing a complex system and is a robust classification method capable of dealing with nonlinear data [188]. SVM demonstrates good performance for solving nonlinear and high dimension machine learning problems, and it has the ability to overcome the drawbacks

of the artificial neural network, such as the complex structure of ANN [189]. For classification tasks, a training SVM model is constructed based on known data or samples.

### 5.3.1 Theory of SVM

SVM is considered as binary for simple cases, where classification is determined by separating data into one of two categories. In Figure 5-2, there are two classes of training sample points. Many different hyperplanes can be constructed and used to separate the data;  $H$  is a classifier hyperplane and one of the separation planes. Moreover, there will be planes parallel to  $H$  that also pass through points close to  $H_1$  or  $H_2$ . The space between  $H_1$  and  $H_2$  is known as the margin. SVM attempts to find the best linear boundary between two different data sets and provide the maximum margin for separating the data.

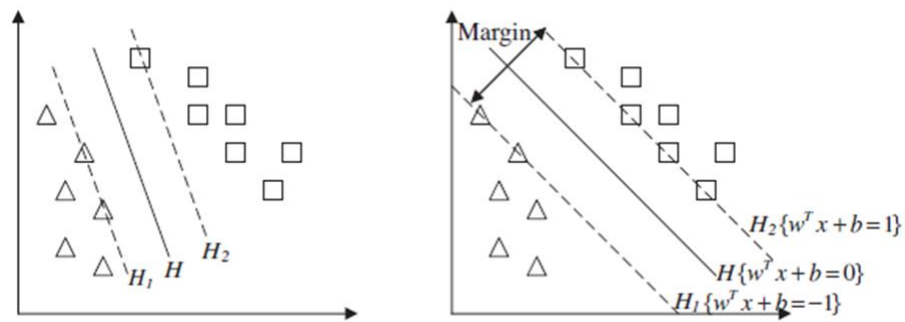


Figure 5-2 A hyperplane separating and classifying two classes (a) small margin and (b) large margin [190]

The theory of SVM is explained below [190, 191]:

Consider a training data set of feature vectors that need to be classified:

$$X = \{x_1, x_2, x_3, \dots, x_n\} \quad (5-1)$$

where  $x_i \in R^D$ , and  $n$  is the number of training data. For simplicity, the target is a binary classification, and  $Y$  is the set of class labels: -1 and 1:

$$Y = \{y_1, y_2, y_3, \dots, y_n\} \quad (5-2)$$

where  $y_n \in \{+1, -1\}$  and every vector in  $x$  is associated with only one value from  $Y$ .

The broad aim of SVM is to find the best hyperplane that will separate the training data, which can be expressed via the following equation:

$$(w^T \cdot x) + b = 0, \text{ where } w \in R^D, b \in R \quad (5-3)$$

where the vector  $w^T$  defines the weights,  $x$  is the input vector, and  $b$  is a constant. From this, the classifier can be expressed as:

$$\tilde{y} = f(x) = \text{sig}(w^T \cdot x + b) \quad (5-4)$$

In a real situation, the two classes can be separated by a margin with two hyperplanes (H1 and H2) as shown in Figure 5-2, The data points that lie closest to these hyperplanes are called support vectors, and a suitable set of support vectors will uniquely define the maximum margin between hyperplanes, giving the greatest separation between the planes to avoid misclassification. In addition, to avoid having data points fall into the margin, the data should satisfy the following constraints:

$$\begin{aligned} (w^T \cdot x) + b &\geq +1 \text{ when } y_i = +1 \\ (w^T \cdot x) + b &\leq -1 \text{ when } y_i = -1 \end{aligned} \quad (5-5)$$

Geometrically, the distance between  $H1$  and  $H2$  is  $\frac{2}{\|w^T\|}$ , and the target is to maximize the margin. To achieve this, the vector  $\|w^T\|$  needs to be minimized. In other words, the combination of the constraints can be expressed as follows:

$$\begin{aligned} \min \frac{2}{\|w^T\|} \\ y_i(w^T \cdot x_i) + b - 1 \geq 0 \quad \forall i \end{aligned} \quad (5-6)$$

In order to include a further elastic separating hyperplane for non-linear data, a slack variable is introduced, and the corresponding constraint optimisation problem must be minimized:

$$\min_{w,b,z} \frac{1}{2} \|w^T\|^2 + C \sum_{i=1}^N \zeta_i \quad (5-7)$$

From the previous formula, the constraints become:

$$y_i(w^T \cdot x_i) + b \geq 1 - \zeta_i \quad (5-8)$$

$$\text{and } \zeta_i \geq 0$$

where the training data  $x_i$  is mapped into a higher-dimensional space in order to separate it (which is easier than separating it in the original space),  $w$  is the weight vector,  $b$  is bias, and  $\zeta_i$  is the slack variable.

To control the flexibility of the resulting SVM, a smoothing parameter  $C$  is used [192]. Equation 5-8 is referred to as a classical optimization problem. By using Lagrange multipliers  $\alpha_i, i=1, \dots, N$ , and using the Kuhn-Tucker formula from optimization theory, the problem can be reduced to:

$$L(w, b, \alpha) = \frac{1}{2} \|w\|^2 - C \sum_{i=1}^N \alpha_i y_i (w^T \cdot x_i + b) + \sum_{i=1}^N \alpha_i \quad (5-9)$$

To resolve Equation (5-9) the derivation of  $b$  with respect to  $w$ , and the derivation of  $L$  with respect to all  $\alpha$  can be removed. Subsequently, the gradient of the Lagrangian equation will consider the following condition:

$$w = \sum_{i=1}^N \alpha_i y_i x_i, \quad \sum_{i=1}^N \alpha_i y_i = 0 \quad (5-10)$$

Coupling 5-9 and 5-10, together, a dual quadratic optimisation problem is obtained:

$$L(\alpha) = \sum_{i=1}^N \alpha_i - \frac{1}{2} \sum_{ij=1}^N \alpha_i \alpha_j y_i y_j x_i \cdot x_j \quad (5-11)$$

$$\text{Subject to } \alpha_i \geq 0, \quad \sum_{i=1}^N \alpha_i y_i = 0 \quad (5-12)$$

By solving the dual quadratic problem, a decision function is obtained:

$$f(x) = \text{sign} \left( \sum_{ij=1}^l \alpha_i y_j x_i \cdot x_j + b \right) \quad (5-13)$$

The features in the original input space are not normally separable. Thus an appropriate kernel function must be introduced into the decision function to separate the features in higher dimensions. The final decision function, according to the kernel function theory, can be expressed as:

$$f(x) = \text{sign} \left( \sum_{ij=1}^l \alpha_i y_j x_i \cdot x_j + b \right) \quad (5-14)$$

where  $\alpha$  donates a coefficient for every training data point, and all parameters are extracted from the optimisation process. Moreover,  $(x)$  is a new sample that needs to be labelled or classified. The most used kernels function in SVM are [193] the Linear, Polynomial and Radial Basis Kernel Functions.

SVM is a binary machine learning algorithm, originally designed to separate two classes but real-world problems usually involve cases of multi-class, and as such, the main target is to carry out a classification task for these problems. There are two techniques that are considered for solving and reducing multi-class classification problems, which can be described as [194]:

- 1- One-Against-All (OAA) classifiers: In this strategy, a set of classifiers is constructed based on the number of classes, where each classifier isolates one class from the combination of all remaining classes. Figure 5-3 illustrates the approach of the OAA multi-class SVM. To classify an unknown sample, the class that has the highest output value is adapted [195].

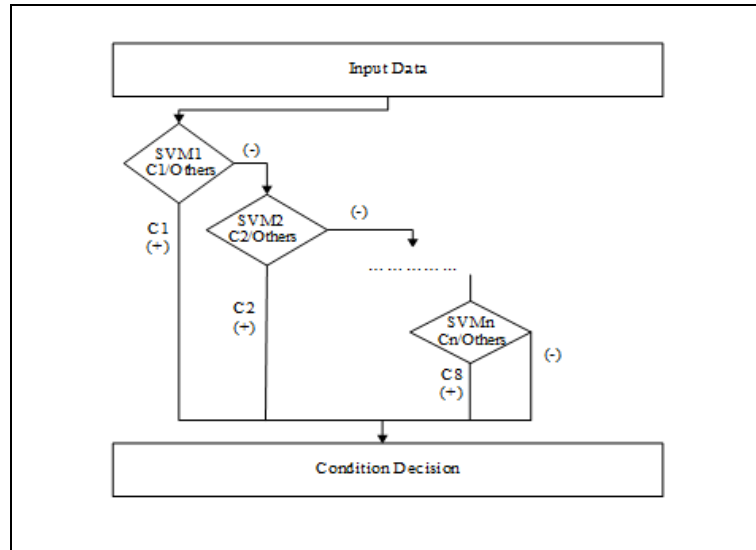


Figure 5-3 The One-Against-All approach of multi-class SVM [196].

- 2- One-Against-One (OAO) classifiers: In this strategy, all possible classifiers are built from the training data depending on the number of classes. If the problem has  $N$  classes, the number of desired classifiers will be  $\frac{N(N-1)}{2}$ . Commonly, in this technique, the number of classifiers is larger than the OAA technique. The flowchart of OAO is shown in Figure 5-4, where maximum voting is applied for classifying new data.

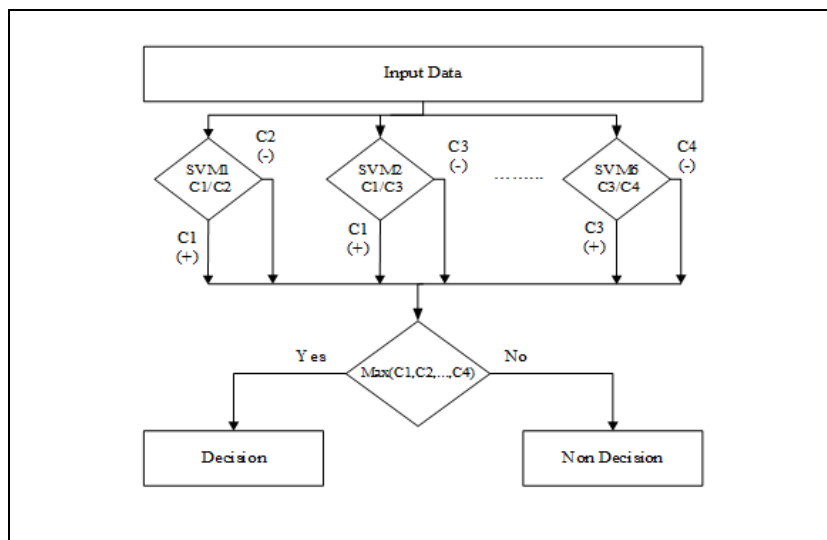


Figure 5-4 The One-Against-One approach of multi-class SVM [196].

For reducing the time for both training and testing the classifiers, and to overcome some of the drawbacks of the above strategies, an interesting modification and development

technique was introduced by Platt, et al., [197] which is an OAO-SVM based on the Directed Acyclic Graph (DAG) method.

Figure 5-5 depicts the structure of the multi-class SVM with a Directed Acyclic Graph approach and shows how it works with a three-class classification problem. The approach has one classifier for every node. Testing or classifying new data involves starting at the root node, where the pairwise decision is evaluated. The next move then depends on the output value, where either the left or the right classifier will be applied in each succeeding step until one of the leaf nodes is reached, which characterizes the class label of the given data.

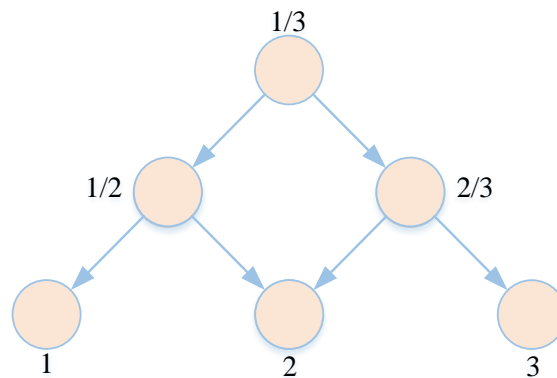


Figure 5-5 SVM with a Directed Acyclic Graph for a multi-classification problem [198].

SVM used for CM has demonstrated good performance regarding fault diagnosis and is very useful due to its generalisation ability compared with other methods such as ANNs. Moreover, SVMs can learn from small data sets, which means that a SVM is an appropriate method for practical cases where it is difficult to gather large data sets [188].

SVM is generally used for classifying the condition of a machine. In this context, selection of the kernel function is vital as it strongly affects the accuracy of the results. Furthermore, it is essential to obtain effective features to be utilised for constructing and training the SVM model. Therefore, SVM is utilized with advanced signal analysis techniques where meaningful features can be extracted to facilitate the distinction between different samples and enhance the overall CM task.

Muralidharan et al. [11] used SVM for fault diagnosis of mono-block centrifugal pumps, where they analysed the vibration signals for different pump conditions. These signals

were decomposed by a CW transform after which a number of transformation coefficient features were extracted from all wavelets, and the distinguishing conditions were classified by SVM. Qu [199] proposed a data processing algorithm for fault classification of the degree of wear of slurry pump impellers, where the acquired vibration data was processed using time and frequency domain features, selected on the basis of the sequential backward selection technique, and the classification was then determined based on SVM, The results indicated that the proposed method was capable of categorised different simulated faults in an effective way.

#### **5.4 Feature Extraction**

Generally, feature extraction takes place before classification, where the main purpose of extracting features is to map a set of measures that represent the original data set into a new space where some specific aspects of the data will be more important for classification decisions than others. Thus, the classification model can be simply constructed based on certain agreed and important features [3].

Statistical parameters have been widely used in CM as diagnostic features to assess a machine's condition, where the extracted features are used to represent the raw signal by minimizing the dimensions of the gathered datasets. The representative extracted features hold the most important data components which can be used to easily classify the health conditions of the machine. It is desirable to employ specific features for training and testing the classification model [200]. Extracting and selecting relevant and meaningful features from the acquired data is vital for obtaining an accurate classification model for CM.

In this research, statistical features are obtained from the current signal. These features are used for building the classification, as well as for detecting and diagnosing the faults of the pump. These features and their formulas are presented below [200] [201, 202]:

1. Root Mean Square (RMS): is the square root of the mean of the squared values of samples, see Section 1.2.1.
2. Kurtosis: determines the shape of the data or signal, whether flat or spiky, see Section 1.2.2.
3. The Crest factor: it is the ratio of the peak value to the RMS value, see Section 1.2.3.

4. Variance: is the average of the squares of the distance for each value from the mean. The formula for variance is given by:

$$X_{\text{var}} = \frac{\sum_{i=1}^n (x_i - \bar{x})^2}{n} \quad (5-15)$$

5. Entropy: can be used to describe the amount of information afforded by a signal [203], and can be computed by this equation by:

$$X_{\text{ent}} = \sum_{i=1}^n p(x_i) \log_2 [p(x_i)] \quad (5-16)$$

where  $p(x_i)$  is the probability for the  $i^{\text{th}}$  point of the signal.

6. Range: is the difference between the maximum and minimum signal point values.

## 5.5 Key Findings

Machine learning can find non-linear patterns from the acquired data, and these patterns can be used to a build model that can be utilised for classifying the health condition of rotating machines. The classification model can be constructed based on learning data and a machine learning algorithm, where the accuracy of such a model depends on both of them. SVM is a robust machine learning technique for settling nonlinear and high dimension data problems and has a good generalisation capability compared with ANNs. The application of ML to CM is influenced by the size of the data, and the feature extraction and selection. Thus, extracting and selecting relevant and meaningful feature using data-driven techniques will contribute to establishing a robust classifier, leading to accurate results for determining the condition of the centrifugal pump.

## Chapter 6 **Experimental Test Facility Setup and Fault Simulation**

*This chapter presents the test facilities utilized in this research. The test rig components are presented in details, which include the description and justification of measuring instrumentation. Then it describes how pump faults were simulated. Finally, the chapter describes the experimental procedure were used for obtaining the current signals from the tests of different faulty cases.*

## **6.1 Introduction**

To investigate the effectiveness of using the proposed method of MCSA analysis to detect and diagnose faults in a centrifugal pump, experimental work was carried out using existing test facilities. This system was used for different tests, collecting the sensor data generated by the centrifugal pump under healthy and faulty conditions, for different faults seeded into the pump, and a range of flow rates. These artificially induced faults included both bearing and impeller defects.

## **6.2 Test Rig Construction**

The test rig used in this study as shown in Figure 6-1, consisted of a centrifugal pump, closed-loop water piping system, and a number of monitoring sensors used to collect data under different load conditions and simulated faults. During the experiment, motor current, and pump pressure, speed, vibration and water flow rate were monitored, and relevant data acquired using the respective sensors.

The pump used in the experimental work was a single-stage Pedrollo Model F32/200 centrifugal pump, used to transfer clean water. The pump has a closed-impeller and was driven by a 4 kW three-phase induction motor. The speed of rotation was 2900 rpm. Figure 6-2 the pump used, and its specification is given in Table 6-1.

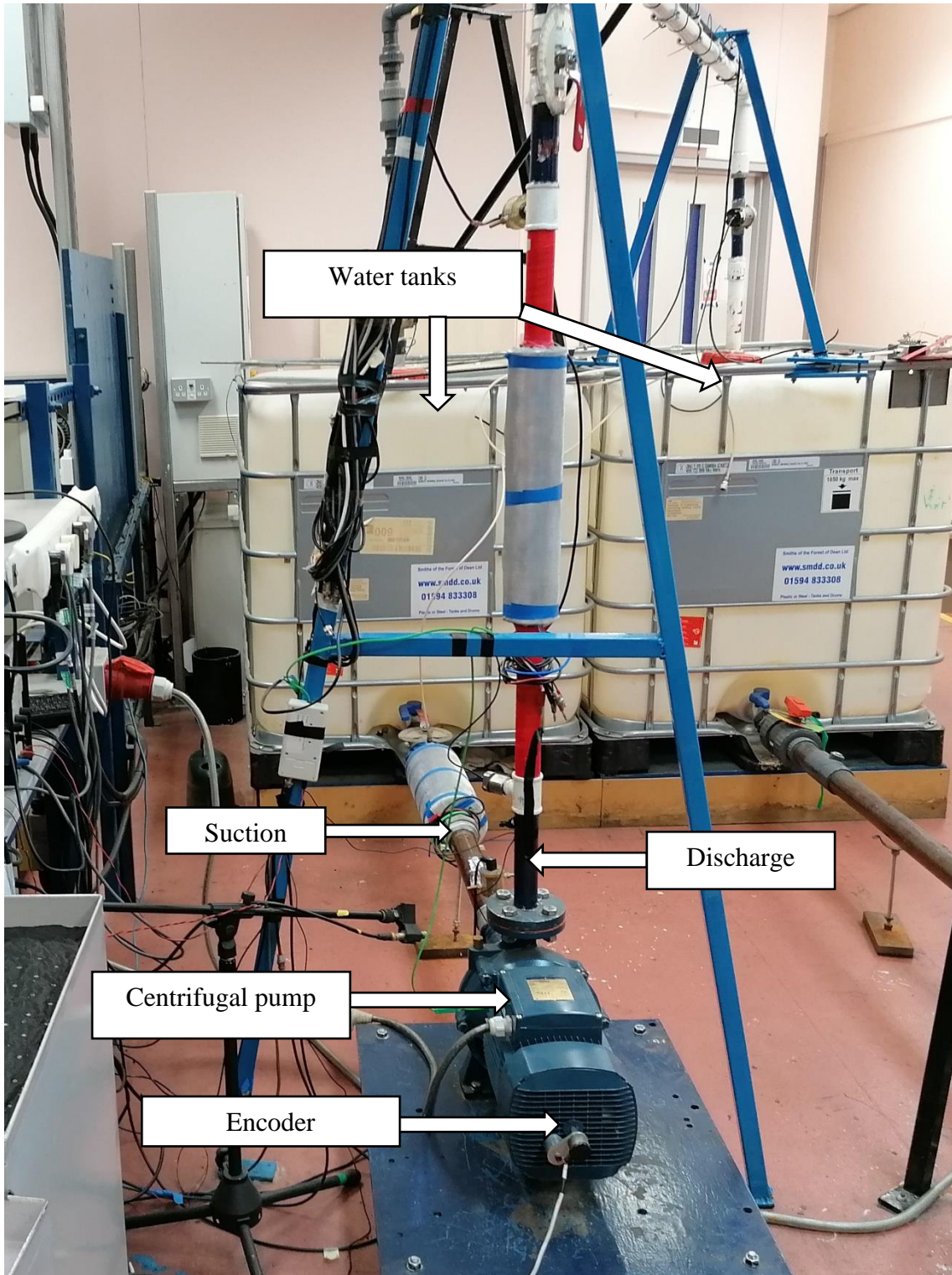


Figure 6-1 The test-rig facility

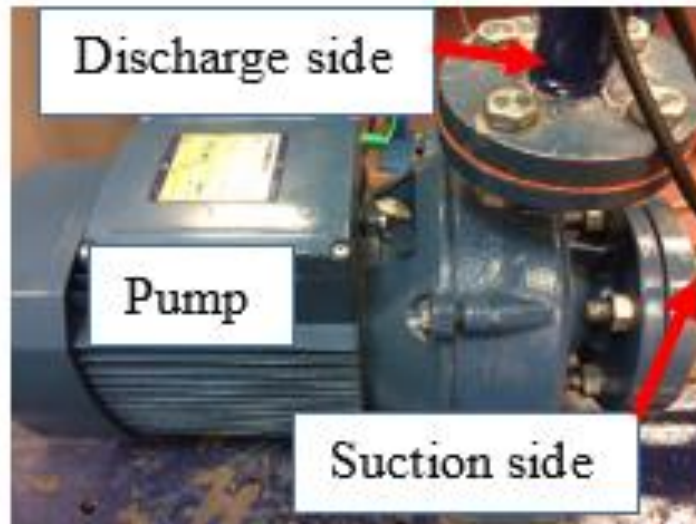


Figure 6-2 The centrifugal pump used in this work (Pedrollo Model F32/200)

Table 6-1 Specification of the centrifugal pump

Parameter	Specification
Capacity	0-19.2 (m <sup>3</sup> /h) 0-320 (l/min)
Head	44— 57(m)
Speed	2900 (rpm)
Maximum Pressure	10 (bar)
Impeller Type	Closed impeller
Number of Stages	Single
Power	4 KW
Frequency	50 Hz
Rated Current	8.9 A
Rated Voltage	400 v
Connection	Closed

### 6.3 Test Rig Facility

To achieve the main objective of this study, a test facility is required for gathering data and evaluating various data analysis techniques. There is such test rig available in the

Centre for Efficiency and Performance Engineering at Huddersfield University. However, it has limited capability to simulate different faults. So it has improved, consequently, different faults including bearing faults, and impeller fault can be simulated to meet the focuses of this research. Moreover, the test rig is able to provide experiments under different flow rates for collecting the necessary data to examine the ability of MCSA on the detection and diagnosis of common pump faults.

In addition, the study also developed a test scheme to operate the test rig to acquire data sets under the baseline and various faults. In particular, up to seven discrete flow rates settings were operated for data acquisition, allowing direct comparison of the results for efficient studies.

The test rig is shown in Figure 6-1, and Figure 6-3 was used to carry out the experiments to examine the response of the centrifugal pump to different operating conditions. The basic structure was in place: water tanks, pipes carrying the water flows, throttle valves, and the flow meters. Also, in place was a speed controller, the selected transducers were properly placed, connected correctly, and the system was able to provide the necessary data. Figure 6-3 shows a schematic diagram of the system, the sensors, and their locations.

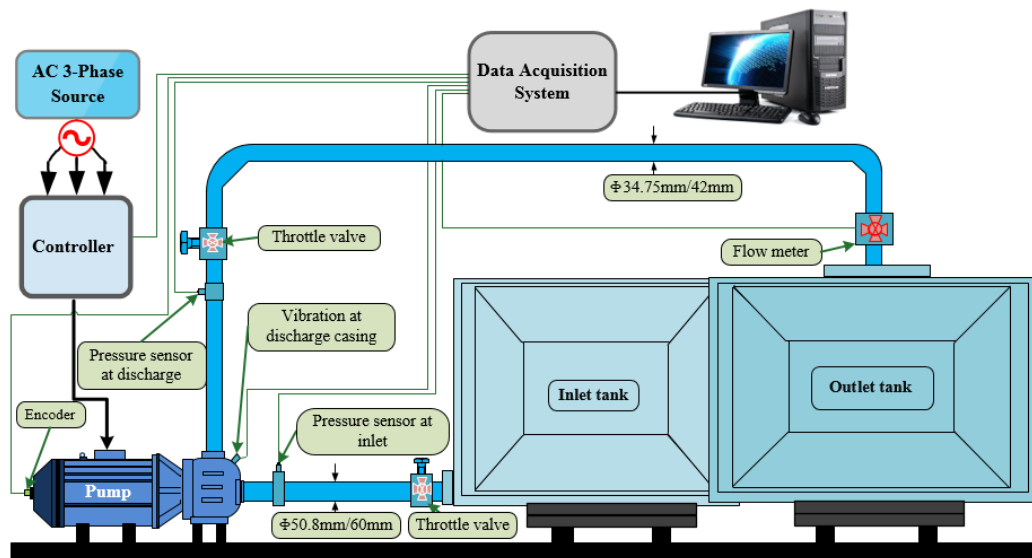


Figure 6-3 A schematic diagram of the test facility.

## 6.4 Instrumentations

This section describes the parameters monitoring and recorded, as well as the measurement transducers. All the measuring devices were connected to the data acquisition system.

### 6.4.1 Power Supply Analyser (Electrical Power Measurement)

The motor current was measured using a mounted Hall-effect Current Transducer (HCT). This transducer can determine the circuit current while not being physically part of the circuit. The transducer generates a voltage output, proportional to the amplitude of the current; knowing the supply voltage, it is possible to also determine electrical power. The HTC was used to measure the three phases of the current separately. Each line was connected into the Data acquisition system (DAQ).

Figure 6-4 shows the HTC unit, Table 6-2 lists the specifications for this unit and. Figure 6-5 shows the typical output current signal.

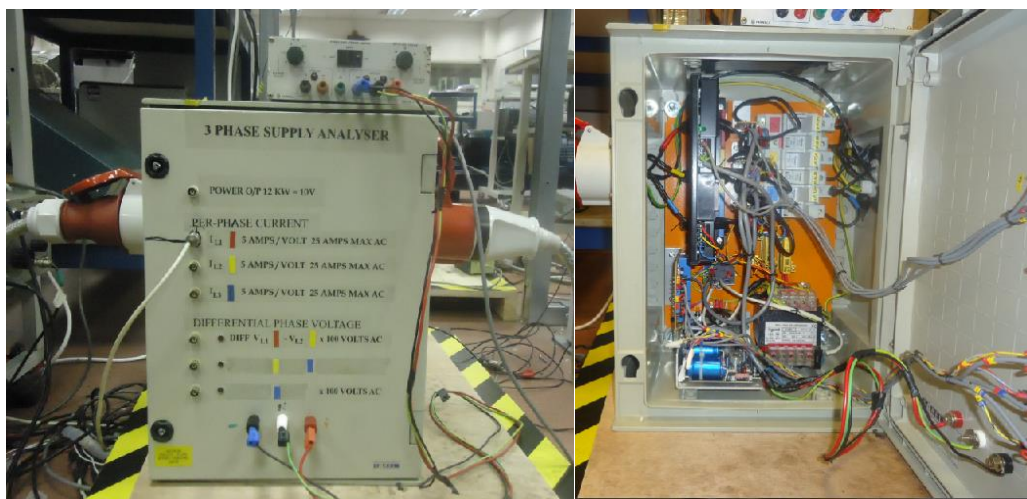


Figure 6-4 The current measurement unit

Table 6-2 Specification of the three-phase HTC unit

Classification	Specification
Phase current	Max. voltage reading: 12.8V at 5A/Volt
Line to Line voltage	Max. voltage reading: 12.8V at 100V/Volt
Total power	Max. power reading 10 VDC at 2kw/Volt

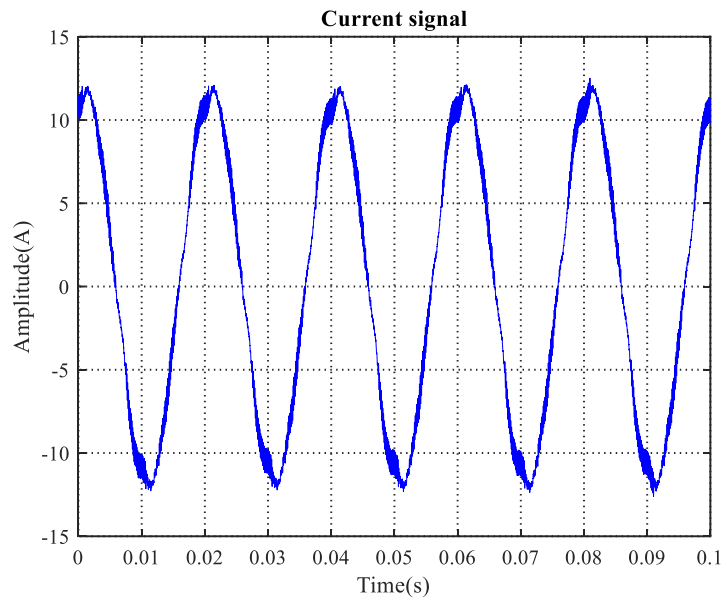


Figure 6-5 The output of the HTC

#### 6.4.2 Flow-Rate Transducer

In order to measure the water flow rate through the pipeline, a GEMS RFO electrical flow rate sensor was chosen as this could easily cope with the calculated pump volumes and pressures in the experimental system. The sensor contains a tubular rotor with six vanes. The movement of the fluid within the device unit generates a series of magnetic fields, producing a sequence of voltage pulses, the rate of which is proportional to the flow rate. The sensor was connected to the DAS, where the flow rate signals were monitored and acquired. Figure 6-6 shows the flow meter and how it works, and Figure 6-7 shows the electronic flow sensor installed on the pump system.

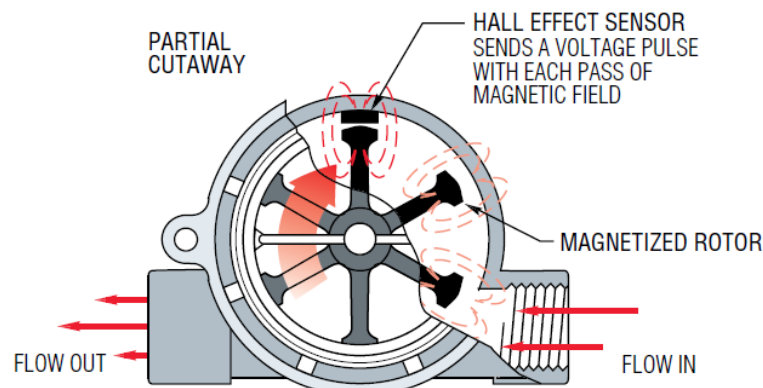


Figure 6-6 Schematic of GEMS RFO electronic flow sensor



Figure 6-7 Electronic flow sensor in the pipeline

The GEMS RFO has the capability of measuring the flow rate of up to 400 l/min with a frequency range of 15 Hz for low flow rates, and up to 225 Hz for the highest flow rate. The output signals of this sensor are presented in Figure 6-8, while the specifications for the flow sensor are given in Table 6-3.

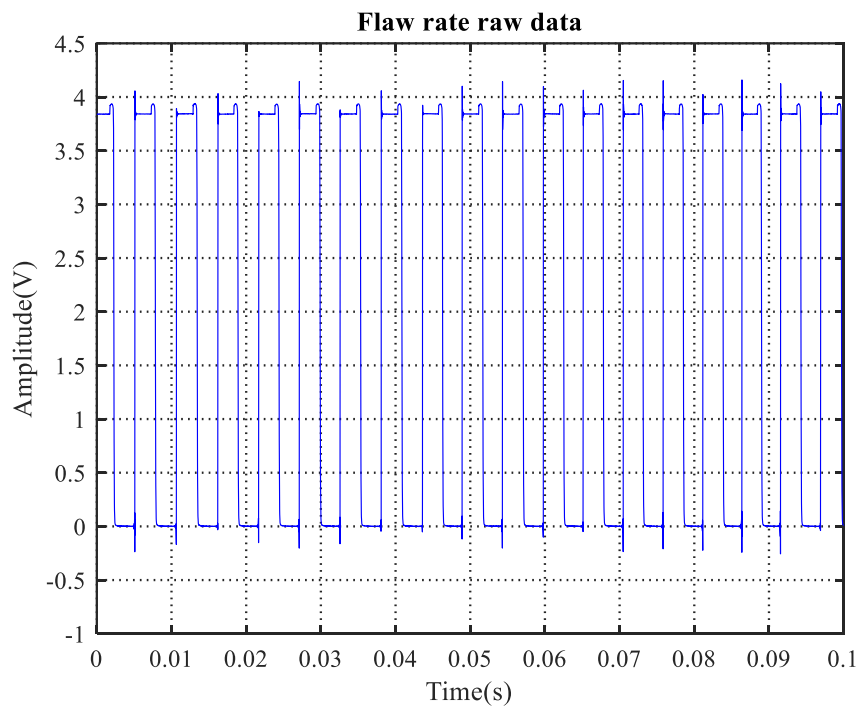


Figure 6-8 Raw data from the GEMS RFO flow rate sensor

Table 6-3 Specifications of GEMS RFO flow rate sensor

Manufacturer	Gems
Type	Rotor flow RFO
Operating pressure, maximum	6.7 bar at 21°C, 2.8 bar max at 80°C
Operating temperature	-29 C to 82°C
Electronics (both bodies)	65°C Ambient
Max. viscosity	45 cSt
Input power	4.5 to 24 Vdc
Current consumption	8mA, no load
Output signal	4.5 to 24 Vdc pulse.
Max. current source output	70 mA
Frequency output range	15 Hz (low flow) to 225 Hz (high flow)

### 6.4.3 Pressure Transducers

Two pressure transducers for measuring the pressure of the pump were fitted in the pumping system, one at the suction pipe inlet to the pump and the other at the discharge pipe of the pump, see Figure 6-9 The sensors used for this experiment were Sinocera CY-YB-025 electromechanical strain gauge transducers. The efficiency of the pump under different operating conditions can be obtained by measuring the pressure over the hydraulic resistor. The essential operation of this transducer is based on the strain gauge principle. Any changes in the fluid pressure will lead to a proportional change to the sensor parameter, which is converted into an electric signal by using a suitable transducer. Then this signal can be analysed for pump condition monitoring. These sensors can measure pressures up to 10-bar gauge. Additional specifications for the transducers are provided in Table 6-4.



Figure 6-9 Pressure transducers installed at the pump inlet and outlet

Table 6-4 Specifications of the pressure transducer

Manufacturer	Sinocera
Product	Strain gauge pressure transducer
Type	CY-YB-025
Measurement range	Suction: 0-0.5mpa Discharge: 0-1mpa
Operating Voltage	12 Vdc
Output Mode	0-5± 0.2 Vdc
Static precision	< 0.3%Fs
Screw joint	1/ 4- NPT external
Operating temperature range	-10°C To 50°

#### 6.4.4 Speed Controller

For this test rig system, an Omron speed controller was used to control the pump speed. Figure 6-10 shows the speed control unit and Table 6-5 device specifications.

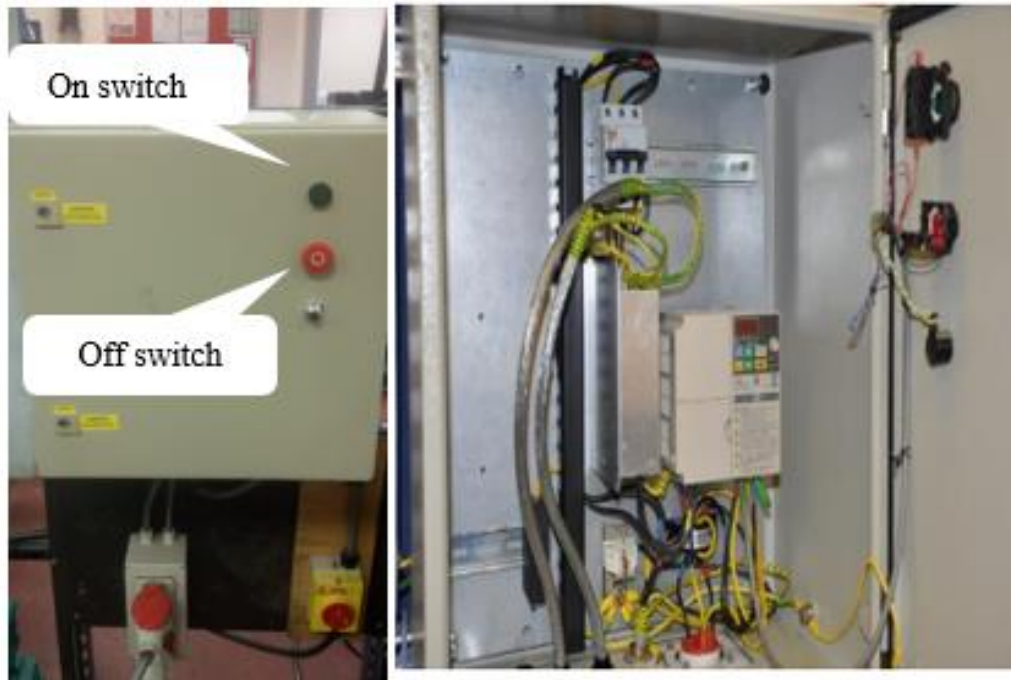


Figure 6-10 Omron speed controller, external and internal views

Table 6-5 Speed controller specifications

Manufacturer	Omron
Model	3G3MV
Allowable voltage fluctuation	$\pm 15\%$ to $10\%$
Allowable frequency fluctuation	$n \pm 5\%$
Power supply	380 to 460 V AC at 50/60 Hz
Max output frequency	400 Hz
Frequency control range	0.1 to 400 Hz
Output frequency resolution	0.01 Hz
Control method	Sine wave PWM
Ambient temperatures	Operating $\pm 10$ to $60^\circ\text{C}$

### 6.4.5 Shaft Encoder

A Hengstler Model: RS-32-0/100ER incremental optical encoder was used to measure instantaneous angular speed (IAS) by which to calibrate the current signal, which could then be analysed to determine the average speed of the pump. Figure 6-11 shows the incremental optical shaft encoder as it was connected to the end face of the pump shaft.



Figure 6-11 Mounted Hengstler shaft encoder

The encoder generates 360 pulses per revolution. The output of the encoder was connected directly to the computer for the propose of recording the speed of the pump. Figure 6-12 shows the online output data acquired from the shaft encoder, and Table 6-6 presents the specifications of the shaft encoder used on the test-rig.

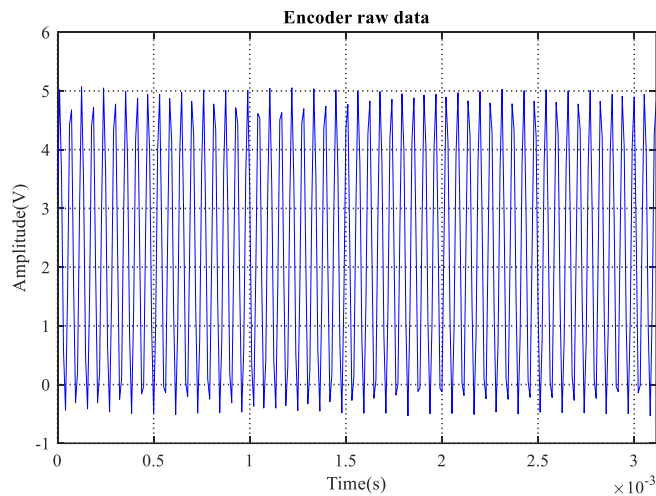


Figure 6-12 Raw data of Shaft encoder

Table 6-6 Specifications of the shaft encoder

Manufacturer	Hengstler
Type	RI 32
Mounting	Round flange
Shaft diameter	5 mm, 6 mm
Output voltage	High 2.5Vdc, Low 0.5 Vdc
Maximum speed	6,000 rpm
Operating temperature	-10 ... +60 °C
Power consumption	5V/40 mA
Shock resistance (IEC 68-2-27)	1000 m/s <sup>2</sup> (6 ms)
Max pulses per rotation	360

#### 6.4.6 Vibration Measurement (Accelerometer)

As shown in Figure 6-13 t a Sinocera YD3-8131 piezoelectric accelerometer to measure vibration data was positioned on the pump casing at the pump cutwater, the location of the smallest clearance between the pump casing and impeller. The accelerometer was used to confirm the characteristics of the pump bearing. It was mounted horizontally, that should acquire the most suitable vibration signal [204].



Figure 6-13 Vibration transducer mounted on the pump

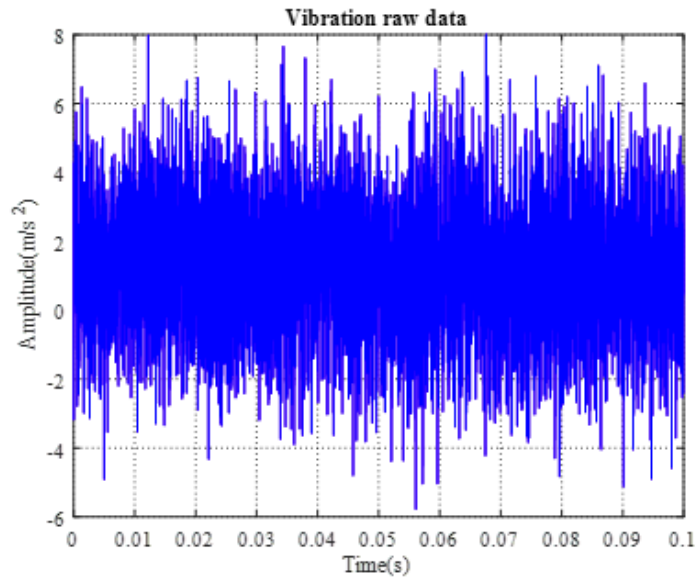


Figure 6-14 Output signal of the accelerometer

The accelerometer was used to measure vibration generated in the pump to provide data to confirm the presence of the mechanical faults seeded into the pump, and to determine the presence of expected fault frequencies corresponding to known bearing defects. The given accelerometer has a frequency range of 10 Hz- 10 kHz, and an upper limit to the acceleration range of  $2000 \text{ ms}^{-2}$ . The specifications for the accelerometer are given Table 6-7.

Table 6-7 Specifications of the accelerometer

Manufacturer	Sinocera
Type	Accelerometer (piezoelectric)
Model	YD38180
Frequency range	10 Hz – 10 KHz
Sensitivity	$1.56 \text{ mv/m.s}^{-2}$
Range accretion	$<2000 \text{ ms}^2$
Temperature Range	To $250^{\circ}\text{c}$

## 6.5 Data Acquisition System

For acquiring data from the test rig, a data acquisition system (DAS) consisting of both hardware and software was required. The DAS system was used to convert the analogue signals acquired from the transducers to digital form for processing and monitoring using specific software. A Sinocera YE6232B multi-channel was used for acquiring the experimental data, see Figure 6-15, and the DAS specifications are shown in Table 6-8.

The DAS system was a 16 channel Global Sensor Technology YE6232B powered by YE7600 software where the vibration levels and current signals could be monitored and analysed in real-time. In this experimental work, the sampling frequency was 96 000 Hz.

The software provided a good graphical interface and allowed the user to easily change several parameters such as data points, sampling time and the sampling frequency.



Figure 6-15 YE6232B Data Acquisition System (DAS)

Table 6-8 Technical specification of the data acquisition

DAQ system manufacturer	Global Sensor Technology YE6232B
Company: SINOCERA	Piezotronics, INC. Version 1.2
Number of Channels	16 (selectable)
A/D Conversion resolution	24 bit
Sampling rate (maximum)	96kHz per channel, Parallel sampling
Maximum sampling	1.5 MHz
Input range	$\pm 10$ V
Internal acquisition card	USB 2.0
Software	YE6232B Analysis Software

### 6.6 Centrifugal Pump Performance

For achieving the best efficiency of pump operation, it is desirable to operate a pump at the best efficiency point, as determined by the characteristics of the pump. Figure 6-16 shows the performance curves of the pump used in these experiments. It represents the relationship between the head, NPSHr and NEPSHa, where the curves represent the equations in Section 3.5.1. The parameters were obtained from the specification of the pump presented in Appendix A. The best operating point is the point where the head required crosses the net positive suction head available.

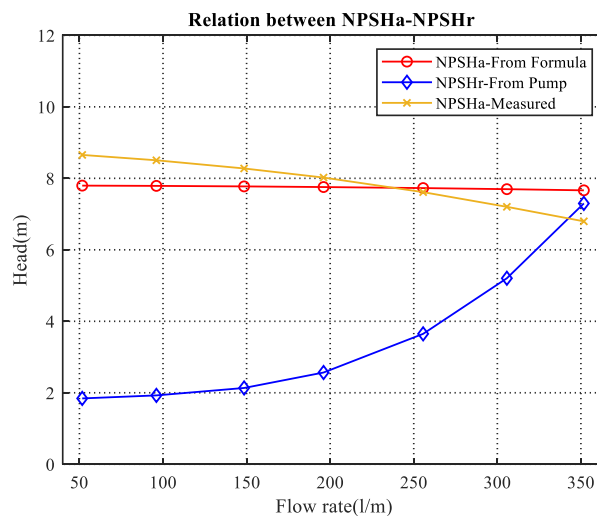


Figure 6-16 The performance of the centrifugal pump

## 6.7 Fault Simulation

### 6.7.1 Bearing Defect

For studying and examining the condition of centrifugal bearing, a small-localised defect is required. This can be achieved by using two techniques. The first one is to fabricate a defect intentionally, then measure and examine the effect of this fault on the operating condition, and compare it with the healthy condition. The other technique is run-to-failure, until the defect occurs and then develops naturally, and to detect this event using some monitoring system. The latter method is both expensive and time-consuming, and so the former method was adopted in this research.

The experimental procedure was carried out using the ball bearing mounts on the pump shaft. The pump bearing type was FAG type 6307, and its parameters are presented in Table 6-9. Three of these bearings were used in the study. First was a healthy bearing, and the other two had localized bearing faults introduced.

Table 6-9 Characteristics of the bearing

Parameters	Measurements
Number of balls	8
Ball Diameter	13.49 mm
Pitch Diameter	58.42 mm
Contact Angle	0°

The seeded local faults were introduced by HB Bearings Ltd. By referring to studies in literature, the size of local faults was agreed to introduce to consistent with abrasive wear marks on both the inner race and outer races. Such faults are a relatively common occurrence and are normally caused by skidding friction between the balls and the raceway surfaces due to the lack of lubricant and contaminated micro debris along with load variations. Again after taking advice from production engineers at HB Bearings Ltd, the defects were set to be “scratches” of 7 mm length and 0.5 mm width in both inner race and outer race. The final shape was decided after discussion with the company, and while it had to represent wear that would occur in the industry, it also had to be made in the laboratory in a way that could be easily reproduced. A simple transverse scratch was

finally decided on, as shown in Figure 6-17. The dimensions of the scratch were estimates made of what could represent a real, in situ, fault.

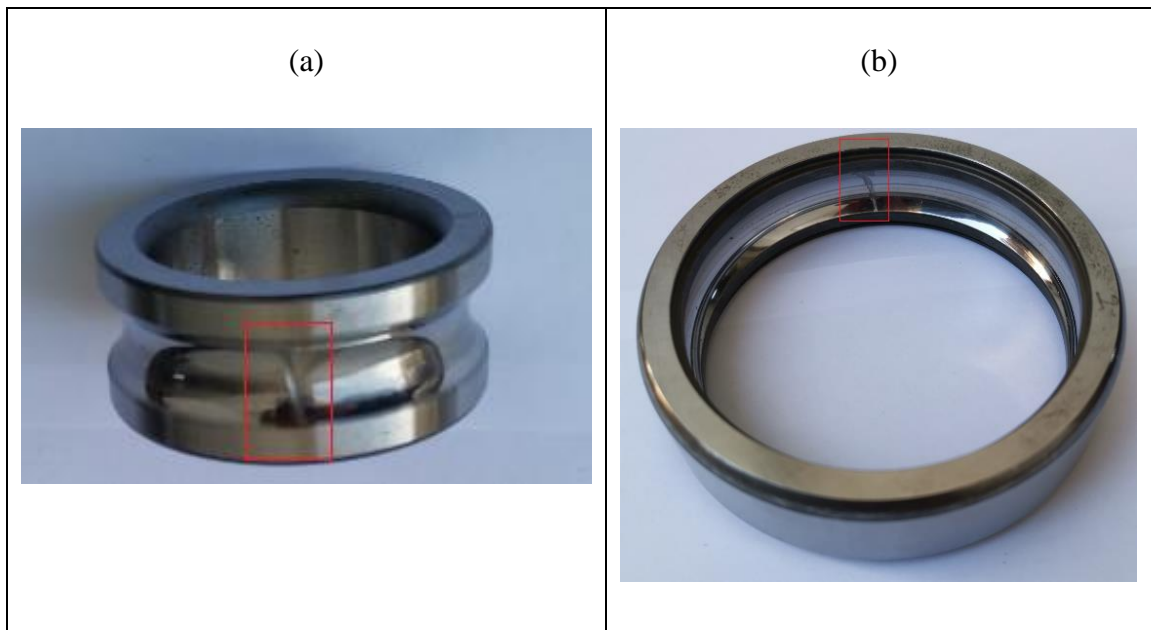


Figure 6-17 (a) Inner race defect (b) Outer race defect

Figure 6-18 shows the relation between the pump head and corresponding flow for the healthy pump, pump with inner race fault, and outer race fault. There is no significant change in pump performance with bearing defects compared to the healthy condition.

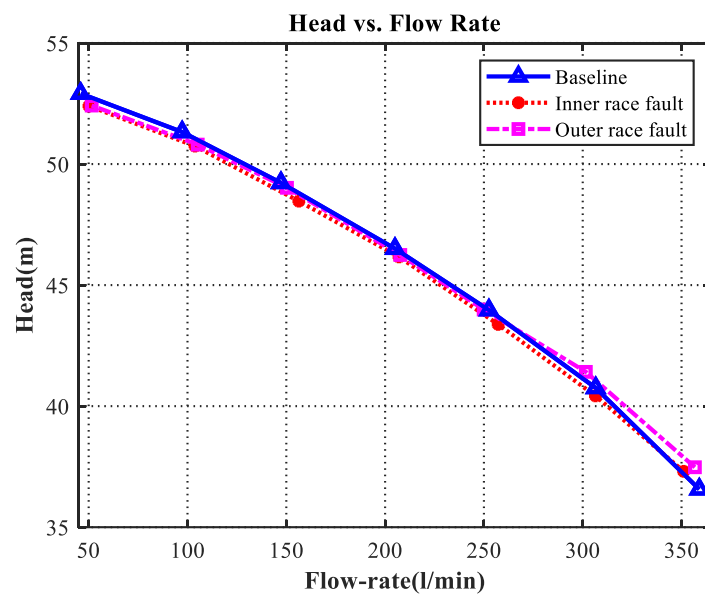


Figure 6-18 Pump head vs Flow rate for (i) healthy pump (baseline), (ii) pump with inner race fault and (iii) pump with outer race fault

### 6.7.2 Impeller Defect

The core of the centrifugal pump is the impeller. Defects can occur on the impeller throughout its lifecycle, which will affect the efficiency of the pump. In this research, a closed impeller type 166GRF3228H was used. The impeller blockage was artificially induced into the inlet vane of the impeller by blocking one of the vanes using a solid material as shown in Figure 6-19

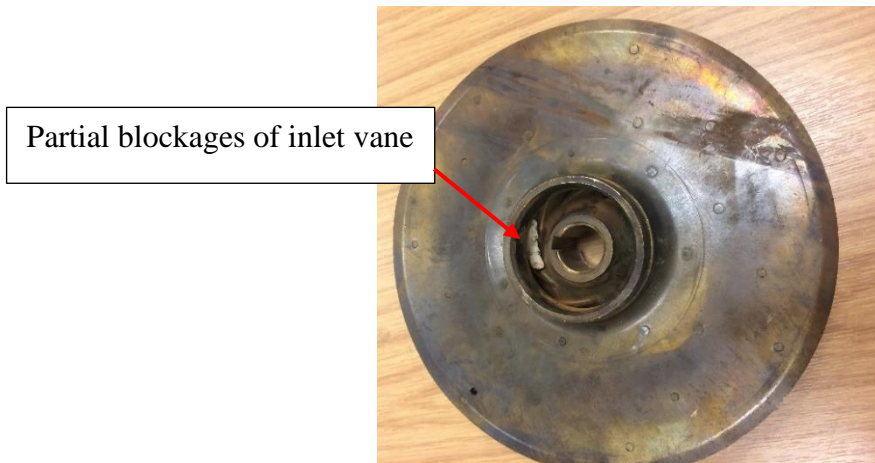


Figure 6-19 Blockage impeller

Next figure presents the head curves for healthy condition (baseline) and combined fault (outer race bearing fault and impeller blockage).

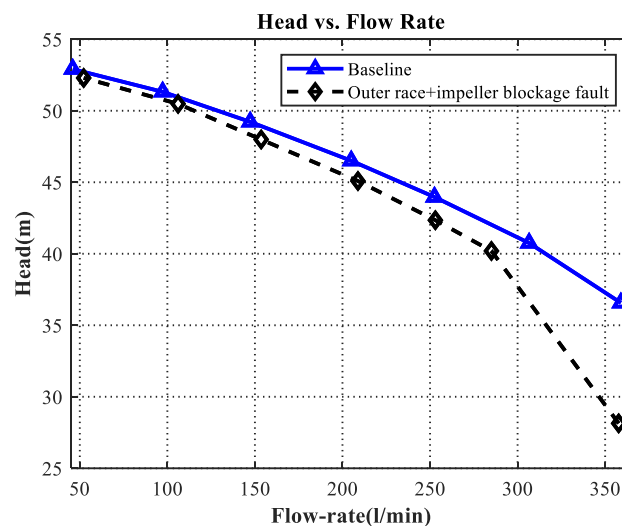


Figure 6-20 Pump head vs Flow rate for (i) healthy pump (baseline), and (ii) pump with outer race fault and impeller blockage

Figure 6-20 shows that the combined defect produces a significant reduction in pump performance compared by the healthy condition. This is what would be expected, as the blockage impacts directly on the flow.

## **6.8 Experimental Procedure**

In this study, various flow rates were investigated to simulate different conditions. The normal condition (baseline/healthy) of the pump and three types of common faults were investigated: the inner race bearing fault alone, the outer race bearing fault alone, and the combined outer race bearing fault with impeller blockage.

For the experiment to be carried out under steady-state conditions, the pump was turned on for half an hour before starting to collect data. Then the data were recorded for different flow rates for durations of 40 seconds. The signals recorded were; motor current and voltage, pump vibration and speed, pressure at inlet to pump and water flow rate. To assess the influence of the faults on the performance of the pump, the signals were measured under different flow rates, which were adjusted manually step by step using the throttling valve in the discharge line. The flow rates were set to be 50, 100, 150 200, 250, 300 and 350 l/min. However, when set the flow rate, the accuracy was less than  $\pm 5$  l/ min, after which the flow was constant.

The experimental procedures for the different tests can be summarised as follows:

- All tests were carried out at a fixed pump speed of 2900 rpm.
- The DAS recorded the current signals from the current transducer, as described in Section 6.4.1.
- The DAS was linked to the computer for online monitoring of the system.
- The pumping system was operated for half an hour before recording the data in order to achieve steady-state conditions for pump operation.
- The test procedure was carried out in the following order: (a) healthy pump (b) bearing with inner race fault (c) bearing with outer race fault (d) a combined fault (outer race fault + blocked impeller ).
- To ensure the accuracy of the acquired data, each test was repeated three times under the same conditions.

- All data sets were recorded for a period of 40 seconds to provide sufficient data samples for understanding the characteristics of motor current for enhancing the diagnostic techniques.
- The obtained current signals were processed and analysed by a MATLAB program written by the author.

## **6.9 Key Findings**

This chapter presents the developed test rig in detail, all the equipment used for simulating and monitoring the centrifugal pump healthy and under different faults are described, including all electrical and mechanical parts. The chapter also presented the specifications of the instruments and transducers. Finally, the fault simulations and test procedures have been explained.

## **Chapter 7 Detection and Diagnosis of Centrifugal Pump Faults using Conventional Current Signal Analysis Technique**

*This chapter evaluates the performances of conventional MCSA regarding fault detection under different pump flow rates. The gathered data were analysed in both the time domain and frequency domain. The healthy condition of the centrifugal pump was adopted as the baseline condition. Also, a comprehensive comparison with the other defect data sets has been made. The results showed that the motor current signatures can provide a solid basis for identifying the given pump faults.*

## **7.1 Introduction**

The current signals were gathered under four pump conditions: healthy pump, inner race fault, outer race fault, and combined fault (impeller blockage and outer race bearing fault). All four conditions were investigated under different flow rates: 50, 100, 150, 200, 250, 300, and 350 l/m. All experiments were conducted at pump speed 2900 rpm, with a sampling rate of 96 kHz, see Section 6.7 for more details.

## **7.2 Time Domain Analysis (waveform)**

It is the primary method for describing the collection data such as electrical signal and, as a function of time. Generally, time domain analysis looks at data over a period of time.

Figure 7-1 shows electrical current waveforms recorded for the centrifugal pump for different flow rates, for the healthy and three faulty conditions described. The current signal for a baseline, healthy pump is presented as a blue line, and the three induced faults are shown as: inner race - red line, outer race - pink line, and combined faults of outer race and impeller blockage - black line. Here the flow rates were 350, 300, and 250 l/min.

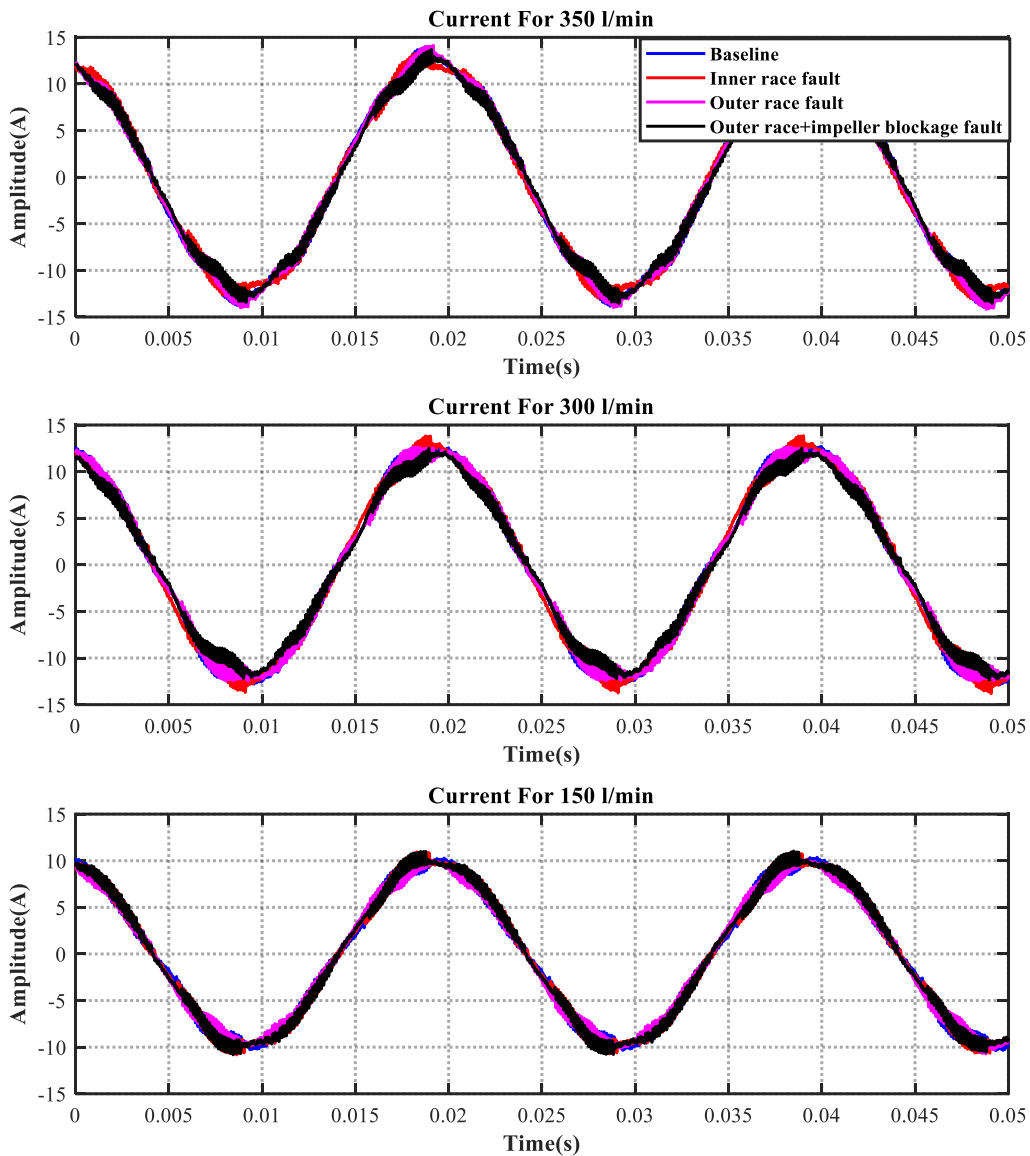


Figure 7-1 Time-domain waveforms for baseline, inner race, outer race and combined fault (outer race and impeller blockage) under different flow rates

From Figure 7-1, the amplitude of the current signal increases with the increase in the flow rate, though this is not easily discernible as the signals have an amplitude modulation, especially at low flow rates. At this stage of analysis of the current data, it is hard to detect changes in the current signatures between the different fault cases, as the amplitude of the current signals is nearly the same for all the cases at a given flow rate. However, a small change was noticed between the combined fault and baseline condition.

From the time waveform representation, it is difficult to detect the seeded faults, as the variation in the waveform is small, and the pump current signal is non-stationary. The time domain trends are usually obtained from well-known parameters, such as RMS which is used to provide an overview of the behaviour of the system. RMS is usually used to detect the presence of a defect in the pump without necessarily identifying the particular defect. The next section presents the results of the RMS and Kurtosis measurements. One simple way to investigate the condition of the pump operation is by observing the RMS values of the current signal. RMS values were calculated for the current data, for all four operating conditions and are presented in Figure 7-2 as a function of flow rate.

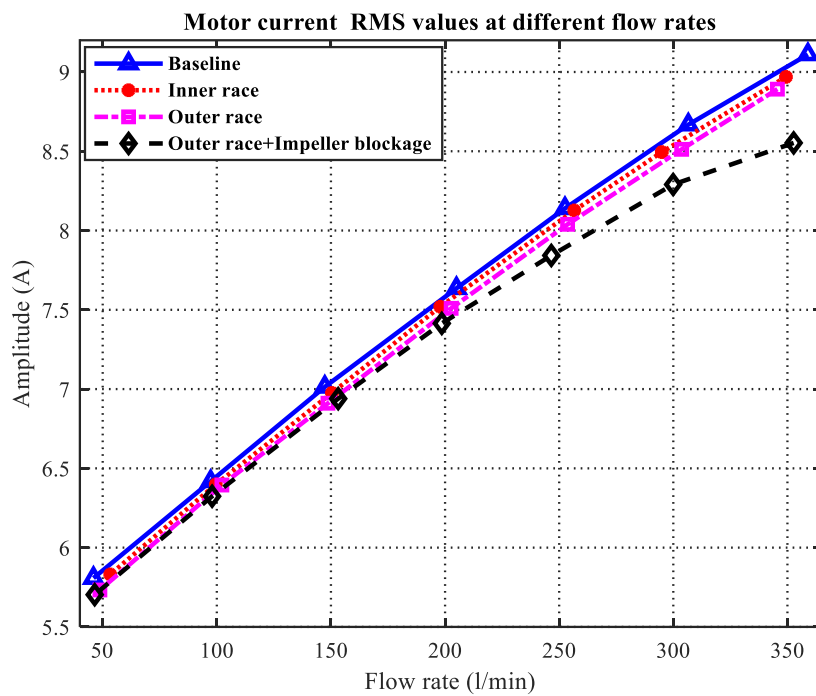


Figure 7-2 Motor current RMS values for a healthy pump, and faulty conditions at different flow rates

Figure 7-2 shows that the trend for RMS values of the phase current was to increase as the flow rate increased for all four conditions. It also shows that the difference in the RMS current values between the healthy pump and the combined fault condition increased with increase in flow rate, and above about 200 l/min flow rates were clearly visible. However, it was not possible to distinguish the baseline from the two remaining fault conditions.

This shows that the RMS values of the raw current signal can differentiate certain, larger, faults but had a limited capability in detecting smaller ones.

Another statistical parameter, Kurtosis, was used to describe the time domain signals of the motor current as it can be very sensitive to the peakedness of the data set.

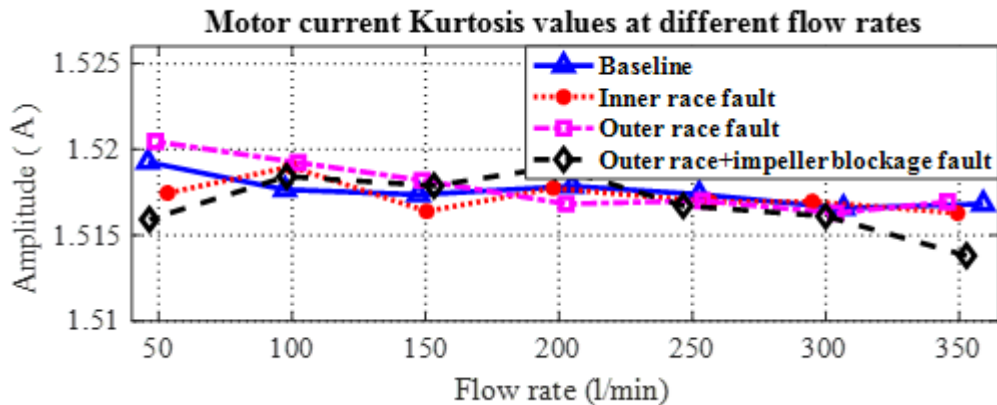


Figure 7-3 Kurtosis values for the current signal for four pump conditions under different flow rates

Figure 7-3 shows the value of the Kurtosis for current data under different flow rates. At very low flow rates, all kinds of apparently random pulsations can occur. The results showed that the Kurtosis values for the baseline condition have a slightly declining trend, kurtosis values for the faulty cases have a fluctuation trend, particularly for the combined fault. Overall, the Kurtosis parameter does not differentiate the faulty conditions from the healthy condition for the flow rates used.

The time-domain analysis has shown that it is unlikely to detect the fault by visual inspection of the time-domain signal, and even the use of statistical features such as RMS and Kurtosis did not prove sufficient.

### 7.3 Frequency Domain (Spectrum)

The most common way of obtaining the spectrum is to use the Discrete Fast Fourier Transform (DFFT). The DFFT has proved itself a tremendously useful and successful tool for investigating the behaviour of rotating machines, in particular centrifugal pumps. The frequency spectrum is analysed to determine particular frequencies that show an unusual amplitude[10, 138].

The current spectrum will contain many operating parameters, such as shaft frequency and supply frequency. The spectrum will show these frequencies and their harmonics as modulated by the fundamental supply frequency ( $f_i \pm f_s$ , where  $f_s = 50$  Hz). Any change in motor load will affect the amplitude of these frequencies. Moreover, it has been shown that common faults show themselves as side-bands around the fundamental frequency,  $f_i$  [205]. Thus, analysing and examining these changes in the spectrum, especially the amplitude information at the frequencies of interest, provided meaningful information on the behaviour of the current signature and hence, the condition of the pump being monitoring.

Before examining the current spectrum, the vibration signals collected from the accelerometer mounted on the centrifugal pump were analysed to confirm the faults induced into the test bearings were affecting pump performance. The characteristic frequencies of the faults which were calculated based on Equations 3-4 and 3-5. In addition, as there is always a slippage when the bearings operate under dynamic loads, the actual frequencies may have slight differences from those calculated using the Equations [206]. Figure 7-4 and Figure 7-5 show the envelope of the vibration spectrum for both the outer race and inner race faults, and for the baseline.

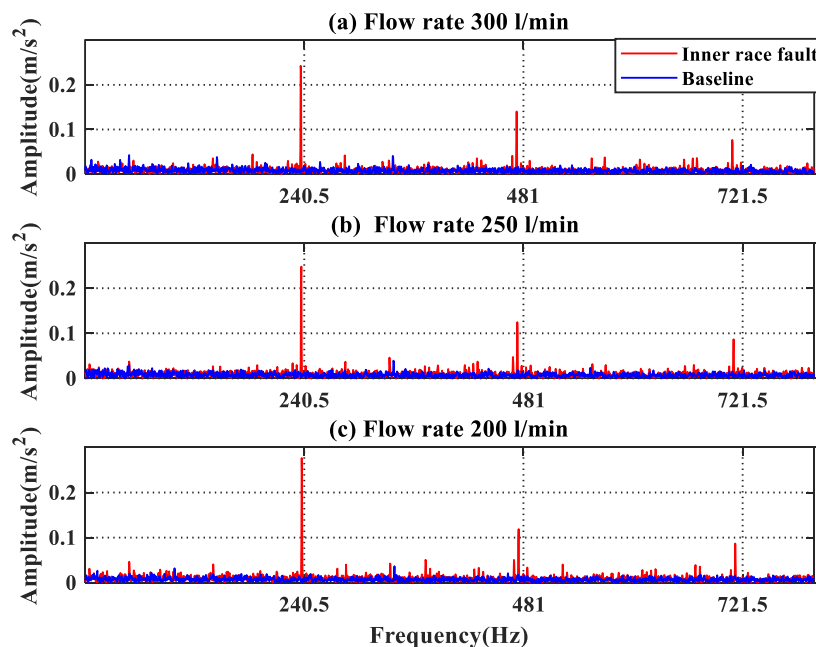


Figure 7-4 Vibration envelope spectral analysis for baseline and inner-race fault under different flow rates

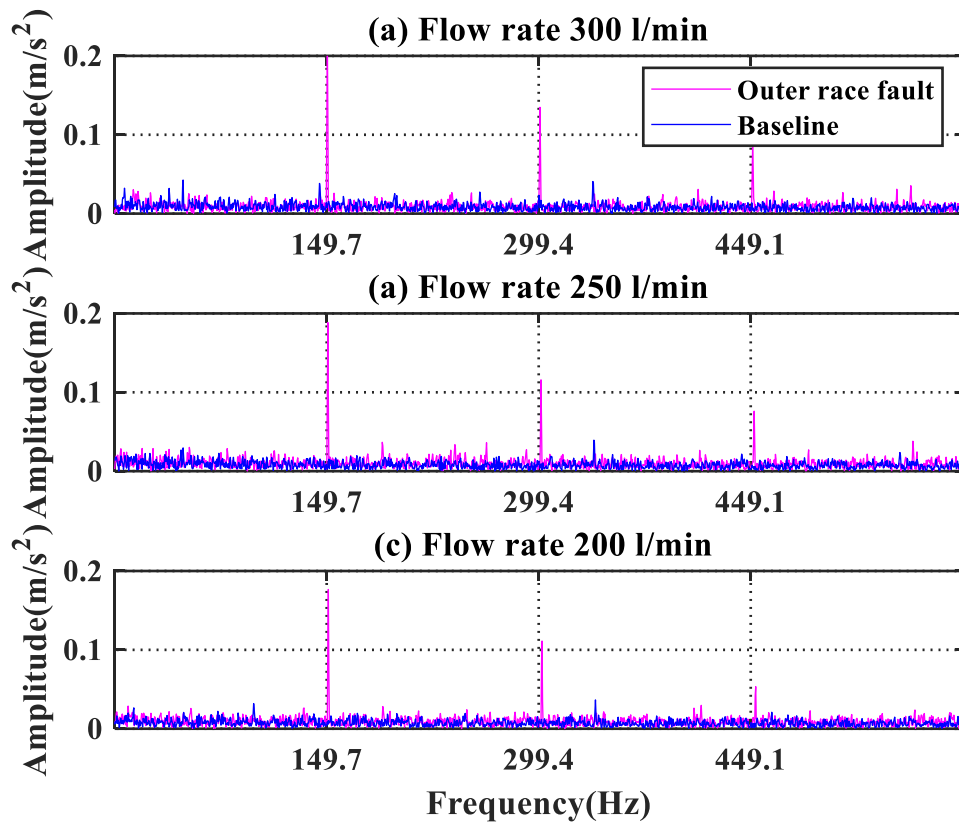


Figure 7-5 Vibration envelope spectral analysis for baseline and outer race fault under different flow rates

The characteristic frequency of inner race fault is  $f_i = 240.4$  and the fundamental fault frequency of the outer race is  $f_o = 149.7$  Hz, also, the harmonics of the faults are shown clearly. These results confirmed that the two types of faults have been induced into the test bearings faults.

Figure 7-6, 7-7, and 7-8 show the current spectra for a healthy pump and the three faulty cases, under different flow rates, The figures show clearly that the supply frequency (50 Hz) and its harmonics (100, 150, 200 and 250 Hz) are present in the spectrum. Also, the frequency band around the fundamental frequency is rich in sidebands. The figures show changes in amplitude of the harmonics of the supply frequency with change in flow and seeded fault. The trends for the fundamental frequency can be used to monitor the condition of the pump.

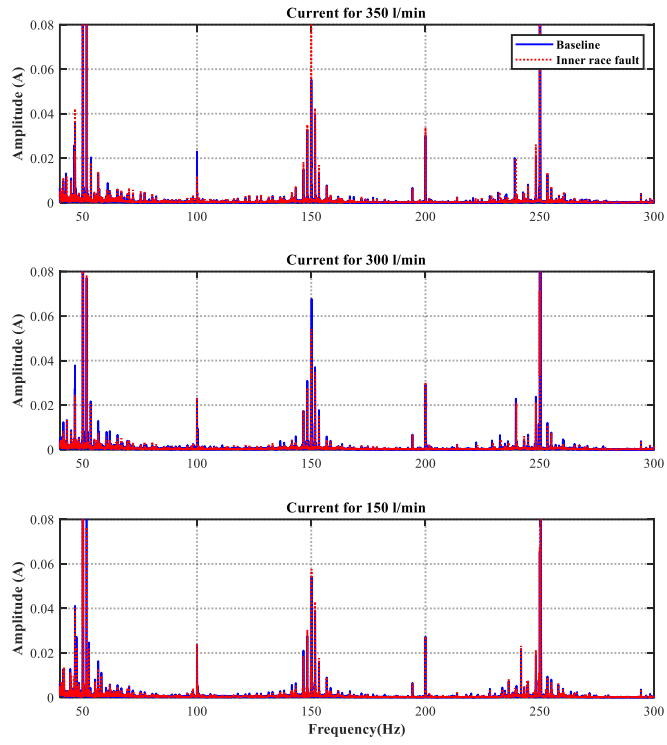


Figure 7-6 Current spectrum for baseline and inner race fault at three flow rates

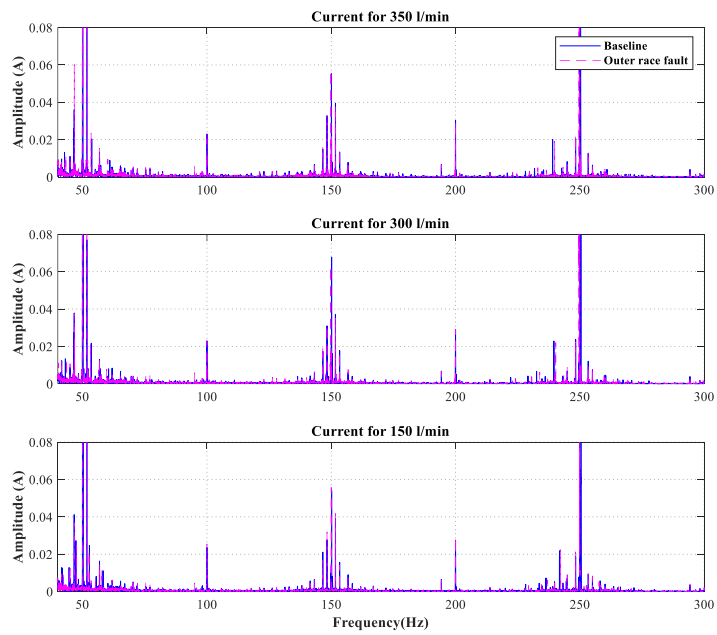


Figure 7-7 Current spectrum for baseline and outer race fault at three flow rates

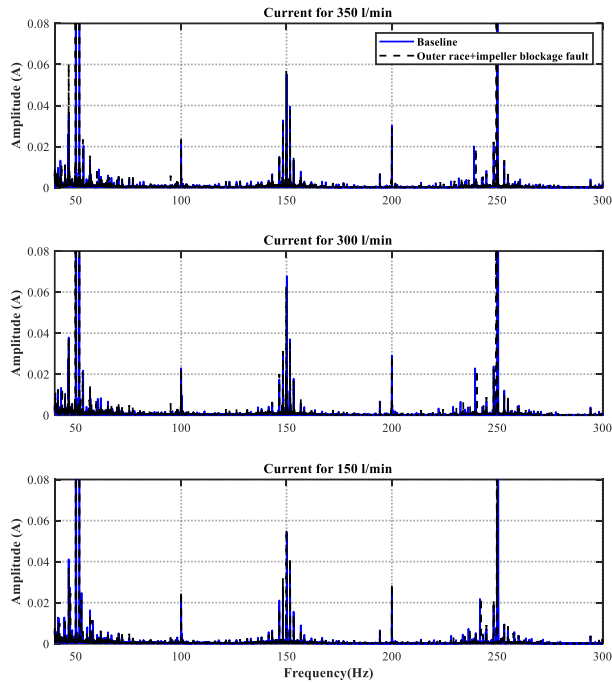


Figure 7-8 Current spectrum for baseline and combined fault (outer race and impeller blockage) for three flow rates

The current spectrum provides information about the pump operation, and it is possible to track the changes in pump operation and condition using the supply frequency. Figure 7-9 presents the amplitude of the peak in the spectrum at the supply frequency (50 Hz) for all cases examined, for all flow rates.

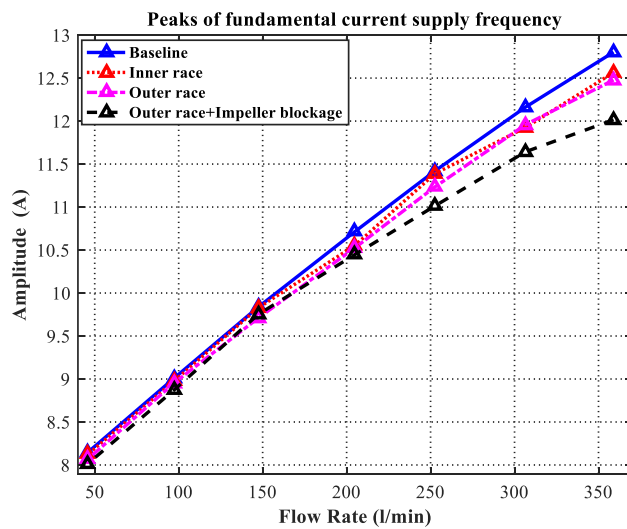


Figure 7-9 Peak value of fundamental supply frequency for the healthy pump and pump with seeded faults under different flow rates

It can be seen that the amplitude of current at the supply frequency increased with increasing flow rate. In the figure, the same trend can be seen for all four conditions, the amplitude of the motor current increased monotonically with flow rate. The figure also shows that the healthy case can be distinguished from the faulty cases, certainly at flow rates higher than 250 l/min, but it is difficult to separate the different conditions for lower flow rates.

At this stage, the bearing fault frequencies could not be directly determined from the current spectrum, and further investigation was carried out based on envelope analysis, to identify these bearing fault frequencies. For envelope analysis, a bandpass filter is required to eliminate the low-frequency noise, then the signal was rectified, and after that, the envelope of the spectrum was obtained, from which the fault frequency components could be detected. The envelope analysis was performed for the current signals for all conditions for three flow rates. Figure 7-10 shows the results of the envelope analysis of the current signals.

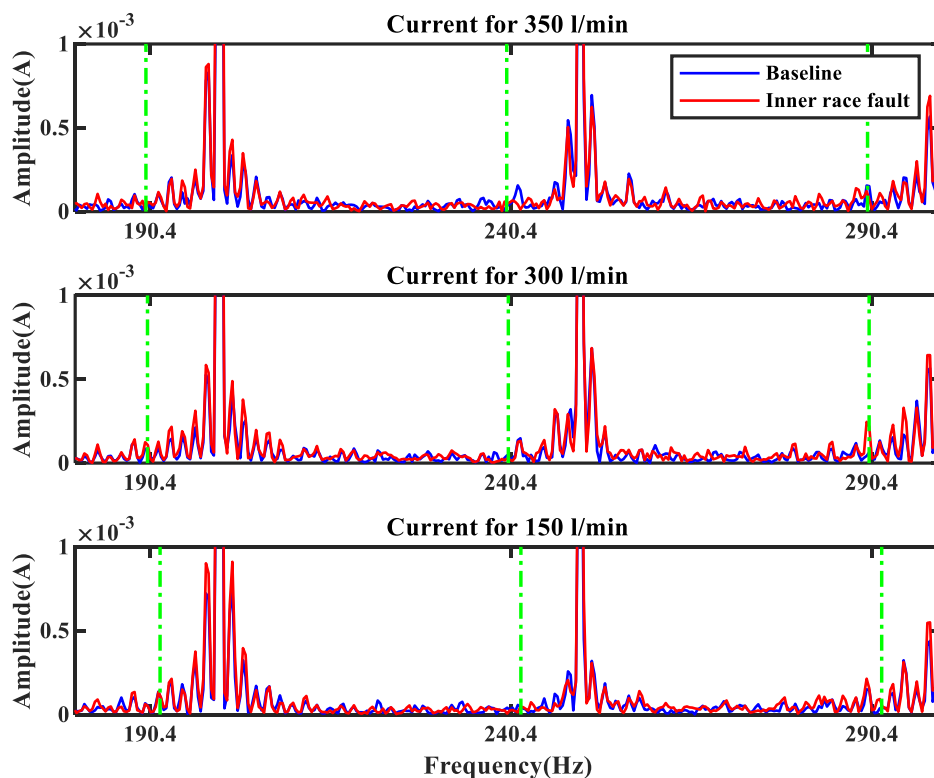


Figure 7-10 Envelope spectrum of current signal for baseline and inner race fault under different flow rates

From Figure 7-10 the current envelope spectrum in the frequency range around the inner race fault frequency ( $f_i = 240.4$  Hz) is presented. The effect of the inner bearing fault on the current spectrum was expected to appear as sidebands around the inner race fault frequency at  $(|f_s \pm f_i|)$  according to the Equation 3-6. It can be seen there was very small change between healthy and faulty cases at  $(|f_s \pm f_i|)$  (190.4 Hz and 290.4 Hz). The faulty peaks can be seen for both the 300 and 150 l/min flow rates, but is not so clear at the flow rate of 350 l/min.

For the outer race fault, Figure 7-11 shows the envelope spectrum for the outer race fault and baseline for the frequency range of interest.

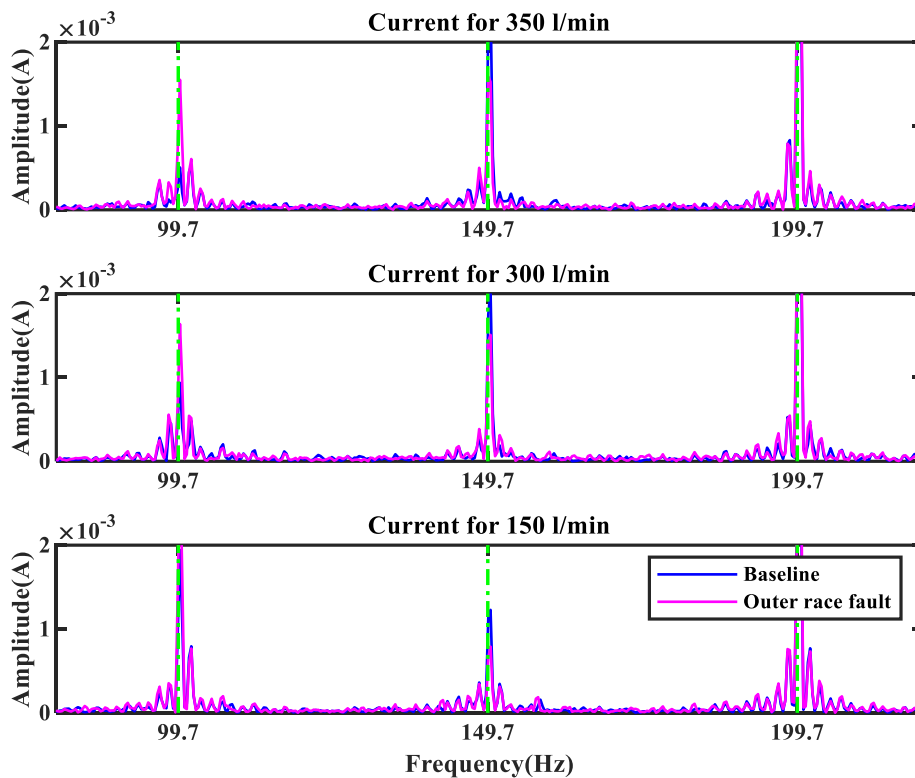


Figure 7-11 Envelope Spectrum Analysis of current signal for baseline and outer race fault under different flow rates

Figure 7-11 shows the spectrum around the characteristic fault frequency of the outer race fault,  $f_o$ , which is 149.7 Hz. The effect of the outer race fault on the current spectrum as calculated by the Equation 3-6 are expected to appear at  $(|f_s \pm f_o|)$ , the figure results show

a peak at the characteristic fault frequency of the outer race  $f_o \pm f_s$ , for all flow rates, while the peaks at  $f_o$  are small than baseline.

However, the modulating components of the bearing faults had very small amplitudes and were masked by the background noise. It would be difficult to detect the peaks belonging to the outer and inner race faults from the current spectrum. Thus, an advanced signal processing technique such as a data-driven technique is required for analysing the current signals to determine the presence of mechanical defects.

#### **7.4 Key Findings**

This chapter has presented an overview of the use of motor current signals for evaluating the condition of the centrifugal pump for fault detection and diagnosis.

Time-domain analysis and frequency domain analysis has carried out for tracking the change of the current signal caused by the induced faults. Although the slight change of the RMS values which has a monotonic increase in amplitude with flow rate, it is unlikely to detect the faults in the centrifugal pump.

Moreover, from the results obtained using current spectrum and the envelope analysis showed that bearing faults have very small amplitudes and were masked by the background noise, it can be concluded that it is still not adequate to identify the pump faults. As the current signals are affected by complicated nonlinear processes such as the fluctuations in the flow rate. Further investigation will be carried out based on the data-driven techniques such as EMD and ITD for analyses and examine the use of current signals for monitoring the performance of centrifugal pumps.

## **Chapter 8 Empirical Mode Decomposition of Motor Current Signal for Centrifugal Pump Diagnostics**

*This chapter offers a data-driven method of extracting characteristics from the motor current signature to detect and diagnose centrifugal pump faults. Specifically, the procedure utilizes the unique advantages of Empirical mode decomposition for decomposing the current signal, and then uses envelope analysis for the demodulation of the decomposed signal. This allows the extraction of features from the current signal to assess the condition of the pump. The results show that the combination of EMD and envelope analysis can be an effective method for detecting the seeded pump faults.*

## 8.1 Introduction

The EMD was used for analysing the current signals. In this method, the analysis is based on the local characteristic time scales of the signal, and that means the procedure will be based on the data itself which makes it reliable and more accurate when analysing non-stationary and non-linear signals, improving the ability of the motor current signature for accurate detection and diagnosis of pump faults. The motor current signals belonging to the defective pumps come with an amplitude-modulating (AM) impact superimposed on the characteristic frequencies of the rotating machine components, and becomes more noticeable as the flow rate increases. Applying EMD allows multicomponent current signals to be decomposed into mono-components, for more details see Section 4.6. The Hilbert transform can be useful for demodulation of the intrinsic mode functions (IMFs) obtained from the EMD process, by generating an envelope that captures the characteristics of both high frequency and low-frequency signatures; this helps to find meaningful information and specific frequencies of interest corresponding to the pump faults.

To demonstrate the performance of the technique, an experimental investigation was carried out on the centrifugal pump under four different conditions: baseline data considered as the healthy condition, inner race fault, outer race fault and a combined fault of the outer race with blockage in the impeller, as described in Section 6.6. The motor current signals corresponding to each of the four conditions were examined for four flow rates: 350, 250, 150, and 50 l/min. These four flow rates were selected to cover the full range for this pump and system. For more details about the test procedure and how the current data were collected, see Chapter 6, Section 6.8. The following section describes the validation of the EMD process on simulated data and shows the diagnostic method in more detail related to the experimental signals.

## 8.2 The Performance of EMD on Numerical Simulation Signal

To validate the efficiency and performance of the EMD method for analyzing a non-stationary signal, a simulated signal with noise-contaminated AM is considered as follows[125]:

$$x = A_L \cos(2\pi f_s t - f_L - \alpha_L) + A_c \cos(2\pi f_s t + \alpha_c) + A_U \cos(2\pi f_s t + f_U - \alpha_U) + A_n n(t)$$

where  $f_s=50.0$  Hz,  $f_L = f_U=48.5$  Hz corresponds to the supply frequency and shaft rotational frequency. The carrier signal,  $A_c$ , has an amplitude of unity, and  $\alpha_c, \alpha_L, \alpha_U$  are random phases from a uniform distribution between 0 and  $2\pi$ .

The modulating signal has an amplitude  $A_L=A_U=0.01$ , and the noise has a uniform distribution between 0 and  $2\pi$ . The signal includes random noise  $n(t)$  which is from a normal distribution denoted as  $N \sim N(\mu=0, \sigma^2=1)$ , where  $\mu$  is the mean and  $\sigma^2$  is the variance; the noise amplitude,  $A_n = 0.1$ .

This simulated signal is analogous to recorded current data where the carrier signal comes with much higher amplitude than other components. The simulated signal, see Figure 8.1(a), was sampled at a frequency of 2048 Hz. Figure 8-1(a) and (b), shows the signal  $x$  in the time domain, also, it contains the same essential features of the AM of the measured signal shown in Figure 4-1. The frequency-domain spectrum corresponding to Figure 8.1(a) is shown in Figure 8-1 (b). This simulation will assist in establishing the analytic characteristics of the measured signals. The simulated signal was decomposed by EMD technique into IMF components, see Figure 8.2. It is clear that the first IMF contains the highest frequency components and, subsequently, the other IMFs contain lower frequencies.

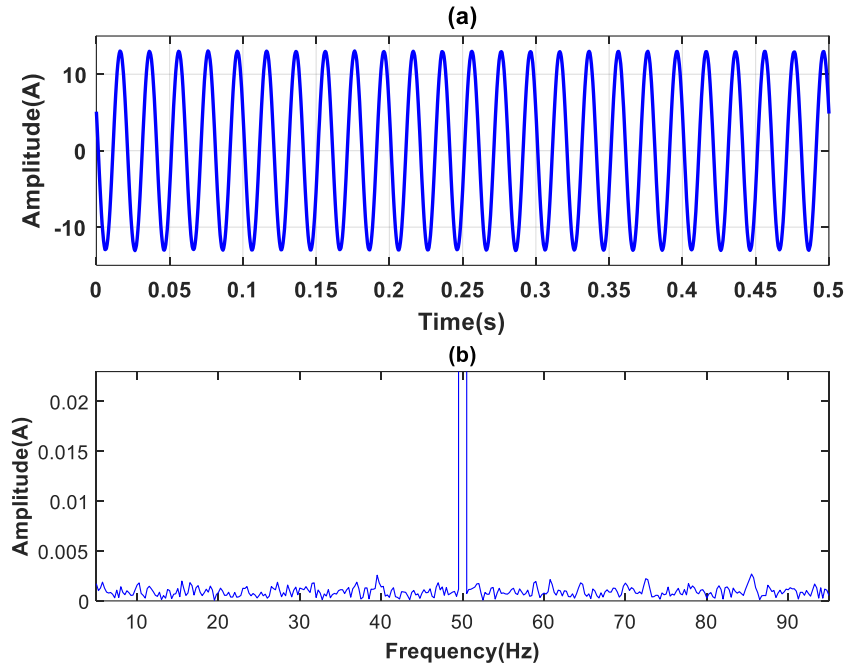


Figure 8-1 Simulated AM signal and its frequency spectrum: (a) a portion of the raw signal and (b) frequency spectrum.

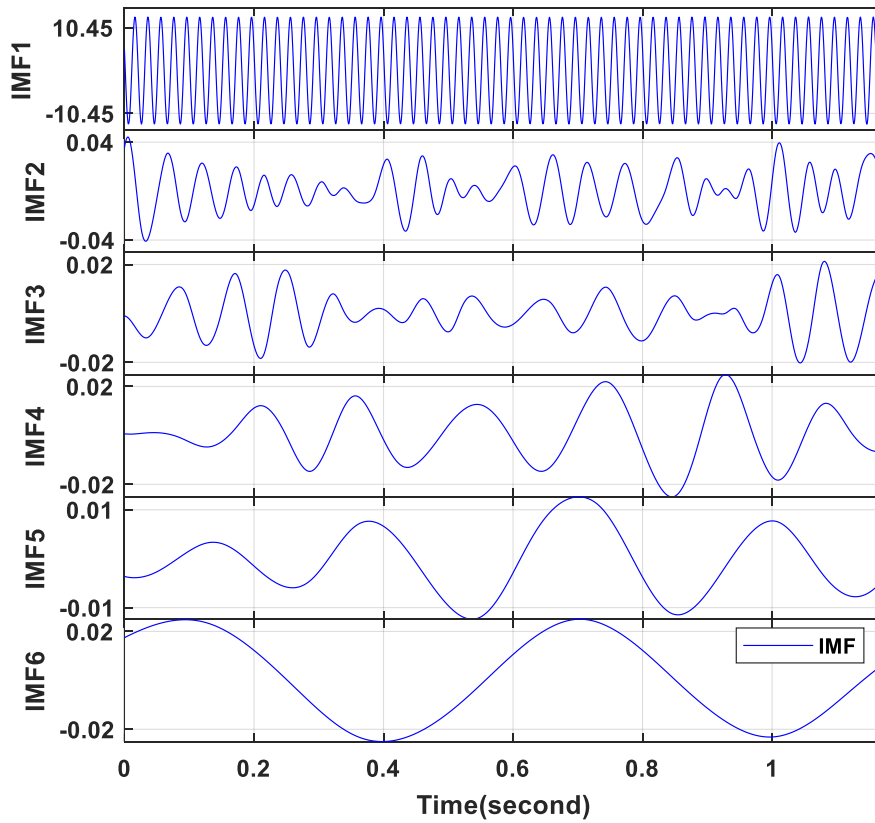


Figure 8-2 EMD results of simulated AM signal.

### 8.3 The Performance of EMD on Experimental Current Signal

The current signals of different cases with a varying range of flow rates were decomposed using the EMD techniques, as shown in figures Figure 8-3 to Figure 8-6 only the six IMFs and their envelopes are presented for all cases with flow rate at 250 l/min. It is obvious that the profiles of the distinct IMF components have some differences, it is clear that the first IMF component has more fluctuations and modulation characteristics.

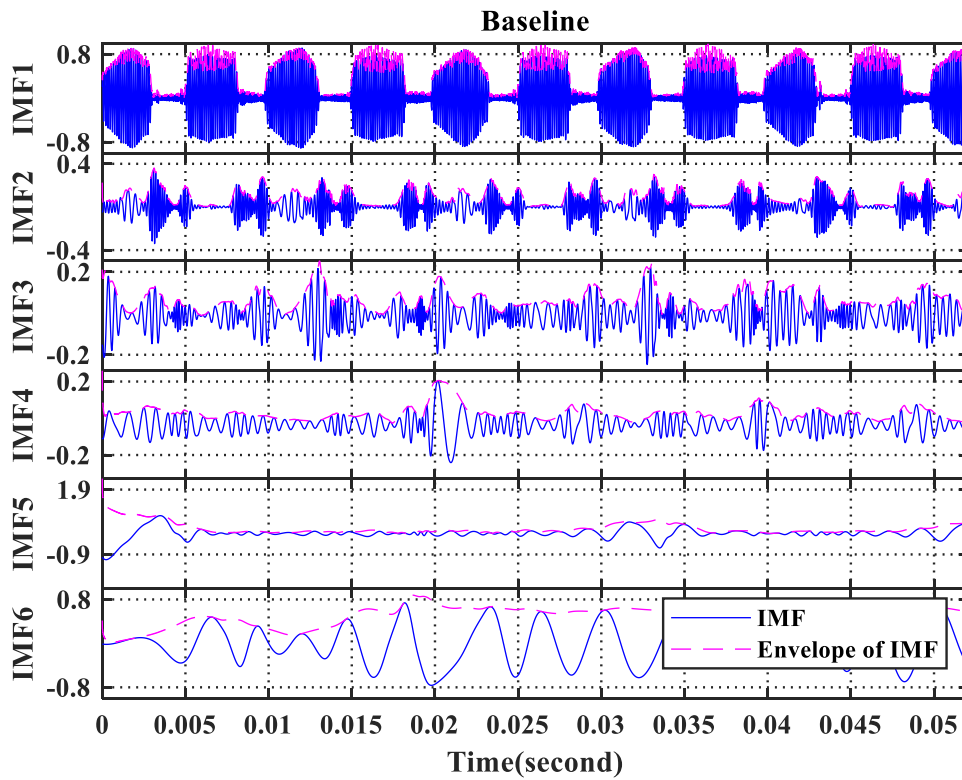


Figure 8-3 EMD decomposition results of Baseline at 250 l/min

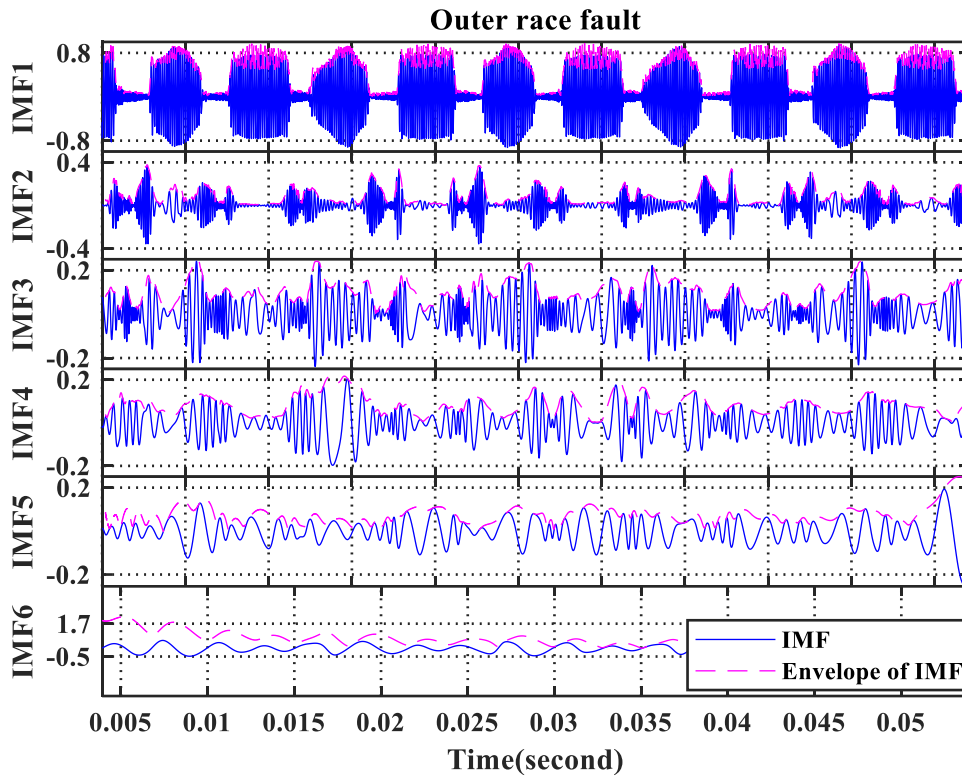


Figure 8-4 EMD decomposition results for the outer race fault at 250 l/min

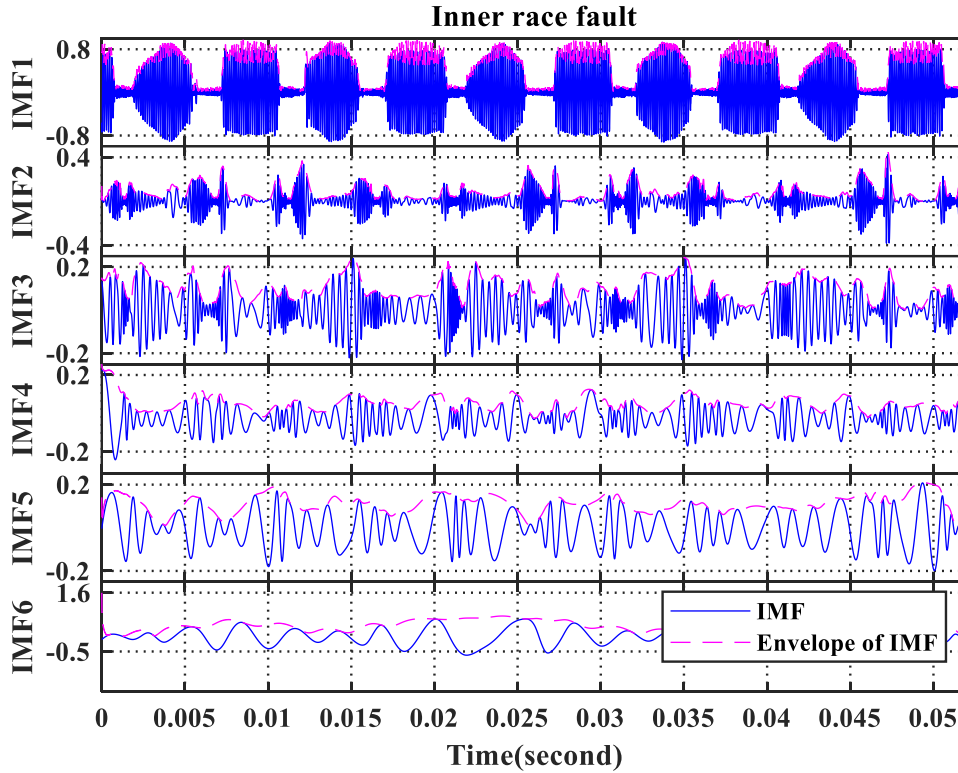


Figure 8-5 EMD decomposition results for the inner race at 250 l/min

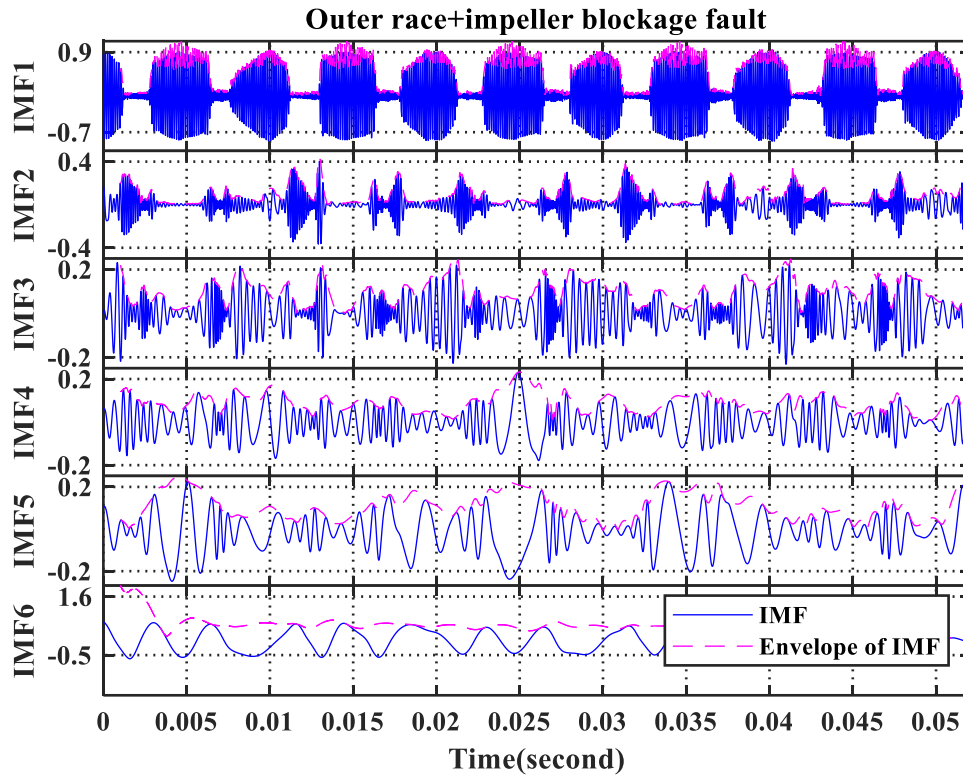


Figure 8-6 EMD decomposition results for the combined fault at 250 l/min

The EMD decomposes the current signal into the different intrinsic modes of oscillations ranging from high frequency, IMF1 through medium frequencies IMF2 and IMF3 to low frequencies IMF4 to IMF6. The IMFs are considered as instantaneous features of the signal at varying windows of frequency measured over time.

It is noticeable that IMF1 contains the dominant higher frequencies contained in the signal, though it can give more detailed information related to the signal characteristics corresponding to the frequencies of interest. Based on the EMD theory mentioned earlier in Chapter 4 Section 4.6. The first IMF is the main component that holds the majority of the current energy for all the current data [59]. Hence, in the present study, more analysis is focused on the first IMF. Moreover, the modulation characteristic is also visible in the first IMF component. It is hard to distinguish between different fault conditions by visual inspection of the IMFs in the time domain. Hence, in the present study, most attention is focused on the first IMF. Moreover, the modulation is clearly visible in the first IMF.

However, it was hard to distinguish between the different fault conditions by visual inspection of the IMFs in the time domain. Thus, spectrum analysis was employed, see the next section, to investigate the motor current signature of each case.

### 8.4 Spectrum of IMFs

The spectrum analysis used to investigate the change of the current signature for IMF1, IMF2 and IMF3 for the different fault cases. Figure 8-7 shows the current spectra for all cases at 250 l/m flow rate.

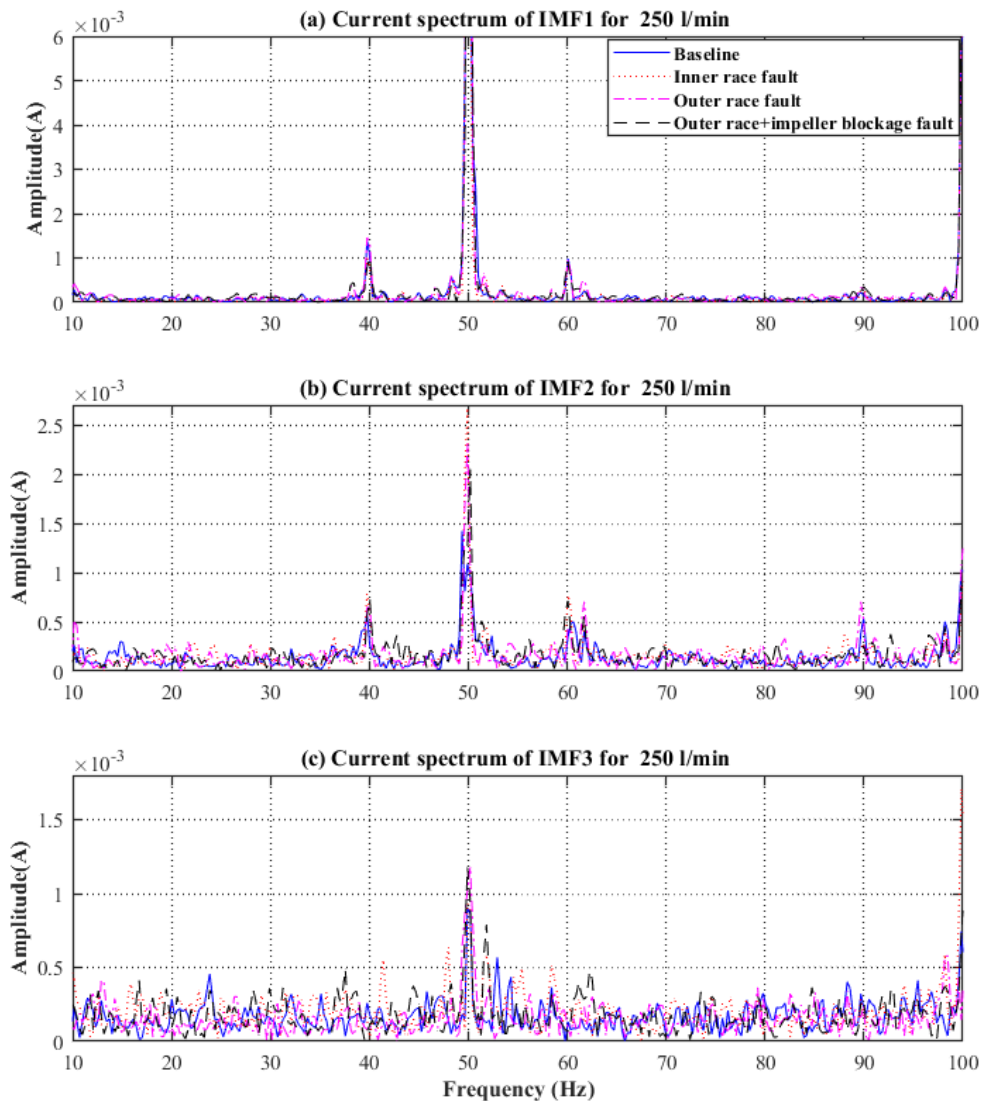


Figure 8-7 Current spectra of the first 3 IMFs for all cases at.250 l/min

Figure 8-7 in (a), (b) and (c) shows the spectrum analysis of the first, second and the third IMFs, respectively. In the first IMF, the fundamental frequency can be seen at 50 Hz, with a higher amplitude compared to the results obtained from IMF2 and IMF3. Figure 8-8 presents comparisons of the peak amplitude values of the supply frequency for the healthy pump and faulty condition.

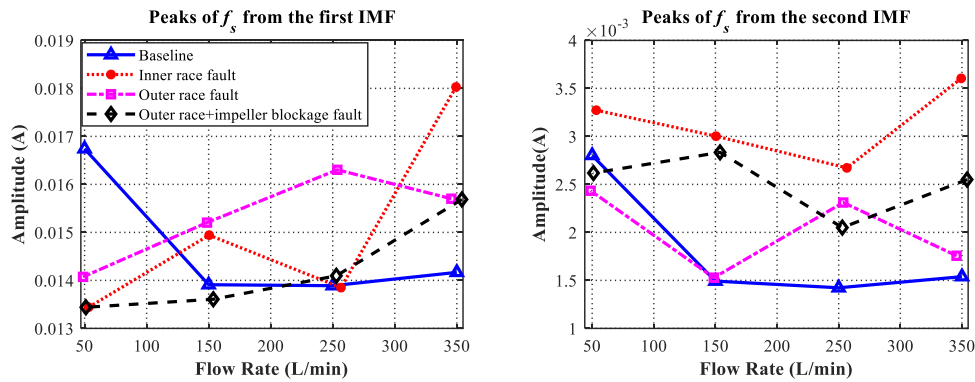


Figure 8-8 Peak values at  $f_s$  from the current spectrums of IMF1 and IMF2

Figure 8-8 presents the peak values of the first and second IMFs, it is obvious that the  $f_s$  values of IMF2 show more fluctuations and a greater spread than IMF1. However, there is no clear trend in either of IMF1 or IMF2. Based on these results, it is not possible to separate the healthy condition from the seeded faults using the characteristic extracted from the spectrums of the IMFs. However, the frequency peaks caused by the defect may be hidden beneath the frequencies from the rotating parts such as the shaft. Thus, envelope spectral analysis was applied to determine the characteristic frequencies from the IMF components of the modulated signal.

### 8.5 Envelope Spectrum of IMFs

The motor current signal has inherent modulation effects generated from the variation of load on the centrifugal pump. The IMF components have an amplitude modulation (AM) effect due to the raw current signal for the various operating conditions of the pump. Thus, envelope analysis of the IMFs was performed in order to obtain envelope spectra from which the mechanical fault might be diagnosed. The Fourier transform of the envelope signal of the first three IMFs was computed as these contain the higher frequencies of the signal that may provide some important diagnostic features.

The envelope of the spectrum is expected to contain the desired diagnostic information, such as the repetition rate of the fault and potential modulations [206], ( see Section 4.5 for details about envelope analysis). The main energy of the current signals is concentrated in the fundamental frequency ( $f_s$ ). The amplitude of  $f_s$  varies with the condition of the machine and the load. Here, the load is proportional to the flow rate [48].

The envelope spectrum was used to demodulate the current data to provide clear peaks at harmonics of the featured defect frequencies. Figure 8-9 exhibits the envelope spectrum of the first three IMFs for all simulated conditions at the flow rate of 250 l/min. The peak values at 50 Hz are shown to present additional information provided by the spectrum.

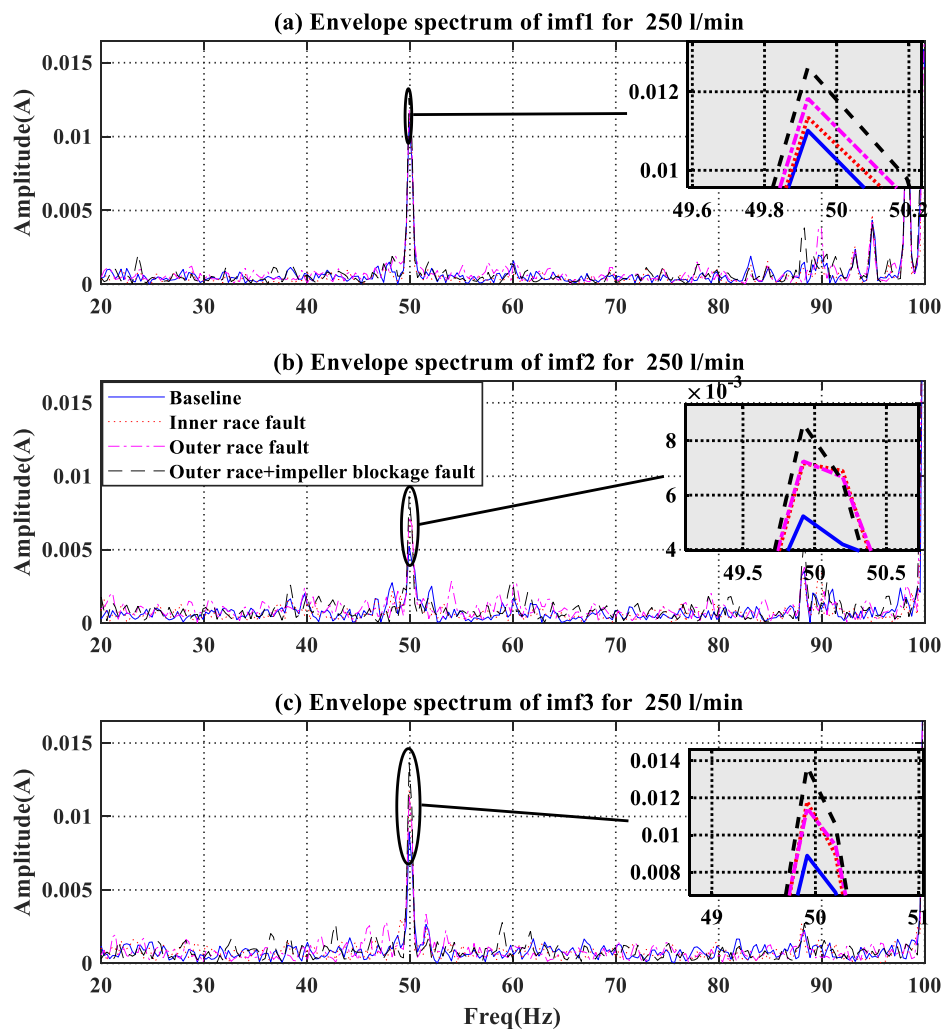


Figure 8-9 Envelope spectrum of IMF1, IMF2 and IMF3 for all cases at 250 l/min.

In Figure 8-9 (a) it is noticeable that the spectral peaks at the fundamental frequency  $f_s$  of 50 Hz for the IMF1 have different amplitudes and show a clear separation between all four the cases, as seen in the magnified graph. This feature provides a good indication of the pump's condition, while the second and third IMFs show the same signal amplitudes for the inner race fault and the outer race fault, see Figure 8-9 (b-c). It is obvious that using IMF2 and IMF3 for the separation of these simulated cases would not be possible.

Figure 8-10 shows the peak values of the fundamental frequency in IMF1 and IMF2 for all cases.

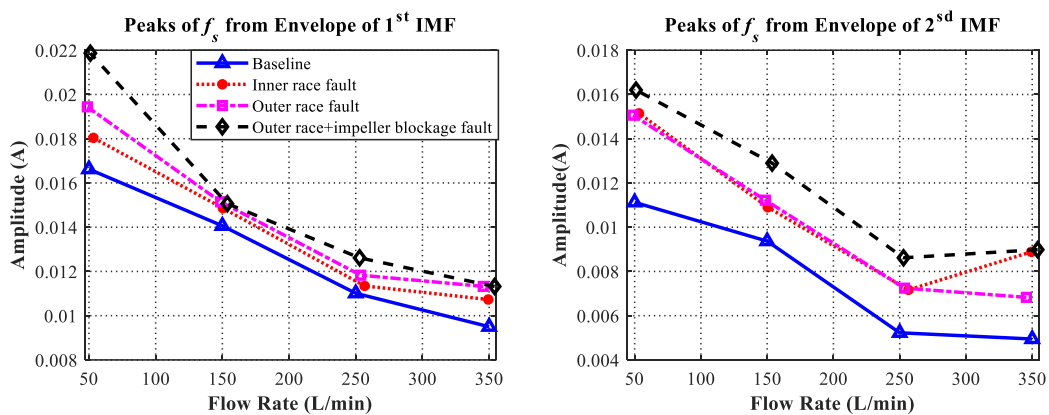


Figure 8-10 Peak value of  $f_s$  from the envelope spectrum for IMF1 and IMF2

From the Figure 8-10, it is clear that the inner and outer race faults have nearly the same peak values for IMF2 in most of the operation conditions, while the peak values for IMF1 provide good results that distinguish between the baseline and the simulated conditions, note the same trend for the magnitudes to decrease as flow increased is observed in all the cases. Thus, the first IMF was adopted for detecting the pump faults, where more information related to the current signals is found.

## 8.6 Key Findings

In this chapter, a centrifugal pump detection method has been applied based on the EMD and Hilbert transform. The EMD characteristics, which include noise reduction and nonlinear signature enhancement combined with envelope analysis, provide more accurate and convincing results. The current signals were decomposed into a number of IMF's that include the fault signatures. The results show that the EMD analysis combined with

envelope spectra of the current signature is proved to be effective in detecting a seeded fault condition in a centrifugal pump under several flow rates, and it is extremely effective than the other conventional analysis method used in this study.

## **Chapter 9 Intrinsic Time Scale Decomposition for Fault Detection and Diagnosis of Centrifugal Pump**

*This chapter provides a data-driven technique to detect and diagnose defects in the centrifugal pump. The method comprises decomposing the current signal by applying an advanced data analysis technique such as intrinsic time scale decomposition (ITD) and investigates its capability for extracting information hidden in the current data.*

## 9.1 Introduction

In this chapter, the intrinsic time scale decomposition (ITD) technique was employed to analyse the current signal of the motor of a centrifugal pump under different conditions. ITD is a robust tool for analysing non-linear and non-stationary data see Chapter 4 Section 7 for more details about the theory of ITD and how it works.

## 9.2 The Performance of ITD on Experimental Current Data

The current signals were decomposed into a set of signals by applying the ITD technique. After decomposing the current signals obtained for different flow rates, useful features could be extracted from the proper rotational components (PRCs) of the ITD. The characteristic features were utilised for evaluating the condition of the centrifugal pump.

The current data were collected from the centrifugal pump test rig and, as described in Chapter 6, four cases were considered: healthy, then simulated faults on the inner and outer races and finally the combined defect of impeller blockage and outer race fault. All the current data were recorded at a sampling rate of 96 kHz and under different flow rates; 350, 300, 250, 200, 150, 100 and 50 (l/min).

Detection of any fault in the pump will require selection of an appropriate component of the signal sensitive to the pump fault. The selected component should contain sufficient energy to construct a feature vector that will be adequate for fault detection and, possibly, identification.

The ITD decomposition should preserve the temporal information contained in each component, and preserve a time scale that will be equal to the occurrence of irregularities in the signal due to the presence of the fault. The ITD should accurately extract amplitude and frequency information and other features relevant to the signal's form and structure.

However, it is important to identify the individual (mono-components) that can accurately estimate the necessary amplitudes and frequencies for fault identification. The optimum would be to select just one PRC from which the necessary fault information can be deduced. This is likely to be the 1st PRC with an instantaneous frequency fluctuating around the shaft frequency and its harmonics will be the mono-component required for

additional analysis. Thus, here the author will investigate whether just the 1st PRC will be sufficient for fault detection and identification.

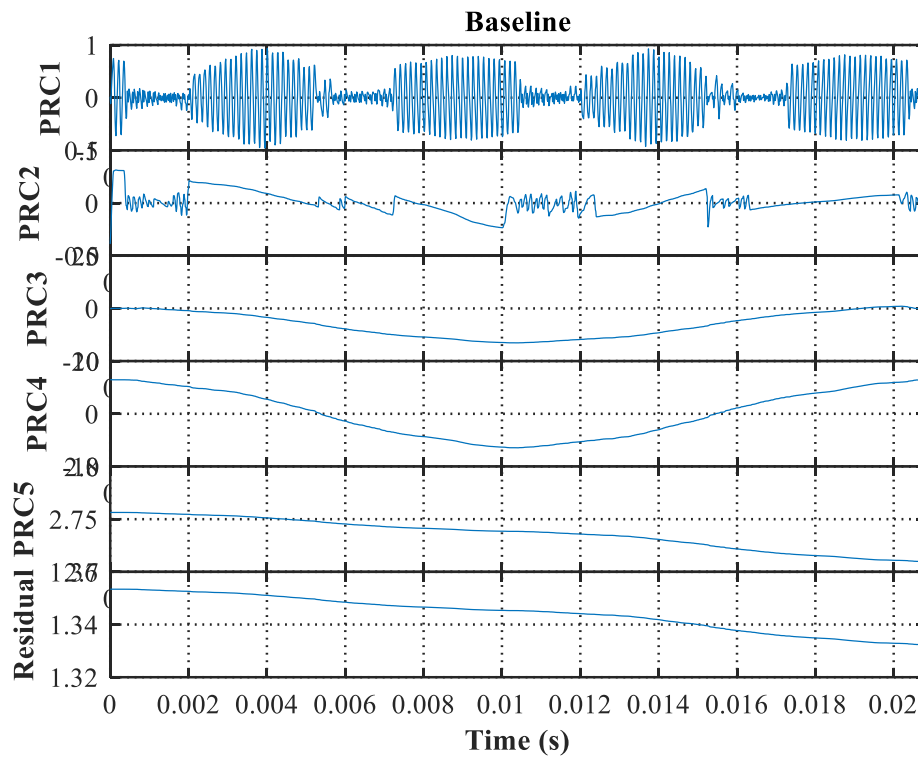


Figure 9-1 ITD decomposition result for the healthy pump at 350 l/min.

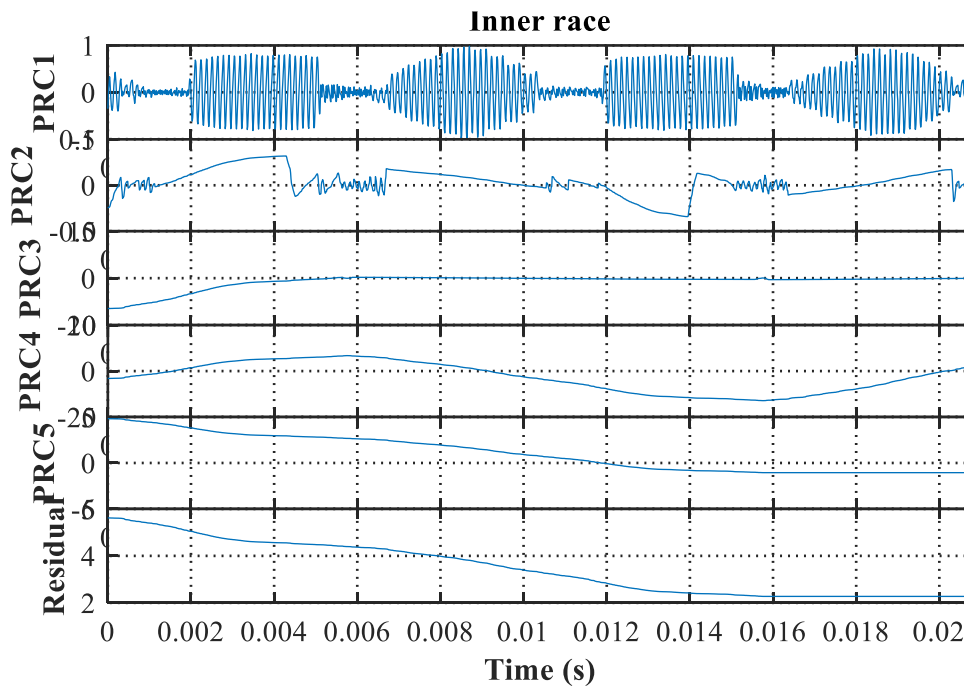


Figure 9-2 ITD decomposition results for inner race bearing fault at 350 l/min.

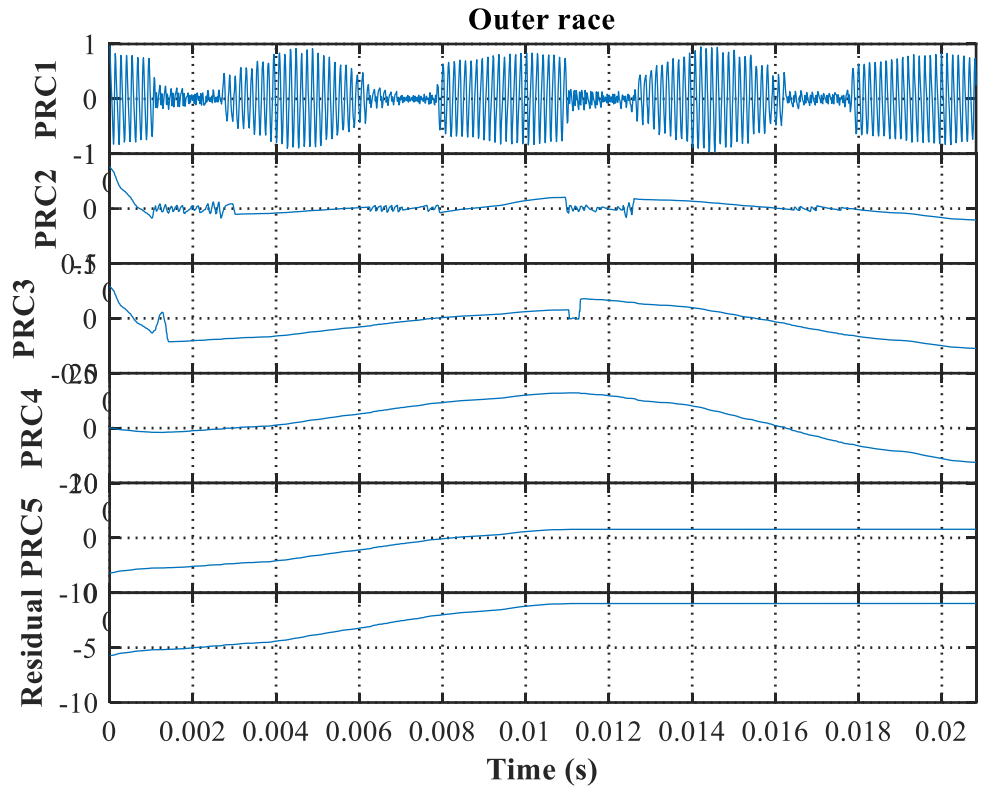


Figure 9-3 ITD decomposition results for outer race bearing fault at 350 l/min.

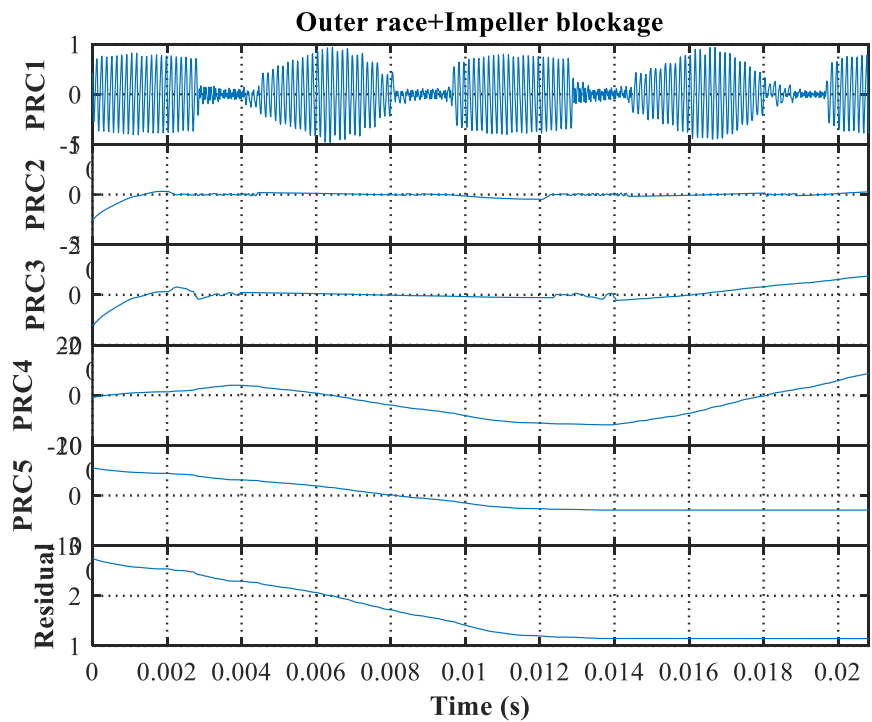


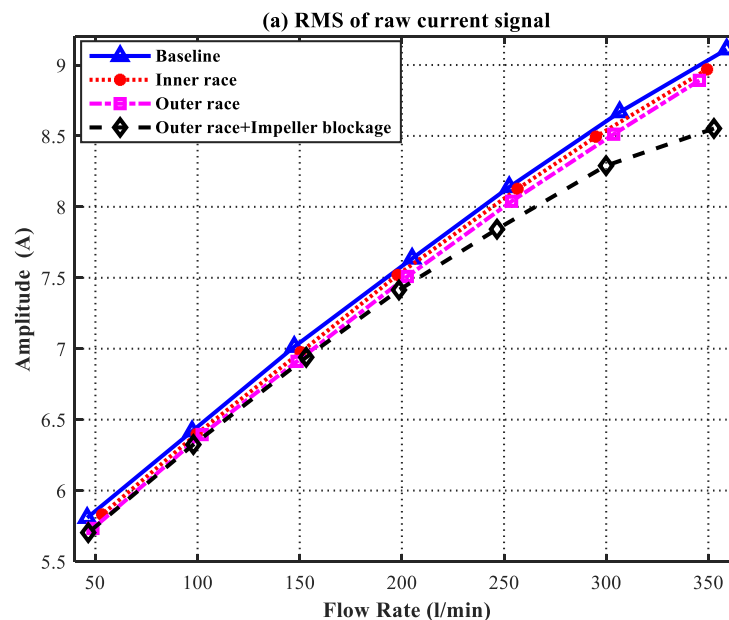
Figure 9-4 ITD decomposition results for the combined fault of impeller blockage and outer race defect, at 350 l/min.

The current data was decomposed into five PRCs and Residual. The decomposition process separated the high frequency components from the low. When comparing the PRCs for all cases, it is hard to find clear differences between the baseline and the faulty cases. Also, it is noticeable that the 1<sup>st</sup> PRC contains the dominant higher frequencies of the signal with important fault information [207]. The 1<sup>st</sup> PRC shows greater fluctuation compared to the other PRCs, which could be a reflection of the nonlinear interactions between the mechanical load and the electrical process [208]. To show the difference between the simulated cases, the RMS values are compared and considered.

### 9.3 Diagnosis Approach based on Motor Current RMS

Extracting diagnostic features is critical in the analysis of the current signal. Here, the root mean square (RMS) has been adopted as a means of revealing the energy in the current, and discrete attributes of the signal. It has been useful for the CM of centrifugal pump faults [209]. The current RMS values for the raw data are shown in Figure 9.5(a) for all flowrates. The RMS values of the 1<sup>st</sup> PRC are shown in Figure 9.5(b).

The trend of the RMS of current versus the flow rate can be used as an indicator to monitor pump operation point [210].



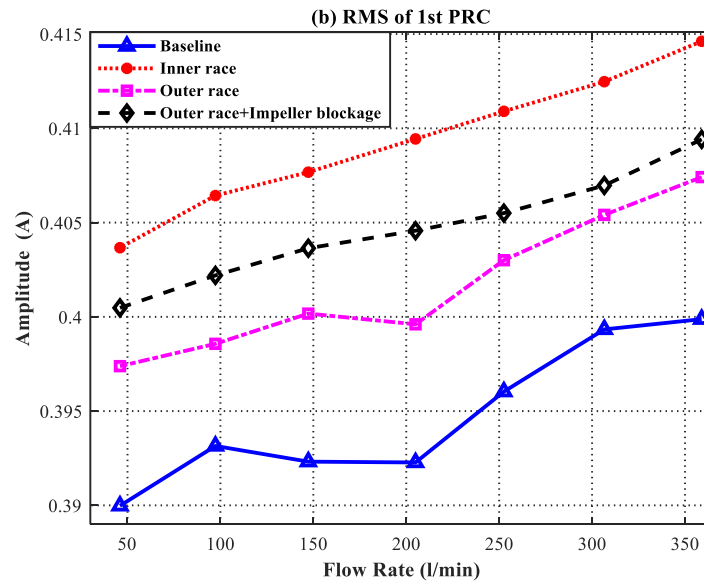


Figure 9-5 RMS of current signals at different flow rates (a) raw data, (b) first PRC.

Figure 9-5 (a) exhibits the RMS values of the raw current data for different conditions for the given range of flow rates; it is obvious that the RMS increases with the flow for all four conditions. It is seen that the RMS does not separate the four condition for flow rates less than 200 l/min. For flow rates greater than 200 l/min, slight differences can be seen between the combined fault (outer race with impeller blockage) and the other three conditions.

The RMS values of the 1<sup>st</sup> PRC for all cases are represented in Figure 9-5 (b). The Figure shows the RMS value of current at different flow rates. From the figure, it can be seen that the RMS increases as the flow rate increases. However, the current in the baseline slightly decreases between 150 – 200 l/min as the flow rate increases. This caused by the development of cavitation. Then after a certain flow rate (about 200 l/min), the current starts to increase again quite sharply as the operation reaches cavitation. Also, it can be seen that the 1<sup>st</sup> PRC values at any given flow rate, for any given condition (faulty or healthy), is measurably different from all others. This indicates that the RMS value of the 1<sup>st</sup> PRC contains useful information for monitoring the condition of the centrifugal pump.

To separate the plots shown in Figure 9.5 (a), and to remove parameters that cannot be measured from the motor current alone, the RMS values of the 1<sup>st</sup> PRC were plotted against the raw signal RMS values, see Figure 9-6. It is seen that valuable information capable of distinguishing between the given faults has been obtained.

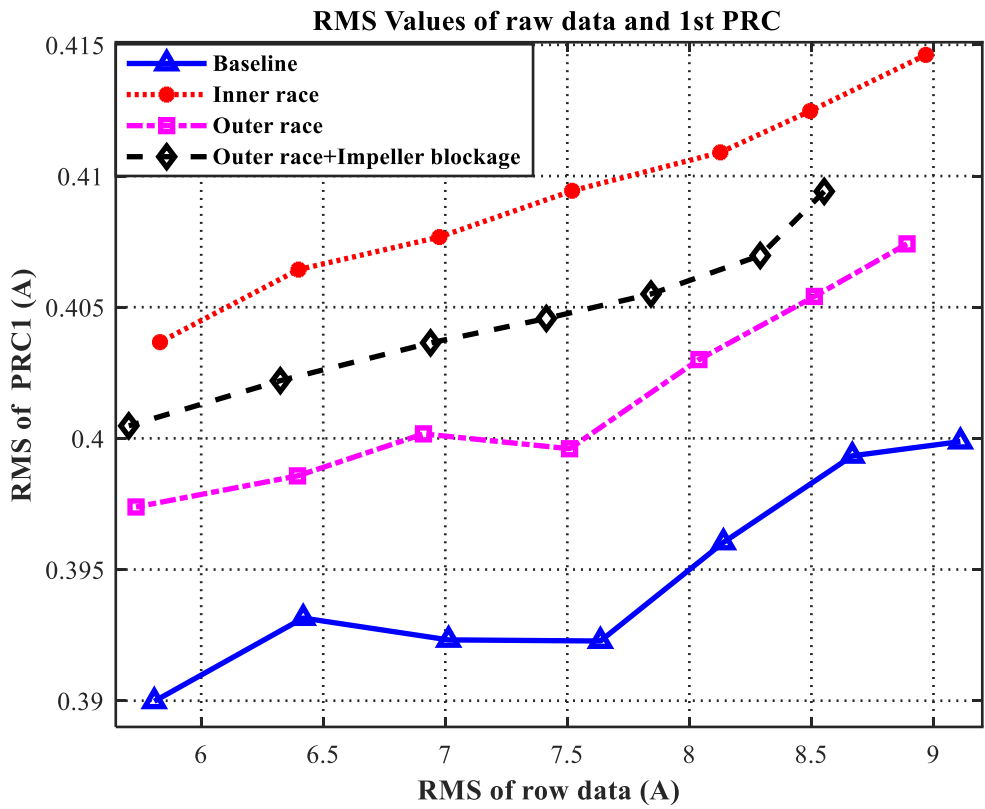


Figure 9-6 Figure 9-7 Fault separation based on static and dynamic features of the current signal

From the above figures, it may be observed that there are obvious and consistent differences between the healthy condition and each of the simulated faults. The proposed method can separate the operating condition of the pump without any other measured parameters such as the pressure and flow rates.

### 9.4 Key Findings

ITD is a data-driven and powerful technique for analysing the current signal, and while it has shown its effectiveness in processing vibration signals for machine fault detection and diagnosis, it has not been used for analysing motor current signals. Here, an approach has been proposed and tested based on ITD analysis of motor current data obtained only from the pump's electrical control system, while operating with three seeded faults under different flow rates.

Firstly, ITD decomposed the current data into a set of PRCs, to obtain characteristic features for maximising the diagnostic efficiency for a set of seeded faults in a centrifugal

pump. The RMS of the motor current and the 1<sup>st</sup> PRC was employed as a useful feature for describing the energy of the current signal. The results have demonstrated that the 1<sup>st</sup> PRC extracted by ITD can adequately represent the motor operation. Also, a new feature parameter is proposed that combined the RMS of the raw signal and RMS of the 1<sup>st</sup> PRC. This has two advantages, firstly it shows a clearer separation among the different pump conditions, at a given flow rate, and secondly, it is in terms of motor current parameters only, it does not require, for example, pipe flow rate. Consequently, this proposed approach performs effectively for detecting common pump faults under a wide range of pressure.

## **Chapter 10 Support Vector Machine for Enhance Detection and Diagnosis of Centrifugal Pump Faults**

*This chapter discusses a proposed method for classifying the three faults seeded into a centrifugal pump, based on current signals. A support vector machine (SVM) was constructed and employed using intrinsic time-scale decomposition (ITD) features, which were extracted from the current data for different fault cases and a range of flow rates. This chapter assesses the capability of the method for centrifugal pump fault detection and diagnosis. Also, the performance of envelope analysis, empirical mode decomposition (EMD), and discrete wavelet transform (DWT) based features were investigated and compared to ITD. The results demonstrate that the analysis method based on SVM and ITD work efficiently for detection and diagnosis of the seeded defects in the centrifugal pump. This diagnostic approach will enhance the condition monitoring of centrifugal pumps.*

## **10.1 Introduction**

In this research, SVM was applied to classify the faults seeded into a centrifugal pump. SVM was adopted due to the advantages it offers, such as having a generalization capability and good classification performance [211]. SVM has the advantage that it can cope with analysing large amounts of data that vary considerably, and data with a high number of dimensions [212]. The principle of SVM is dependent on statistical learning concepts and is generally considered to be very effective for finding an optimal solution for classification problems. It is a robust machine learning technique that is appropriate for machine fault diagnosis [213]. Hence, a multi-class SVM was applied to features extracted from different signal processing techniques: ITD, envelope analysis, EMD, and DWT. The next section explains the diagnostic approach to the centrifugal pump faults.

## **10.2 Centrifugal Pump Diagnostic Approach based on SVM**

In this approach, the current data of a centrifugal pump are investigated for all four cases: baseline, inner race fault, outer race fault, and the combined fault impeller blockage and outer race bearing fault. Figure 10-1 presents a flowchart of the proposed diagnostic approach based on SVM for centrifugal pump faults.

The diagnostic approach has three main processing stages. The process starts with the current signals being acquired from the centrifugal pump test rig (see Section 6.8). In the second stage, the current signals are analysed to extract statistical features to be used for the classification task. These features are: Mean, RMS, Crest factor Kurtosis, Entropy, Variance, and Range, (for more details about their formulas see Section 5.4), then in the last stage, the SVM algorithm was employed for generating the classifier, which was used to detect and diagnose the particular fault determining the condition of the pump.

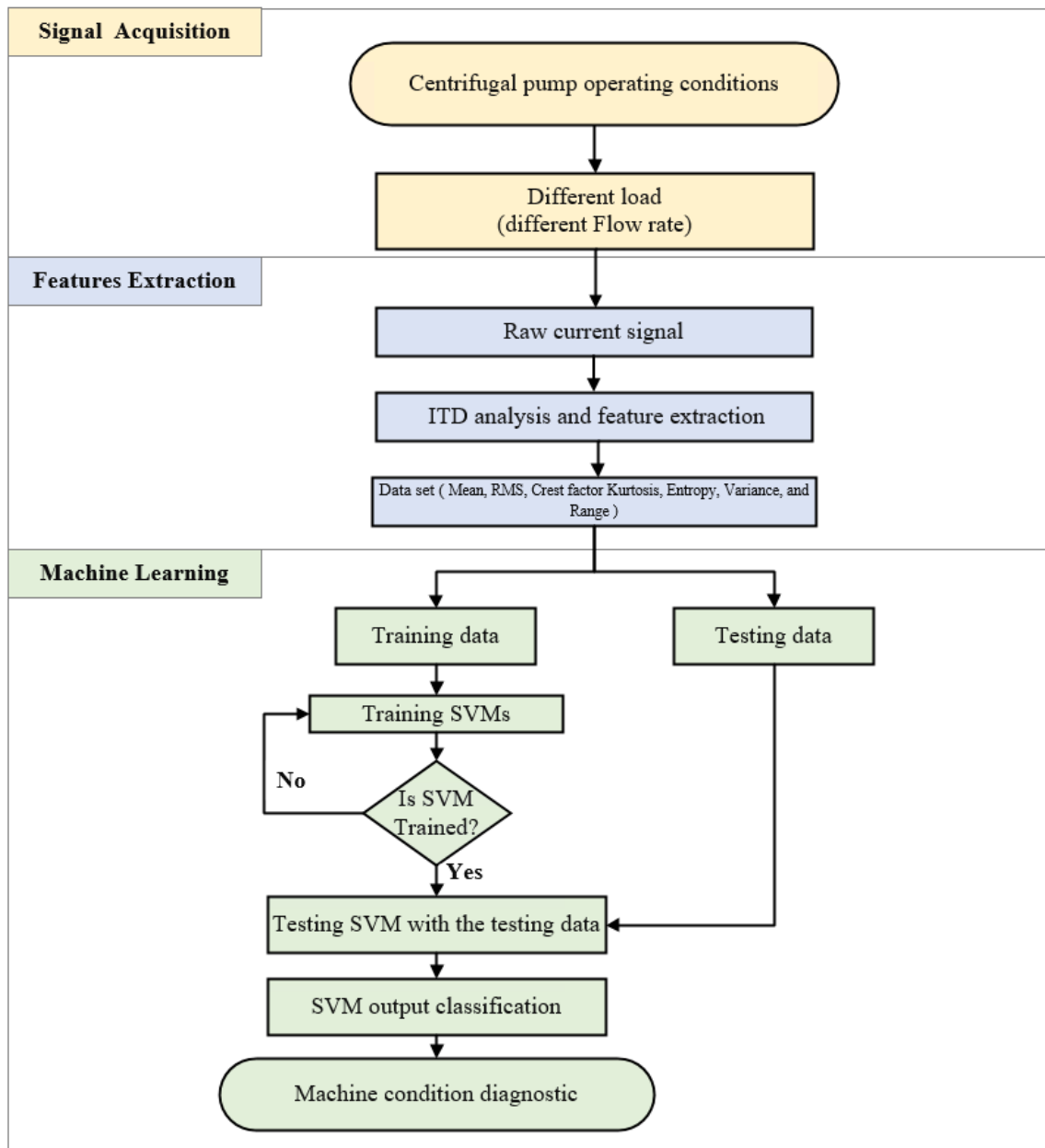


Figure 10-1 An adaptive diagnostic approach for a centrifugal pump based on data analysis and SVM.

### 10.3 SVM classifier based on ITD features

The current signals for each fault condition were analysed by ITD then the envelope analysis method was applied to the signals. After that, the statistical features (Mean, RMS, Crest factor Kurtosis, Entropy, Variance, and Range) were extracted from the first of the proper rotation components (PRCs) that contains substantial information concerning the current signal and used to generate the data sets.

For each case, the calculation of the seven features was obtained from 20 segments of the current signal for each of seven flow rates. Then data sets were combined together, in which the data corresponding to each of the four cases were distributed as 140 feature vectors for each case. As shown in Table 10-1. The dataset is split into two data sets; a training set (50%) and a testing set (50%). Each set contained the same number of cases, which were randomly selected, the training set was used for classifier construction and the test set for testing the model.

Table 10-1 Data set of statistical features (experimental data)

Fault Number	Fault condition	batch size	Training set	Test set
1	Baseline	140	70	70
2	Inner race fault	140	70	70
3	Outer race fault	140	70	70
4	Outer race fault with impeller blockage	140	70	70

The multi-SVM classifier was constructed using the MATLAB's built-in function 'fitcecoc', which required the training data set as input arguments, where each row of this matrix was given a class name that corresponded to the type of fault. Table 10-2 presents the class designation number and the class name. It should also be noted that the kernel function RBF was used to train the SVM classifier, that function was used because it has been shown to be better than other kernel functions such as the polynomial kernel, as the hyperparameters are fewer than in other functions [189].

Table 10-2 Multiclass SVM class names

Class number	Class label
1	Baseline
2	Inner race fault
3	Outer race fault
4	Outer race fault with blockage impeller

The constructed multiclass SVM classifier was then tested on the testing data set, where the class label was unseen by the classifier. The accuracy of SVM classification was computed using the standard formula for accuracy rate:

$$AC = \frac{\text{number of correctly classified samples}}{\text{total number of samples in dataset}} \times 100 \quad 10-1$$

A confusion matrix that conveniently presents comparable information was used to evaluate the SVM performance. The accuracy of results obtained from the classification of testing data is presented in Figure 10-2.

**ITD based Confusion Matrix**

Output Class	1	70 25.0%	0 0.0%	0 0.0%	0 0.0%	
	2	0 0.0%	70 25.0%	0 0.0%	0 0.0%	
	3	0 0.0%	0 0.0%	70 25.0%	1 0.4%	
	4	0 0.0%	0 0.0%	0 0.0%	69 24.6%	
		100% 0.0%	100% 0.0%	100% 0.0%	98.6% 1.4%	99.6% 0.4%
	1	2	3	4		Total
	<b>Target Class</b>					

Figure 10-2 Confusion matrix of multi-class SVM based on ITD features

Figure 10-2 shows the percentage of correct and incorrect classifications, that the classifier produced from the test data according to their corresponding class label (machine condition). The correct rate of the classification achieved across all cases was 99.6%, giving a mis-classification of just 0.4%. The classifier was 100% accurate classifying all

cases of baseline (healthy pump), inner race fault and outer race fault, while the compound fault had just one mis-classified.

Figure 10-3 shows the classification results in more detail, cases appear on blue trace are correctly classified, whilst, only single misclassified case (shifted from the blue trace) is the combined fault (outer race fault impeller blockage).

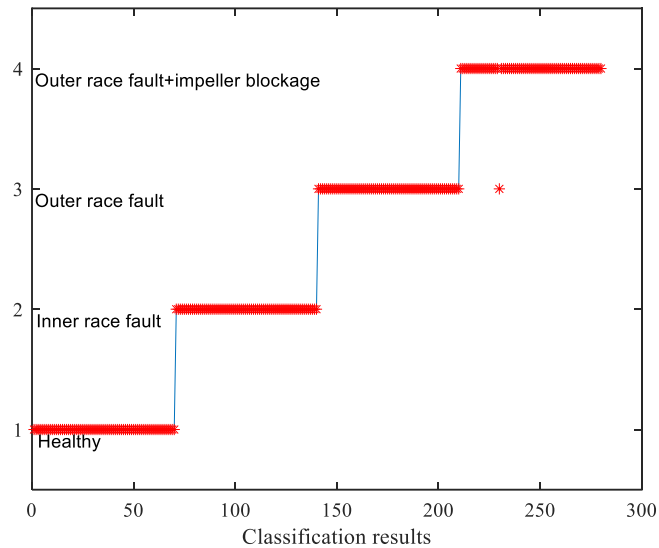


Figure 10-3 Multi-class SVM classification results using ITD features

#### 10.4 SVM classifier based on EMD features

The current signals of each of the four conditions were analysed using EMD, the envelope signals obtained, and statistical features (Mean, RMS, Crest factor Kurtosis, Entropy, Variance, and Range), were extracted from the first IMF that contains most of the information in the current signal, and using these features to generate the data sets. For each fault case, the calculated statistical features were, again, obtained from 20 segmentations of the current signal for each of the seven flow rates. Then the data sets were combined, in which the data corresponding to the fault cases were distributed as 140 feature vectors for each fault case.

The same procedure was carried out for dividing the dataset into training and testing sets, and constructing the multi-SVM classifier. The confusion matrix, including the accuracy rate of using EMD features is presented in Figure 10-4.



Figure 10-4 Confusion matrix of multi-class SVM based on EMD features

Figure 10-4 shows the accuracy of the classification results. The classifier was able to correctly identify the test data with their corresponding class label (machine condition) across 98.9% of cases, mis-classifying just 1.1%. The classifier classified all baseline (healthy) and inner race faults with 100% accuracy, while there were two mis-classified outer race faults and one mis-classified compound fault. The results indicated that the features extracted from EMD signals are highly efficient for diagnosing the pump faults. Figure 10-5 shows the correct and incorrect classification in more detail, where the correct classification appears on blue trace, and the mis-classified results are (shifted from the blue trace).

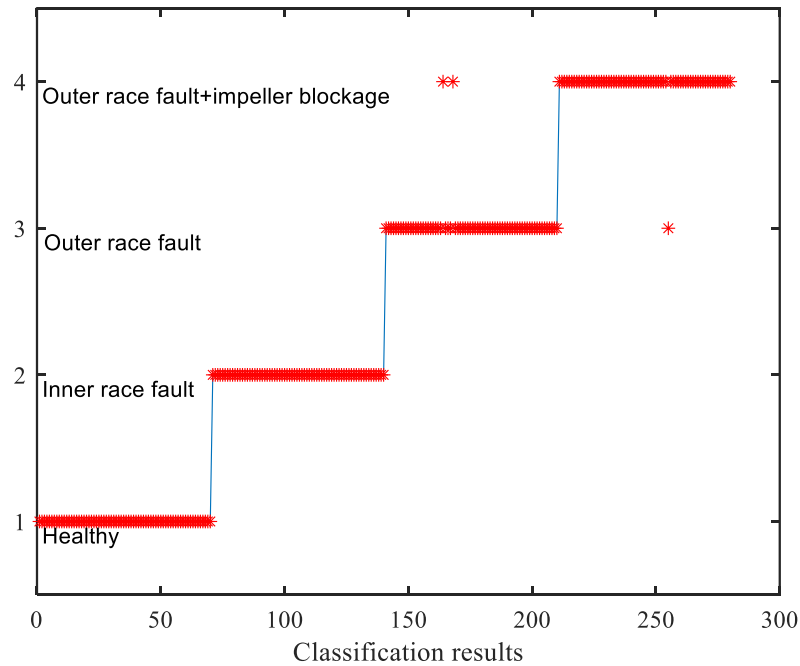


Figure 10-5 Multi-class SVM classification results using EMD features

### 10.5 SVM classifier based on DWT features:

The DWT is an implementation of the wavelet transform using discrete sets of the wavelet scales. The application of DWT is faster than CWT with fewer parameters, and has a good time and frequency resolutions [214]. The given signal is decomposed into low-pass approximation coefficient and high-pass detailed coefficients, and then on the next levels, only the approximation coefficients are decomposed into low-pass approximations while the high-pass details are kept. Then the reconstruction signal is obtained through the inverse wavelet transform of the detail coefficients [215].

The current signals for all the experimental conditions were analysed by DWT. The signal was decomposed into six levels, then envelope analysis was applied to the reconstructed signals, after that the same statistical features as listed above were extracted from 20 segmentations of each level of DWT results for each of the seven flow rates. When the data sets were combined together, there are 140 feature vectors for each fault case.

The same procedure was carried out for dividing the dataset into training and testing sets, and constructing the SVM classifier. The confusion matrix for showing the accuracy rate obtained using DWT features is presented in Figure 10-6.

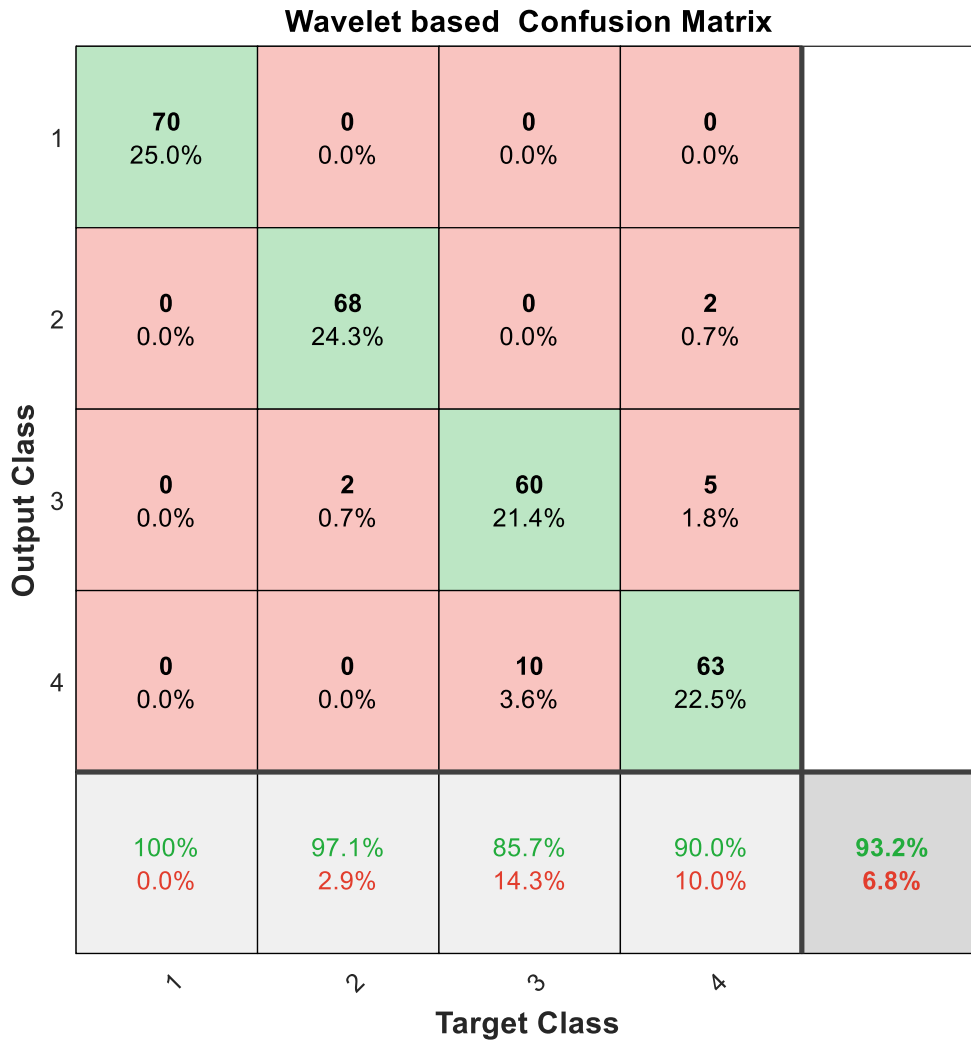


Figure 10-6 SVM Confusion matrix of multi-class SVM based on DWT features

The classifier classified all baseline (healthy) conditions correctly. There were two inner race faults, ten outer race faults and seven compound faults mis-classified. The overall accuracy rate was 93.2%.

Figure 10-7 shows the correct and incorrect classification based on DWT features in more detail.

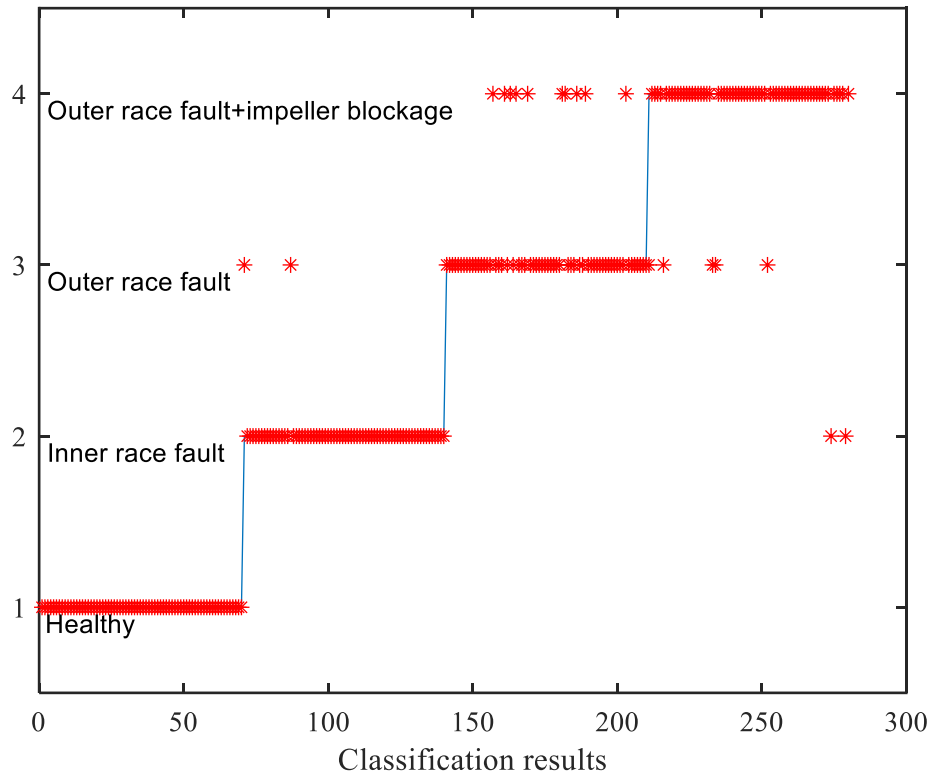


Figure 10-7 Multi-class SVM classification results using DWT features

### 10.6 SVM classifier based on Envelope features:

In this method, envelope analysis was applied to the current signals, after that the same statistical features stated previously were extracted. Data sets were generated and using these features from 20 segments of each envelope and for the seven flow rates. Then the data sets were combined to provide 140 feature vectors for each fault case.

The same procedure as described above, was carried out for dividing the dataset into training and testing sets, and constructing the multi-SVM classifier. The confusion matrix, including the accuracy rate using envelope features is presented in Figure 10-8.

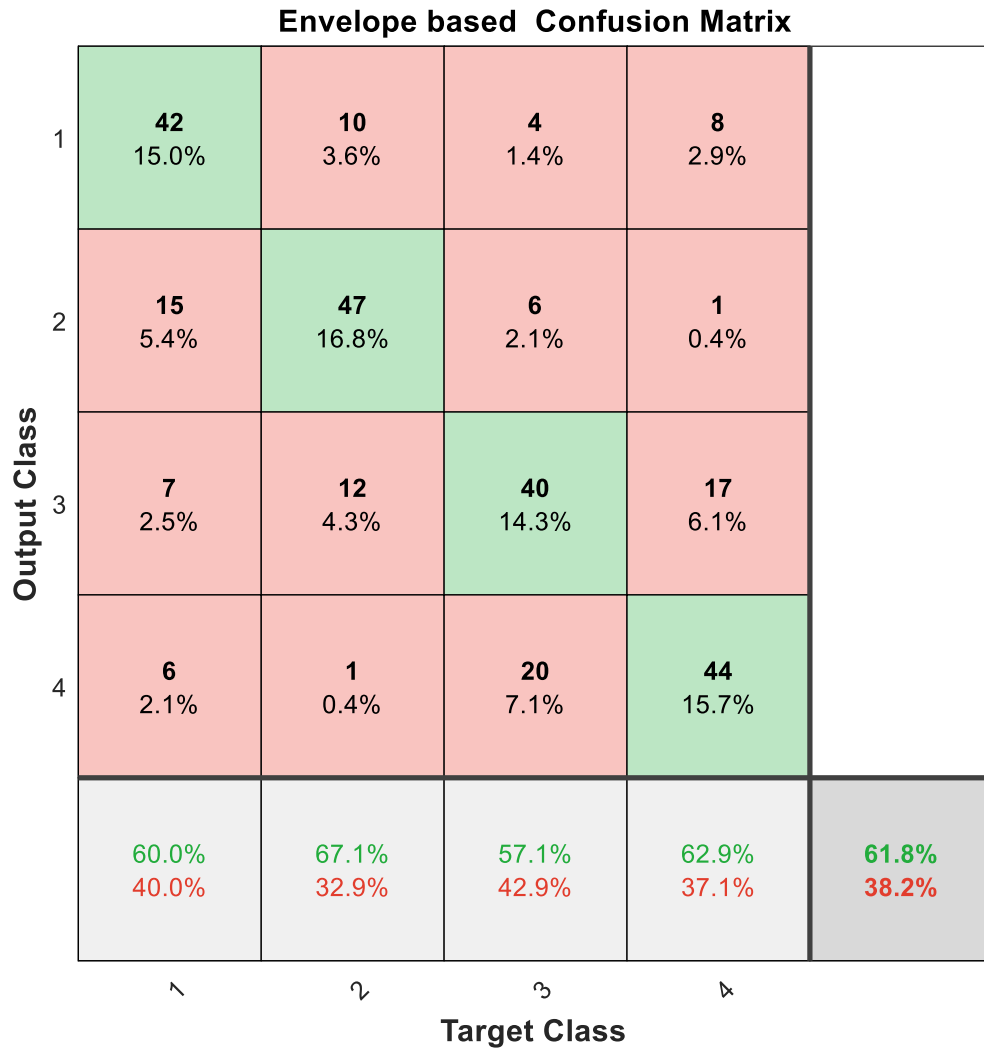


Figure 10-8 SVM Confusion matrix of multi-class SVM based on envelope features

From the figure, it can be seen that the overall accuracy of diagnosis was low (61.8%). For the healthy case, about 40% of were mis-classified. For the inner, outer and combined faults, the corresponding percentages were 32.9%, 42.9% and 37.1%, respectively. The results indicated that the feature extracted from envelope signals have relatively low accuracy and are not suited for diagnosing the given pump faults.

Figure 10-9 shows the correct and incorrect classification based on envelope features in more detail, again, the correct classification appear on the blue trace.

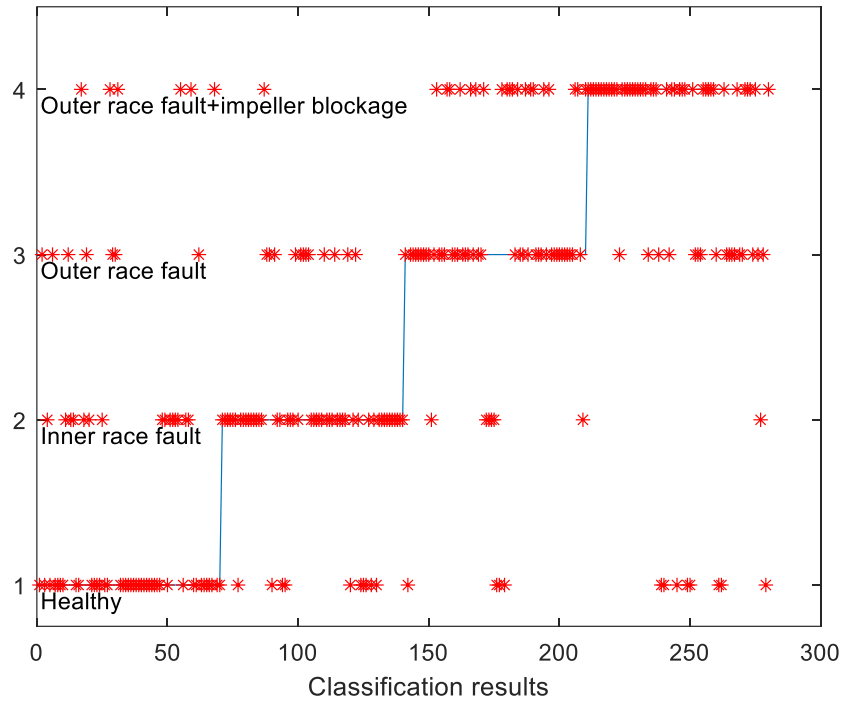


Figure 10-9 multi-class SVM classification results using envelope features

### 10.7 Comparison of the diagnostic approach with different methods:

To evaluate the proposed diagnostic approach, the results of the multi-class SVM classifier based on ITD features was compared with SVM multi-class classifier based on features obtained from the EMD, WDT, and envelope analysis. Table 10-3 shows the accuracy rate achieved from the SVM with different feature extraction techniques.

Table 10-3 Comparison of diagnostic results obtained using the different techniques for all cases

Machine condition	Accuracy rate			
	Envelope features	DWT features	EMD features	ITD features
Baseline	60 %	100 %	100 %	100 %
Inner race fault	67.1 %	97.1 %	100 %	100 %
Outer race fault	57.1 %	85.7 %	97.1 %	100 %
Outer race fault & impeller blockage	62.9 %	90.0 %	98.6 %	98.6 %
	61.8 %	93.2 %	98.9 %	99.6 %

From Table 10.3, it can be seen that the classifier SVM based on ITD features provides the best diagnostic information, for classification of the pump faults considered. The ITD features are marginally better than EMD because of the better diagnosis of the outer race fault (100% compared to 97.1%). However, a comparison of proportions showed no significant difference overall between the results obtained from ITD and EMD features. Also, ITD was significantly better at the 5% confidence level than DWT, mainly because of the lower score of the DWT on the outer race fault. ITD was very much better at diagnosis than the Envelope features at the 1% confidence level. Here a simple two-tailed difference of proportions test was used.

The classification rates for the different methods tested are presented in Figure 10-10. By examining the results of the table, it can be stated that utilizing ITD features for fault diagnosis can significantly enhance the prediction accuracy of SVM compared to the envelope, DWT and EMD. To compare the performance of the SVM classifier based on ITD features with other studies from literature, a further comparison is presented in Table 10-4.

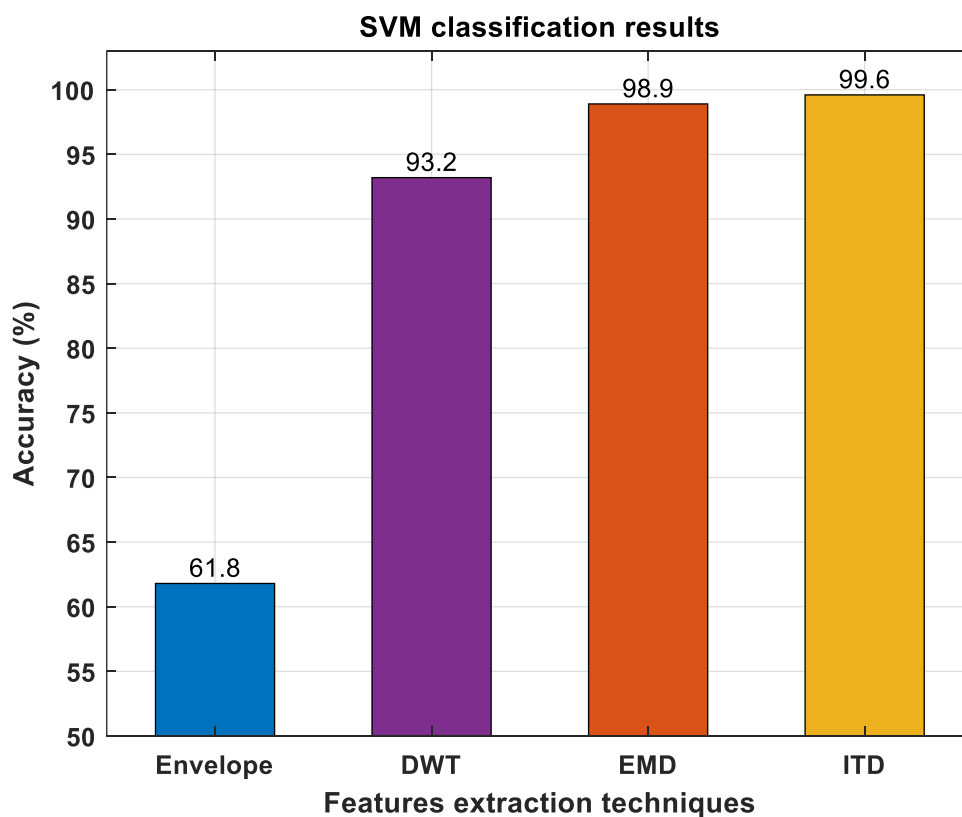


Figure 10-10 Comparison between different feature extraction techniques

Table 10-4 Comparison of the current work with the comparable work reported in the literature

Authors/Year	Types of faults	Sampling rate	Domain used	Classification method	Classification /best prediction accuracy	Remarks
Kumar [216]	Broken impeller, clogged impeller, bearing inner race defect, outer race defect	70 kHz	Time-frequency analysis	Genetic algorithm - SVM	96.66 %	Vibration signal
Yuvaraj, [217]	Bearing fault	2.06 kHz	Time domain	SVM	64.71%	Current signal
Jami and Haynes[218]	Cracked impeller, impeller imbalance	4.8 kHz	Time-frequency analysis	ANN - WPT	97.6 %	Vibration signal
Ebrahimi [219]	impeller wear, seal wear, cavitation	n/a	Time-frequency analysis	WT-SVM	96.67	Vibration signal
Wang, et al., [220]	Bearing roller defect, bearing inner race defect, bearing outer race defect, and impeller wear	10.24 kHz	Time frequency domain	Ensemble EMD-random forest	97.08%	Vibration signal
Sami (present work)	Inner race fault, outer race fault, compound fault (outer race fault and impeller blockage)	96 kHz	Time frequency domain	ITD-SVM	99.6%	Current signal

From Table 10-4, it can be seen that the diagnostic accuracy attained using different methods with different pump faults is high, mostly better than 96%, and that the method proposed and tested in the present work (ITD and SVM) has a higher prediction performance, 99.6%.

It is concluded that the data-driven technique based on the ITD method represents an effective and meaningful technique for processing the current signals, the features based

on ITD provide a good basis for describing the signature of the current signals. The diagnostic approach based on ITD with SVM is very effective for classifying the simulated faults of a centrifugal pump.

### **10.8 Key Findings**

In this chapter, an intelligent diagnostic approach was proposed based on a data-driven and machine learning technique for extracting meaningful features and distinguishing between seeded faults. Remarkably high classification accuracy was achieved when the SVM classifier was applied to ITD features, it shows the effectiveness of ITD in the task of extracting informative features from the motor current signals. ITD based features outperform envelope and DWT.

The results showed that the diagnostic approach (SVM and ITD) performed effectively, enhanced the monitoring of the pump operation under different flow rates, thereby demonstrating that it is capable of detecting and distinguishing between the given faults based on their motor current signatures. Comparison of these with published results show that SVM with ITD is effective as all other available techniques known to the author for diagnosing pump faults.

## Chapter 11      **Conclusions and Suggestions for Future Work**

*This chapter summarises the main findings of this study, and provides an overview of its major accomplishments. Additionally, a summary of the contributions of this research to knowledge is presented. Finally, suggestions for possible future work on the CM of centrifugal pumps are provided.*

## 11.1 Review of the Aims, Objectives and Achievements

The main objective of this study was to produce a platform using advanced ML paradigms capable of analysing the motor current signals of centrifugal pumps to detect developing faults and produce an accurate diagnosis, to improve CM performance. A comprehensive investigation, extracting fault features from current signals was carried out by using a variety of motor current analysis techniques. For fault detection and identification, a diagnostic approach based on data-driven methods, such as ITD and EMD, resulted in a machine learning technique being adopted for this research programme. Advanced MCSA techniques have been used to improve the diagnostic methods for three specific centrifugal pump defects under a wide range of flow rates.

In this section, the achievements of this thesis are reviewed corresponding with the research Objectives listed in Section 5.1. The objectives of this research have been fulfilled as follows:

**Objective 1.** To review CM methods and maintenance strategies and explain the most common techniques used for fault detection of centrifugal pumps.

**Achievement:** A comprehensive review of CM was presented to evaluate the techniques most frequently used for monitoring rotating machines. These techniques were discussed in Chapter 2; maintenance strategies and some essential concepts were considered in Sections 2.3 and 2.4. It has been demonstrated that motor current analysis is a reliable technique for detecting and diagnosing machine faults. This provided motivation for investigating accurate and reliable monitoring techniques to achieve a more sensitive and more accurate monitoring technique.

**Objective 2.** To refine the existing test facility and use it for monitoring the condition of a centrifugal pump with different simulated pump faults under various flow rates.

**Achievement:** The existing facilities, suitably adapted, were used for investigating the condition of the centrifugal pump under different operating conditions. A full description and explanation of this test rig is presented in Chapter 6. The experimental tests were performed on a healthy centrifugal pump and pump with three common faults seeded into it. During the tests, several parameters were monitored and recorded, including flow rate,

vibration and suction pressure, to assess the pump condition. Motor current data were gathered for the healthy and simulated fault conditions under various flow rates.

**Objective 3.** To examine the ability of motor current data obtained from the electrical control system for detecting various mechanical faults of the pump by examining the current signature using various signal process techniques.

**Achievement 3:** A comprehensive review has been presented in Section 2.6.4, to assess the MCSA as a means of detecting and diagnosing faults in rotating machines. Also, some theoretical background is presented to aid understanding of the characteristics of the current data when the pump operates under different conditions and different loads. In Section 3.8, the behaviour of the motor current is explained when changes in the load torque resulted from change of working conditions, such as due to a mechanical defect, will require corresponding modifications of the motor torque to maintain the desired pump speed. This review demonstrated that the MSCA is reliable and accurate for fault detection and diagnosis, and it can be employed in an effective means of monitoring the health of a centrifugal.

**Objective 4.** To explore the current signal under different operating conditions using conventional data analysis methods to identify and obtain the most critical fault defining feature, that will be used for comparison with those obtained from the data-driven techniques.

**Achievement 4:** Conventional signal processing techniques according to the time and frequency domain were applied to detect and diagnose the simulated pump faults. In Chapter 7, it is shown that the given mechanical faults lead to a rise in the amplitude of the current signals, also shown are some AM effects. However, though the statistical parameters presented some differences between the cases, this method was not adequate for distinguishing between the different seeded faults and defining the condition of the pump. Hence a more advanced signal processing technique was required.

**Objective 5.** To explore and apply data-driven techniques for extraction of the weak nonlinear characteristics of the current signals that are affected by, for example, fluctuations in pump operating pressures and flow rate, and various electromagnetic noises interfering with the measured signals.

**Achievement:** Effective adaptive analysis techniques have been explained in Sections 4.6 and 4.7. These were implemented to reduce noise and determine the diagnostic features from modulating motor current data that corresponded to the pump operation. EMD and Hilbert transform were used in an attempt to detect the centrifugal pump faults as presented in Chapter 8, where the envelope was used to obtain the demodulated current signals. The proposed method based on EMD analysis with envelope spectra of the current signature is demonstrated to be valuable in detecting the presence of the seeded centrifugal pump faults under different flow rates. In addition, ITD was used to decompose the motor current signal to extract the most informative features for increasing the diagnostic efficiency. Chapter 9 explained this technique and the analysis results show that the 1<sup>st</sup> PRC can explain the characteristics of the motor current, and can be used for detecting the presence of seeded, common pump faults under a wide range of pump operating conditions

**Objective 6.** To examine supervised machine learning techniques such as SVM, for enhancement of CM performances based on the electrical data from the motor.

**Achievement:** A comprehensive review is presented in Chapter 5 to explain the structure of the supervised classification technique that was used to classify the conditions of the rotating machine. The SVM algorithm was chosen to be used for the classification task.

**Objective 7.** To investigate and evaluate the use of ITD combined with SVM classification algorithm to detect and diagnose the seeded faults. Also, to compare the results of the proposed method with those adopted using a combination of the SVM algorithm with EMD, with DWT and with envelope analysis. The results will also be compared with those of other researchers in this area.

**Achievement:** The SVM and ITD combination is shown in Chapter 10 to successfully diagnose a given fault in 99.6% of cases. Utilizing ITD features for fault diagnosis significantly enhanced the prediction accuracy of SVM compared to DWT and envelope analysis, and marginally better than EMD, see Table 10-3. The results were compared with those of other researchers in this topic area, see Table 10-4. It can be seen that the diagnostic accuracy attained by those researchers, using different methods with different pump faults is high, mostly better than 96%, and that the method proposed and tested in the present work (ITD and SVM) has a higher prediction performance, 99.6%.

**Objective 8.** To provide meaningful recommendations for future research in this particular subject.

**Achievement:** A number of recommendations for future research in the CM of centrifugal pumps are presented in Section 11.34.

## 11.2 Conclusion

The results show that the proposed framework (diagnostic approach ) is robust and effective for fault detection and diagnosis based on a combined ITD with SVM method. The ITD gave good results in feature extraction and accurate fault diagnosis based on SVM classification.

From the research work and the investigation procedures described in the previous chapters, a number of conclusions and primary findings can be summarized as:

1. It is confirmed that MCSA is a non-intrusive method and can be carried out with low-cost equipment. The motor current signature of the centrifugal pump is influenced by the operating conditions and the defects incorporated in it. The motor current signal has meaningful information for detecting and diagnosing the machine faults.
2. A comprehensive investigation was successful for developing reliable and robust diagnosis methods based on the motor current signatures. MCSA using conventional techniques was able to detect the presence of faults but not able to distinguish between the seeded faults, because faults were similar with very similar characteristics. Advanced data analysis technique was found to be necessary to extract features contaminated by the noise that contained the necessary relevant characteristics of the signals for successful diagnosis.
3. EMD analysis was effective in decomposing the complicated nonlinear component of the current data and reducing the noise to extract the main frequency components that provide useful information for detecting centrifugal pump faults.
4. Envelope spectral analysis was utilized to demodulate the current signal and reveal the weak nonlinear components of the current signals. A combined method based on EMD and envelope analysis of the current signature was demonstrated to be great for detecting the presence of centrifugal pump faults under different flow rates.

5. ITD data-driven technique was used for MCSA of the centrifugal pump. It allows accurate extraction of the modulation features, which are due to the nonlinear effects of the various pump faults. The proposed ITD technique shows an effective method for extracting useful diagnostic information, leading to an accurate diagnosis. It was able to differentiate between the seeded faults only with prior knowledge of their relative magnitudes
6. Supervised machine learning techniques have been employed to distinguish between the seeded pump faults using features extracted from the current signals of the centrifugal pump under different flow rates.
7. The results of the diagnostic approach for classifying the pump faults have demonstrated the capability of using the current signature for monitoring the centrifugal pump condition. It is concluded that ITD with SVM has a high capability for characterizing and distinguishing the faults depending on their current signature
8. The diagnostic approach based on ITD features is relatively reliable and accurate for fault detection and diagnosis compared with the results obtained from other means, as listed in Table 10-3, envelope, EMD and DWT based features.

### **11.3 Contributions to the Knowledge**

This research offered several contributions to the literature in the field of CM, by applying a number of techniques based on the MCSA for accurately evaluating the pump's condition and diagnosing the faults in the centrifugal pump. The principal contributions in this thesis are:

**Contribution 1:** The novel data-driven technique (SVM + ITD) developed in this research programme has been shown to be very effective for extracting diagnostic features from the motor current data and distinguishing between seeded faults.

**Contribution 2:** The results show that the EMD analysis combined with envelope spectra of the current signature is effective in detecting the presence of the seeded pump faults. This proposed method becomes more efficient than the other conventional methods used in this study.

**Contribution 3:** Fault classification of the centrifugal pump using the proposal adaptive diagnostic approach, constructed based on the data-driven method and ML algorithm has demonstrated to be a powerful approach for fault diagnosis. The analysis results of the diagnostic approach using ITD features increased the accuracy of monitoring the condition of the pump, compared with the other conventional methods techniques. This diagnostic approach, based on ITD for pre-processing current signal and SVM for classification, has not been found in previous studies.

The author believes that the application of ITD for analysis the current signals for CM of a centrifugal pump and SVM for classification the faults is novel as no reports in the literature used the method applied in this thesis for detection and diagnosis of centrifugal pump faults.

#### **11.4 Recommendations for Future Work**

Based on this thesis, a number of recommendations for future works are made that could improve CM and fault diagnosis of centrifugal pumps:

**Recommendation 1:** Investigate condition monitoring of rotating machine using data fusion of both current and other data such as vibration. The effectiveness of these methods could be compared with MCSA.

**Recommendation 2:** More experimental work is required on a suitable test rig for gathering a wide range of datasets including vibration, acoustic emissions and so on and develop data fusion methods with AI techniques for reliable and interpretable diagnostics method.

**Recommendation 3:** Investigate current analysis using other data-driven methods to improve the accuracy of the CM by examining characteristics in the frequency domain, including higher-order harmonics and implementing an optimization algorithm for selecting the optimal features.

**Recommendation 4:** Examine fault diagnosis methods to enhance CM by developing more effective signal processing techniques for detecting common combined pump faults such as mechanical and electrical faults.

**Recommendation 5:** Develop a fault diagnosis approach using other machine learning methods such as CNN and other state of the art deep learning algorithms for feature extraction and classification, and compare systematically the results with the proposed methods.

**Recommendation 6:** Extend the proposed diagnostic approach to diagnose other faults such as incipient leakages and faults with different severity.

## References

1. Soliman, H., Wang, H., and Blaabjerg, F., "A review of the condition monitoring of capacitors in power electronic converters." *IEEE Transactions on Industry Applications*, 2016. **52**(6): p. 4976-4989.
2. Randall, R.B., "Vibration-based condition monitoring: industrial, aerospace and automotive applications." 2011: John Wiley & Sons.
3. Yang, O.S. and Widodo, A., "Introduction of intelligent machine fault diagnosis and prognosis." 2009, New York: Nova Science Publishers.
4. Tavner, P., Ran, L., Penman, J., and Sedding, H., "Condition monitoring of rotating electrical machines." Vol. 56. 2008: IET.
5. Stetco, A., Dinmohammadi, F., Zhao, X., Robu, V., Flynn, D., Barnes, M., Keane, J., and Nenadic, G., "Machine learning methods for wind turbine condition monitoring: A review." *Renewable Energy*, 2018.
6. Stetco, A., Dinmohammadi, F., Zhao, X., Robu, V., Flynn, D., Barnes, M., Keane, J., and Nenadic, G., "Machine learning methods for wind turbine condition monitoring: A review." *Renewable Energy*, 2018.
7. Tian, X., Feng, G., Chen, Z., Albraik, A., Gu, F., and Ball, A., "The investigation of motor current signals from a centrifugal pump for fault diagnosis." in *The investigation of motor current signals from a centrifugal pump for fault diagnosis*. 2014, COMADEM.
8. Hussein, N.A., Mahmood, D.Y., and Abdul-Baki, E.M., "3-phase induction motor bearing fault detection and isolation using MCSA technique based on neural network Algorithm." *Journal of Engineering and Sustainable Development*, 2012. **16**(3): p. 175-189.
9. Verma, A.K., Radhika, S., and Padmanabhan, S. "Wavelet Based Fault Detection and Diagnosis Using Online MCSA of Stator Winding Faults Due to Insulation Failure in

- Industrial Induction Machine." in IEEE Recent Advances in Intelligent Computational Systems (RAICS). 2018. IEEE.
10. Jardine, A.K., Lin, D., and Banjevic, D., "A review on machinery diagnostics and prognostics implementing condition-based maintenance." *Mechanical Systems and Signal Processing*, 2006. **20**(7): p. 1483-1510.
  11. Muralidharan, V., Sugumaran, V., and Indira, V., "Fault diagnosis of monoblock centrifugal pump using SVM." *Engineering Science and Technology, an International Journal*, 2014. **17**(3): p. 152-157.
  12. Kostyukov, V. and Tarasov, E., "Centrifugal pumps in downstream: operational safety increase." *Procedia Engineering*, 2016. **152**: p. 505-510.
  13. Selvakumar, J. and Natarajan, K., "Failure analysis of centrifugal pumps based on survey." *ARPN Journal of Engineering and Applied Sciences*, 2015. **10**(4).
  14. Saad, N., Irfan, M., and Ibrahim, R., "Condition Monitoring and Faults Diagnosis of Induction Motors: Electrical Signature Analysis." 2018.
  15. Choudhary, A., Goyal, D., Shimi, S.L., and Akula, A., "Condition monitoring and fault diagnosis of induction motors: A review." *Archives of Computational Methods in Engineering*  
2019. **26**(4): p. 1221-1238.
  16. Frei, M.G. and Osorio, I. "Intrinsic time-scale decomposition: time–frequency–energy analysis and real-time filtering of non-stationary signals." in *Proceedings of the Royal Society of London A: Mathematical, Physical and Engineering Sciences*. 2007. The Royal Society.
  17. Vaimann, T. and Kallaste, A. "Condition Monitoring of Electrical Machines." in *11th Int. Symp. "Topical problems in the field of el. and power eng.* 2012.
  18. Awadallah, M.A. and Morcos, M.M., "Application of AI tools in fault diagnosis of electrical machines and drives-an overview." *IEEE Transactions on energy conversion*, 2003. **18**(2): p. 245-251.

19. Isermann, R. and Isermann, R., "Fault-Diagnosis Applications: Model-Based Condition Monitoring: Actuators, Drives, Machinery, Plants, Sensors, and Fault-tolerant Systems." 1st ed. 2011, Berlin, Heidelberg: Springer Berlin Heidelberg.
20. Singh, K. and Komal, S., "Condition Monitoring of Induction Motor." International Journal of Engineering & Technical Research, 2015. **3**(4): p. 290-293.
21. Boyce, M.P., "Centrifugal compressors: a basic guide." 2003: PennWell Books.
22. Tavner, P.J., "Wave and tidal generation devices: reliability and availability." Vol. 18. 2017, London: Institution of Engineering and Technology.
23. Scheffer, C. and Girdhar, P., "Practical machinery vibration analysis and predictive maintenance." 2004: Elsevier.
24. Deighton, M.G., "Facility Integrity Management - Effective Principles and Practices for the Oil, Gas, and Petrochemical Industries." in Facility Integrity Management - Effective Principles and Practices for the Oil, Gas, and Petrochemical Industries. 2016, Elsevier.
25. Mehta, B.R. and Reddy, Y.J., "Industrial process automation systems: design and implementation." 2014: Butterworth-Heinemann.
26. Vamsi, I., Sabareesh, G., Penumakala, P.J.M.S., and Processing, S., "Comparison of condition monitoring techniques in assessing fault severity for a wind turbine gearbox under non-stationary loading." 2019. **124**: p. 1-20.
27. Cheng, S., Du, Y., Restrepo, J.A., Zhang, P., and Habetler, T.G., "A nonintrusive thermal monitoring method for induction motors fed by closed-loop inverter drives." IEEE Transactions on Power Electronics, 2012. **27**(9): p. 4122-4131.
28. Janssens, O., Loccafier, M., Van de Walle, R., Van Hoecke, S.J.I.P., and Technology, "Data-driven imbalance and hard particle detection in rotating machinery using infrared thermal imaging." 2017. **82**: p. 28-39.
29. Barksdale, H., Smith, Q., and Khan, M. "Condition Monitoring of Electrical Machines with Internet of Things." in SoutheastCon 2018. 2018. IEEE.

30. Albla, A.A., Brkovic, B.M., Jecmenica, M.M., and Lazarevic, Z.M., "Online temperature monitoring of a grid connected induction motor." *International Journal of Electrical Power & Energy Systems*, 2017. **93**: p. 276-282.
31. Zhou, Z., Gui, L., Tan, Y., Liu, M., Liu, Y., and Li, R., "Actualities and development of heavy-duty CNC machine tool thermal error monitoring technology." *Chinese Journal of Mechanical Engineering*, 2017. **30**(5): p. 1262-1281.
32. Gulati, R. and Smith, R., "Maintenance and reliability best practices." 2009: Industrial Press Inc.
33. Goyal, D. and Pabla, B., "The vibration monitoring methods and signal processing techniques for structural health monitoring: a review." *Archives of Computational Methods in Engineering*, 2015: p. 1-10.
34. Singh, G. and Ahmed, S., "Vibration signal analysis using wavelet transform for isolation and identification of electrical faults in induction machine." *Electric Power Systems Research*, 2004. **68**(2): p. 119-136.
35. Kia, S.H., Henao, H., and Capolino, G., "Gear tooth surface damage fault detection using induction machine stator current space vector analysis." *IEEE Transactions on Industrial Electronics*, 2014. **62**(3): p. 1866-1878.
36. Loutas, T., Sotiriades, G., Kalaitzoglou, I., and Kostopoulos, V., "Condition monitoring of a single-stage gearbox with artificially induced gear cracks utilizing on-line vibration and acoustic emission measurements." *Applied Acoustics*, 2009. **70**(9): p. 1148-1159.
37. Yang, Z., Jin, L., Yan, Y., and Mei, Y., "Filament breakage monitoring in fused deposition modeling using acoustic emission technique." *Sensors*, 2018. **18**(3): p. 749.
38. Salameh, J.P., Cauet, S., Etien, E., Sakout, A., and Rambault, L., "Gearbox condition monitoring in wind turbines: A review." *Mechanical Systems and Signal Processing*, 2018. **111**: p. 251-264.
39. Wu, H., Yu, Z., and Wang, Y., "Real-time FDM machine condition monitoring and diagnosis based on acoustic emission and hidden semi-Markov model." *The*

International Journal of Advanced Manufacturing Technology, 2017. **90**(5-8): p. 2027-2036.

40. Baydar, N. and Ball, A., "Detection of gear failures via vibration and acoustic signals using wavelet transform." *Mechanical Systems and Signal Processing*, 2003. **17**(4): p. 787-804.
41. Alfayez, L. and Mba, D., "Detection of incipient cavitation and determination of the best efficiency point for centrifugal pumps using acoustic emission." *Proceedings of the Institution of Mechanical Engineers, Part E: Journal of process mechanical engineering*, 2005. **219**(4): p. 327-344.
42. Haynes, H. and Kryter, R., "Condition monitoring of machinery using motor current signature analysis." 1989, Oak Ridge National Lab., TN (USA).
43. Naid, A., Gu, F., and Ball, A., "Fault detection and diagnosis of reciprocating compressors using motor current signature analysis." 2009, PhD Thesis. University of Huddersfield.
44. Karmakar, S., Chattopadhyay, S., Mitra, M., and Sengupta, S., "Induction Motor Fault Diagnosis : Approach Through Current Signature Analysis." 2016, Singapore: Springer.
45. Mohanty, A.R., "Machinery condition monitoring: Principles and practices." 2014: CRC Press.
46. Pradhan, P.K., Roy, S., and Mohanty, A., "Detection of Broken Impeller in Submersible Pump by Estimation of Rotational Frequency from Motor Current Signal." *Journal of Vibration Engineering and Technologies*, 2019: p. 1-8.
47. Miljković, D., "Brief Review of Motor Current Signature Analysis." *HDKBR info magazin*, 2015. **5**(1): p. 14-26.
48. Luo, Y., Zhixiang, X., Sun, H., Yuan, S., and Yuan, J., "Research on the induction motor current signature for centrifugal pump at cavitation condition." *Advances in Mechanical Engineering*, 2015. **7**(11).

49. Singh, S., Kumar, A., and Kumar, N., "Motor current signature analysis for bearing fault detection in mechanical systems." *Procedia Materials Science*, 2014. **6**: p. 171-177.
50. Popaleny, P., Duyar, A., Ozel, C., and Erdogan, Y. "Electrical Submersible Pumps Condition Monitoring Using Motor Current Signature Analysis." in *Abu Dhabi International Petroleum Exhibition & Conference*. 2018. Society of Petroleum Engineers.
51. Riera-Guasp, M., Fernández Cabanas, M., Antonino-Daviu, J.a., Pineda-Sanchez, M., and Rojas García, C.H. "Influence of non-consecutive bar breakages in motor current signature analysis for the diagnosis of rotor faults in induction motors." in *IEEE Transactions on energy conversion*. 2010. Institute of Electrical and Electronics Engineers.
52. Rangel-Magdaleno, J., Ramirez-Cortes, J., and Peregrina-Barreto, H. "Broken bars detection on induction motor using MCSA and mathematical morphology: An experimental study." in *IEEE International Instrumentation and Measurement Technology Conference (I2MTC)*. 2013. IEEE.
53. Picazo-Ródenas, M.J., Antonino-Daviu, J., Climente-Alarcon, V., Royo-Pastor, R., and Mota-Villar, A., "Combination of noninvasive approaches for general assessment of induction motors." *IEEE Transactions on Industry Applications*, 2015. **51**(3): p. 2172-2180.
54. Niu, G., Widodo, A., Son, J.-D., Yang, B.-S., Hwang, D.-H., and Kang, D.-S., "Decision-level fusion based on wavelet decomposition for induction motor fault diagnosis using transient current signal." 2008. **35**(3): p. 918-928.
55. Bravo-Imaz, I., Ardakani, H.D., Liu, Z., García-Arribas, A., Arnaiz, A., and Lee, J., "Motor current signature analysis for gearbox condition monitoring under transient speeds using wavelet analysis and dual-level time synchronous averaging." *Mechanical Systems and Signal Processing*, 2017. **94**: p. 73-84.

56. Lau, E.C. and Ngan, H., "Detection of motor bearing outer raceway defect by wavelet packet transformed motor current signature analysis." *IEEE Transactions on Instrumentation and measurement*, 2010. **59**(10): p. 2683-2690.
57. Kar, C. and Mohanty, A., "Monitoring gear vibrations through motor current signature analysis and wavelet transform." *Mechanical Systems and Signal Processing*, 2006. **20**(1): p. 158-187.
58. Kompella, K.D., Rao, M.V.G., and Rao, R.S., "Bearing fault detection in a 3 phase induction motor using stator current frequency spectral subtraction with various wavelet decomposition techniques." *Ain Shams Engineering Journal*, 2017.
59. Sun, H., Luo, Y., Yuan, S., and Yin, J., "Hilbert spectrum analysis of unsteady characteristics in centrifugal pump operation under cavitation status." *Annals of Nuclear Energy*, 2018. **114**: p. 607-615.
60. Amirat, Y., Benbouzid, M., Wang, T., Bacha, K., and Feld, G., "EEMD-based notch filter for induction machine bearing faults detection." *Applied Acoustics*, 2018. **133**: p. 202-209.
61. Badr, H.M. and Ahmed, W.H., "Pumping Machinery Theory and Practice." 2014: John Wiley & Sons, Incorporated.
62. Prosoli, M. "Centrifugal pump Overview ". 2005 [cited 12/06/2007]; Available from: [https://www.mi-wea.org/docs/Prosoli%20-%20Centrifugal\\_Pumps\\_Overview.pdf](https://www.mi-wea.org/docs/Prosoli%20-%20Centrifugal_Pumps_Overview.pdf).
63. Hall, S. and Branan, C.R., "Rules of thumb for chemical engineers, fifth edition." 5th ed. 2012, Waltham, Mass; Oxford, U.K: Butterworth-Heinemann.
64. Girdhar, P. and Moniz, O., "Practical centrifugal pumps." 2011: Elsevier.
65. Nolan, D.P., "Fire Pump Arrangements at Industrial Facilities." 2017: Gulf Professional Publishing.
66. Chaurette, J. "Centrifugal pump system tutorial." 2005 [cited 04/06/2018]; Available from: <http://www.pumpfundamentals.com/images/tutorial/tutorial.pdf>.
67. Gülich, J.F., "Centrifugal pumps." 2008: Springer.

68. Choi, J.-H., "Model based diagnostics of motor and pumps." 2006.
69. Ellis, J., "Pressure transients in water engineering: a guide to analysis and interpretation of behaviour." 2008, London: Thomas Telford.
70. Kamiel, B.P., "Vibration-Based Multi-Fault Diagnosis for Centrifugal Pumps." 2015.
71. Parrondo, J.L., Velarde, S., and Santolaria, C., "Development of a predictive maintenance system for a centrifugal pump." *Journal of Quality in Maintenance Engineering*, 1998. **4**(3): p. 198-211.
72. Taylor, D.A., "Introduction to marine engineering." 1996: Elsevier.
73. Smith, R. and Mobley, R.K., "Industrial machinery repair: best maintenance practices pocket guide." 2003: Butterworth-Heinemann.
74. Bing, H., Cao, S., Tan, L., and Zhu, B., "Effects of meridional flow passage shape on hydraulic performance of mixed-flow pump impellers." *Chinese Journal of Mechanical Engineering*, 2013. **26**(3): p. 469-475.
75. Sahdev, M. "Centrifugal Pumps: Basic Concepts of Operation, Maintenance, and Troubleshooting (Part- I), Presented at the Chemical Engineers." [cited 24/07/2017]; Available from: : <http://www.plant-maintenance.com/articles/centrifugalpumps.pdf>
76. Mackay, R., "The practical pumping handbook." 2004, New York; Oxford; Elsevier.
77. Nolan, D.P., "Fire fighting pumping systems at industrial facilities." 2011: William Andrew.
78. Steele, A., "Advanced Plumbing Technology 2." 2015: American Society of Plumbing Engineers.
79. Gülich, J.F., "Centrifugal Pumps." 2010, Berlin, Heidelberg, GERMANY: Springer Berlin Heidelberg.
80. Karassik, I. and McGuire, J.T., "Centrifugal pumps." 2012: Springer Science & Business Media.

81. Bachus, L. and Custodio, A., "Know and understand centrifugal pumps." 2003: Elsevier.
82. Garr M. Jones and Robert L. Sanks, "Pumping Station Design: Revised 3rd Edition." 2011: Elsevier Science.
83. Bachus, L. and Custodio, A., "Know and understand centrifugal pumps." 2003, New York; Oxford; Elsevier.
84. Lobanoff, V.S. and Ross, R.R., "Centrifugal pumps: design and application." 2013: Elsevier.
85. Sulzer Pumps, L., "Centrifugal Pump Handbook." 2010, San Diego, CA, USA: Elsevier Science.
86. Bloch, H.P. and Budris, A.R., in Pump User's Handbook - Life Extension (4th Edition). 2014, Fairmont Press, Inc.
87. Towler, G. and Sinnott, R.K., "Chemical engineering design: principles, practice and economics of plant and process design." 2012: Elsevier.
88. King, M.L. "Selecting mechanical seals." 2005 [cited 26/07/2018]; Available from: [http://www.peerlessxnet.com/documents/tibs/TIB-29\\_selecting-mechanical-seals.pdf](http://www.peerlessxnet.com/documents/tibs/TIB-29_selecting-mechanical-seals.pdf).
89. Mishra, C., Samantaray, A., and Chakraborty, G., "Rolling element bearing fault diagnosis under slow speed operation using wavelet de-noising." Measurement, 2017. **103**: p. 77-86.
90. Boglietti, A. and Cavagnino, A., "Analysis of the endwinding cooling effects in TEFC induction motors." IEEE Transactions on Industry Applications, 2007. **43**(5): p. 1214-1222.
91. Coker, A.K. and Ludwig, E.E., "Ludwig's applied process design for chemical and petrochemical plants." 4th ed. 2007, Boston: Elsevier Gulf Professional Pub.
92. Bentley, S., Walski, T.M., Barnard, T.E., Harold, E., Merritt, L.B., Walker, N., and Whitman, B.E., "Wastewater Collection System Modeling and Design." 2007, Bentley Institute Press.

93. Oberg, E., Horton, H.L., Ryffel, H.H., and McCauley, C., "Machinery's Handbook Guide." 2016: Industrial Press, Incorporated.
94. Savic, D.A., Savic, D., Banyard, J.K., and Savic, D.A., "Water distribution systems." 2011, London: ICE Pub.
95. Smith, K. and Slabaugh, R., "Water Quality in Distribution Systems-M68." 2017, AWWA.
96. Walski, T.M. and Barnard, T.E., "Wastewater collection system modeling and design." Vol. 1. 2004: Haestad Press.
97. Oberg, E., Jones, F.D., Horton, H.L., and Ryffel, H.H., "Machinery's Handbook (30th Edition)." 2016: Industrial Press.
98. Sun, H., Yuan, S., Luo, Y., and Energy, "Characterization of cavitation and seal damage during pump operation by vibration and motor current signal spectra." Proceedings of the Institution of Mechanical Engineers, Part A: Journal of Power, 2019. **233**(1): p. 132-147.
99. Weidong, C., Lingjun, Y., Bing, L., and Yining, Z., "The influence of impeller eccentricity on centrifugal pump." Advances in Mechanical Engineering, 2017. **9**(9).
100. Reid, R.N., "Water Quality and Systems - A Guide for Facility Managers (2nd Edition)." 2004, Fairmont Press, Inc.
101. Urbanowski, R., "IADC Drilling Manual." Vol. Volume 1 and 2 (12th Edition) 2015, Houston, Texas: International Association of Drilling Contractors (IADC).
102. Zarei, J., "Induction motors bearing fault detection using pattern recognition techniques." Expert Systems with Applications, 2012. **39**(1): p. 68-73.
103. Gu, F., Tian, X., Chen, Z., Wang, T., Rehab, I., and Ball, A., "Fault severity diagnosis of rolling element bearings based on kurtogram and envelope analysis." 2014.
104. Pise, S.M. and Kulkarni, S.S., "A Review on Investigation of Effect of Surface Defect on Ball Bearing Vibration Response." 2016.

105. Akin, B., Orguner, U., Toliyat, H.A., and Rayner, M., "Low order PWM inverter harmonics contributions to the inverter-fed induction machine fault diagnosis." *IEEE Transactions on Industrial Electronics*, 2008. **55**(2): p. 610-619.
106. Stack, J.R., Habetler, T.G., and Harley, R.G., "Fault classification and fault signature production for rolling element bearings in electric machines." *IEEE Transactions on Industry Applications*, 2004. **40**(3): p. 735-739.
107. Singh, S. and Kumar, N., "Detection of bearing faults in mechanical systems using stator current monitoring." *IEEE Transactions on Industrial Informatics*, 2016. **13**(3): p. 1341-1349.
108. Schoen, R.R., Habetler, T.G., Kamran, F., and Bartfield, R., "Motor bearing damage detection using stator current monitoring." *IEEE Transactions on Industry Applications*, 1995. **31**(6): p. 1274-1279.
109. Zhou, W., Habetler, T.G., and Harley, R.G. "Stator current-based bearing fault detection techniques: A general review." in *2007 IEEE International Symposium on Diagnostics for Electric Machines, Power Electronics and Drives*. 2007. IEEE.
110. Alwodai, A., Wang, T., Chen, Z., Gu, F., Cattley, R., and Ball, A., "A study of motor bearing fault diagnosis using modulation signal bispectrum analysis of motor current signals." *Journal of Signal and Information Processing*, 2013. **4**(03): p. 72.
111. Forsthoffer, W.E., "Forsthoffer's best practice handbook for rotating machinery." 2011: Elsevier.
112. Sagoo, K.S., "Wear and corrosion of mechanical seals." 1988, Aston University Thesis.
113. Affonso, L.O.A., "Machinery failure analysis handbook: sustain your operations and maximize uptime." 2013: Elsevier.
114. Erjavec, J., "Hybrid, electric, and fuel-cell vehicles." 2012: Cengage Learning.
115. Mehala, N., "Condition monitoring and fault diagnosis of induction motor using motor current signature analysis." 2010, National Institute Of Technology Kurukshetra, India.

116. Alwodai, A., Gu, F., and Ball, A. "Motor current signature analysis of a variable speed drive for motor fault diagnosis." 2011. COMADEM.
117. Electrotechnical-officer. "Operation of ship's induction motors." [cited 12/03/2019]; Available from: <http://electrotechnical-officer.com/operation-of-ships-induction-motors/>.
118. Chattopadhyay, S., Karmakar, S., Sengupta, S., and Mitra, M., "Induction Motor Fault Diagnosis." 2016, Singapore: Springer Singapore.
119. Faiz, J., Ghorbanian, V., and Joksimović, G., "Fault Diagnosis of Induction Motors." 2017, Stevenage: The Institution of Engineering and Technology.
120. Janevska, G. "Mathematical Modeling of Pump System." in Electronic International Interdisciplinary Conference. 2013. EDIS - Publishing Institution of the University of Zilina.
121. Bettaieb, N. and Taïeb, E.H., "Theoretical study and measurement of the characteristic curves of a centrifugal pump." in Design and Modeling of Mechanical Systems-II. 2015, Springer. p. 745-754.
122. Gu, F., Wang, T., Alwodai, A., Tian, X., Shao, Y., and Ball, A., "A new method of accurate broken rotor bar diagnosis based on modulation signal bispectrum analysis of motor current signals." *Mechanical Systems and Signal Processing*, 2015. **50**: p. 400-413.
123. Tripathi, A. and Narayanan, G., "Evaluation and minimization of low-order harmonic torque in low-switching-frequency inverter-fed induction motor drives." *IEEE Transactions on Industry Applications*, 2016. **52**(2): p. 1477-1488.
124. Filippetti, F., Franceschini, G., Tassoni, C., and Vas, P. "AI techniques in induction machines diagnosis including the speed ripple effect." in IAS'96. Conference Record of the 1996 IEEE Industry Applications Conference Thirty-First IAS Annual Meeting. 1996. IEEE.

125. Gu, F., Shao, Y., Hu, N., Naid, A., and Ball, A., "Electrical motor current signal analysis using a modified bispectrum for fault diagnosis of downstream mechanical equipment." *Mechanical Systems and Signal Processing*, 2011. **25**(1): p. 360-372.
126. Huang, B., Feng, G., Tang, X., Gu, J.X., Xu, G., Cattley, R., Gu, F., and Ball, A.D., "A Performance Evaluation of Two Bispectrum Analysis Methods Applied to Electrical Current Signals for Monitoring Induction Motor-Driven Systems." *Energies*, 2019. **12**(8): p. 1438.
127. Khan, M., Hasnain, S.K., and Jamil, M., "Digital Signal Processing: A Breadth-First Approach." 2016: Stylus Publishing, LLC.
128. Sakthivel, N., Sugumaran, V., and Babudevasenapati, S., "Vibration based fault diagnosis of monoblock centrifugal pump using decision tree." *Expert Systems with Applications*, 2010. **37**(6): p. 4040-4049.
129. Peng, Z. and Kessissoglou, N., "An integrated approach to fault diagnosis of machinery using wear debris and vibration analysis." *Wear*, 2003. **255**(7-12): p. 1221-1232.
130. Liu, C., Wu, X., Mao, J., and Liu, X., "Acoustic emission signal processing for rolling bearing running state assessment using compressive sensing." *Mechanical Systems and Signal Processing*, 2017. **91**: p. 395-406.
131. Boyd, D.W., "Systems analysis and modeling: a macro-to-micro approach with multidisciplinary applications." 2000: Elsevier.
132. Hytti, H. "Efficient signal reconstruction and analysis for integrated SHM system." in In: Uhl, T., Ostachowicz, W. & Holnicki-Szulc, Proceedings of the Forth European Workshop, Structural Health Monitoring. 2008. Cracow, Poland.
133. Goyal, D., Pabla, B., and Dhami, S., "Condition monitoring parameters for fault diagnosis of fixed axis gearbox: a review." *Archives of Computational Methods in Engineering*, 2017. **24**(3): p. 543-556.
134. Antoni, J., "The spectral kurtosis: a useful tool for characterising non-stationary signals." *Mechanical Systems and Signal Processing*, 2006. **20**(2): p. 282-307.

135. Luo, J., Yu, D., and Liang, M., "A kurtosis-guided adaptive demodulation technique for bearing fault detection based on tunable-Q wavelet transform." *Measurement Science and Technology*, 2013. **24**(5): p. 055009.
136. Lacey, S., "Using vibration analysis to detect early failure of bearings." *Insight-Northampton-Including European Issues*, 2007. **49**(8): p. 444-446.
137. Jayaswal, P. and Aherwar, A., "Fault Detection and Diagnosis of Gear Transmission System via Vibration Analysis." *The IUP Journal of Mechanical Engineering*, 2012.
138. Khan, M.N., Hasnain, S., and Jamil, M., "Digital Signal Processing: A Breadth-First Approach." Vol. 1. 2016: River Publishers.
139. Lu, S., Zhou, P., Wang, X., Liu, Y., Liu, F., and Zhao, J., "Condition monitoring and fault diagnosis of motor bearings using undersampled vibration signals from a wireless sensor network." *Journal of Sound and Vibration*, 2018. **414**: p. 81-96.
140. Zhang, H., Krooswyk, S., and Ou, J., "High Speed Digital Design: Design of High Speed Interconnects and Signaling." 2015: Elsevier.
141. Ball, A., Wang, T.T., Tian, X., and Gu, F., "A robust detector for rolling element bearing condition monitoring based on the modulation signal bispectrum." 2016.
142. Kay, S.M. and Marple, S.L., "Spectrum analysis—a modern perspective." *Proceedings of the IEEE*, 1981. **69**(11): p. 1380-1419.
143. Bouhlel, A., Sakly, A., and Ikki, S. "Performance analysis of DWT based OFDM with index modulation under channel estimation error." in *2017 International Conference on Engineering & MIS (ICEMIS)*. 2017. IEEE.
144. Boashash, B. and Barkat, B., "Introduction to time-frequency signal analysis." in *Wavelet Transforms and Time-Frequency Signal Analysis*. 2001, Springer. p. 321-380.
145. Qian, S. and Chen, D., "Joint time-frequency analysis." *IEEE Signal Processing Magazine*, 1999. **16**(2): p. 52-67.

146. Peng, Z. and Chu, F., "Application of the wavelet transform in machine condition monitoring and fault diagnostics: a review with bibliography." *Mechanical Systems and Signal Processing*, 2004. **18**(2): p. 199-221.
147. Kronland-Martinet, R., Morlet, J., and Grossmann, A., "Analysis of sound patterns through wavelet transforms." *International Journal of Pattern Recognition and Artificial Intelligence*, 1987. **1**(02): p. 273-302.
148. Grossmann, A., Kronland-Martinet, R., and Morlet, J., "Reading and understanding continuous wavelet transforms." in *Wavelets*. 1990, Springer. p. 2-20.
149. Liu, Y., Ouyang, J., and Yan, Y. "De-Noising of Life Feature Signals Based on Wavelet Transform." in *Industrial Engineering, Machine Design and Automation (IEMDA 2014) & Computer Science and Application (CCSA 2014)*. 2015. World Scientific.
150. Tan, C.Z. and Leong, M.S., "An experimental study of cavitation detection in a centrifugal pump using envelope analysis." *Journal of System Design and Dynamics*, 2008. **2**(1): p. 274-285.
151. Bechhoefer, E., Kingsley, M., and Menon, P. "Bearing envelope analysis window selection using spectral kurtosis techniques." in *2011 IEEE Conference on Prognostics and Health Management*. 2011. IEEE.
152. Randall, R.B., Antoni, J., and Chobsaard, S., "The relationship between spectral correlation and envelope analysis in the diagnostics of bearing faults and other cyclostationary machine signals." *Mechanical Systems and Signal Processing*, 2001. **15**(5): p. 945-962.
153. Huang, N.E., Shen, Z., Long, S.R., Wu, M.C., Shih, H.H., Zheng, Q., Yen, N.-C., Tung, C.C., and Liu, H.H. "The empirical mode decomposition and the Hilbert spectrum for nonlinear and non-stationary time series analysis." in *Proceedings of the Royal Society of London A: mathematical, physical and engineering sciences*. 1998. The Royal Society.
154. Kıymık, M.K., Güler, İ., Dizibüyük, A., and Akın, M., "Comparison of STFT and wavelet transform methods in determining epileptic seizure activity in EEG signals for real-time application." *Computers in biology and medicine*, 2005. **35**(7): p. 603-616.

155. Cao, H., Zhou, K., and Chen, X., "Chatter identification in end milling process based on EEMD and nonlinear dimensionless indicators." *International Journal of Machine Tools and Manufacture*, 2015. **92**: p. 52-59.
156. Bin Queyam, A., Kumar Pahuja, S., and Singh, D., "Quantification of Feto-Maternal Heart Rate from Abdominal ECG Signal Using Empirical Mode Decomposition for Heart Rate Variability Analysis." *Technologies*, 2017. **5**(4): p. 68.
157. Hassan, H.H., "Empirical mode decomposition (EMD) of potential field data: airborne gravity data as an example." in *SEG Technical Program Expanded Abstracts*. 2005, Society of Exploration Geophysicists. p. 704-706.
158. Lin, W., Chuang, L., and Young, H., "Condition-based shaft fault diagnosis with the empirical mode decomposition method." *Proceedings of the Institution of Mechanical Engineers, Part B: Journal of Engineering Manufacture*, 2011. **225**(5): p. 723-734.
159. Miao, Q., Wang, D., and Pecht, M. "Rolling element bearing fault feature extraction using EMD-based independent component analysis." in *Prognostics and Health Management (PHM), 2011 IEEE Conference on*. 2011. IEEE.
160. Georgoulas, G., Tsoumas, I.P., Antonino-Daviu, J.A., Climente-Alarcón, V., Stylios, C.D., Mitronikas, E.D., and Safacas, A.N., "Automatic pattern identification based on the complex empirical mode decomposition of the startup current for the diagnosis of rotor asymmetries in asynchronous machines." *IEEE Transactions on Industrial Electronics*, 2014. **61**(9): p. 4937-4946.
161. Yunlong, Z. and Peng, Z., "Vibration fault diagnosis method of centrifugal pump based on emd complexity feature and least square support vector machine." *Energy Procedia*, 2012. **17**: p. 939-945.
162. Ali, J.B., Fnaiech, N., Saidi, L., Chebel-Morello, B., and Fnaiech, F., "Application of empirical mode decomposition and artificial neural network for automatic bearing fault diagnosis based on vibration signals." *Applied Acoustics*, 2015. **89**: p. 16-27.
163. Bin, G., Gao, J., Li, X., and Dhillon, B., "Early fault diagnosis of rotating machinery based on wavelet packets—Empirical mode decomposition feature extraction and neural network." *Mechanical Systems and Signal Processing*, 2012. **27**: p. 696-711.

164. Liu, B., Riemenschneider, S., and Xu, Y., "Gearbox fault diagnosis using empirical mode decomposition and Hilbert spectrum." *Mechanical Systems and Signal Processing*, 2006. **20**(3): p. 718-734.
165. Haba, U., Feng, G., Shaeboub, A., Peng, X., Gu, F., and Ball, A., "Detection and Diagnosis of Compound Faults in a Reciprocating Compressor based on Motor Current Signatures." 2016.
166. Zhang, J.-h. and Liu, Y., "Application of complete ensemble intrinsic time-scale decomposition and least-square SVM optimized using hybrid DE and PSO to fault diagnosis of diesel engines." *Frontiers of Information Technology & Electronic Engineering*, 2017. **18**(2): p. 272-286.
167. Lang, X., Zhang, Z., Xie, L., Horch, A., and Su, H., "Time-frequency analysis of plant-wide oscillations using multivariate intrinsic time-scale decomposition." *Industrial and Engineering Chemistry Research*, 2018. **57**(3): p. 954-966.
168. Feng, Z., Lin, X., and Zuo, M.J., "Joint amplitude and frequency demodulation analysis based on intrinsic time-scale decomposition for planetary gearbox fault diagnosis." *Mechanical Systems and Signal Processing*, 2016. **72**: p. 223-240.
169. Yang, Y., Pan, H., Ma, L., and Cheng, J., "A roller bearing fault diagnosis method based on the improved ITD and RRVPMCD." *Measurement*, 2014. **55**: p. 255-264.
170. Yu, L., Junhong, Z., Fengrong, B., Jiewei, L., and Wenpeng, M., "A fault diagnosis approach for diesel engine valve train based on improved ITD and SDAG-RVM." *Measurement Science and Technology*, 2014. **26**(2): p. 025003.
171. Li, Y., Xu, M., Wei, Y., and Huang, W., "Rotating machine fault diagnosis based on intrinsic characteristic-scale decomposition." *Mechanism and Machine Theory*, 2015. **94**: p. 9-27.
172. Yu, J. and Liu, H., "Sparse coding shrinkage in intrinsic time-scale decomposition for weak fault feature extraction of bearings." *IEEE Transactions on Instrumentation and measurement*, 2018. **67**(7): p. 1579-1592.

173. An, X., Jiang, D., Chen, J., and Liu, C., "Application of the intrinsic time-scale decomposition method to fault diagnosis of wind turbine bearing." *Journal of Vibration and Control*, 2012. **18**(2): p. 240-245.
174. Hu, A., Yan, X., and Xiang, L., "A new wind turbine fault diagnosis method based on ensemble intrinsic time-scale decomposition and WPT-fractal dimension." *Renewable Energy*, 2015. **83**: p. 767-778.
175. Liu, Y., Zhang, J., Qin, K., and Xu, Y., "Diesel engine fault diagnosis using intrinsic time-scale decomposition and multistage Adaboost relevance vector machine." *Proceedings of the Institution of Mechanical Engineers, Part C: Journal of Mechanical Engineering Science*, 2018. **232**(5): p. 881-894.
176. Bo, L. and Peng, C., "Fault diagnosis of rolling element bearing using more robust spectral kurtosis and intrinsic time-scale decomposition." *Journal of Vibration and Control*, 2016. **22**(12): p. 2921-2937.
177. Mohammed, M., Khan, M.B., and Bashier, E.B.M., "Machine learning: algorithms and applications." 2016: Crc Press.
178. Mohri, M., Talwalkar, A., and Rostamizadeh, A., "Foundations of machine learning (adaptive computation and machine learning series)." 2012: Mit Press Cambridge, MA.
179. Murty, M.N. and Devi, V.S., "Introduction to pattern recognition and machine learning." Vol. 5;5.;. 2015, New Jersey: World Scientific.
180. Jap, D. and Breier, J. "Overview of machine learning based side-channel analysis methods." in *Integrated Circuits (ISIC), 2014 14th International Symposium on*. 2014. IEEE.
181. Kotsiantis, S.B., Zaharakis, I., and Pintelas, P., "Supervised machine learning: A review of classification techniques." 2007.
182. Sharma, R., "Supervised Learning for Text Classification." 2005.
183. Dayan, P., Sahani, M., and Deback, G., "Unsupervised learning." *The MIT encyclopedia of the cognitive sciences*, 1999.

184. Huang, G., Song, S., Gupta, J.N., and Wu, C., "Semi-supervised and unsupervised extreme learning machines." *IEEE Transactions on Cybernetics*, 2014. **44**(12): p. 2405-2417.
185. Shao, H., Jiang, H., Lin, Y., and Li, X.J.M.S.S.P., "A novel method for intelligent fault diagnosis of rolling bearings using ensemble deep auto-encoders." *Mechanical Systems and Signal Processing*, 2018. **102**: p. 278-297.
186. Mao, W., He, L., Yan, Y., and Wang, J., "Online sequential prediction of bearings imbalanced fault diagnosis by extreme learning machine." *Mechanical Systems and Signal Processing*, 2017. **83**: p. 450-473.
187. Cortes, C. and Vapnik, V., "Support-vector networks." *Machine learning*, 1995. **20**(3): p. 273-297.
188. Widodo, A. and Yang, B.-S., "Support vector machine in machine condition monitoring and fault diagnosis." *Mechanical Systems and Signal Processing*, 2007. **21**(6): p. 2560-2574.
189. Saidi, L., Ali, J.B., and Fnaiech, F., "Application of higher order spectral features and support vector machines for bearing faults classification." *ISA transactions*, 2015. **54**: p. 193-206.
190. Kankar, P., Sharma, S.C., and Harsha, S., "Fault diagnosis of ball bearings using machine learning methods." *Expert Systems with Applications*, 2011. **38**(3): p. 1876-1886.
191. Bonaccorso, G., "Machine Learning Algorithms." 2017: Packt Publishing Ltd.
192. Huang, J., Hu, X., and Yang, F., "Support vector machine with genetic algorithm for machinery fault diagnosis of high voltage circuit breaker." *Measurement*, 2011. **44**(6): p. 1018-1027.
193. Lantz, B., "Machine learning with R." 2013: Packt Publishing Ltd.

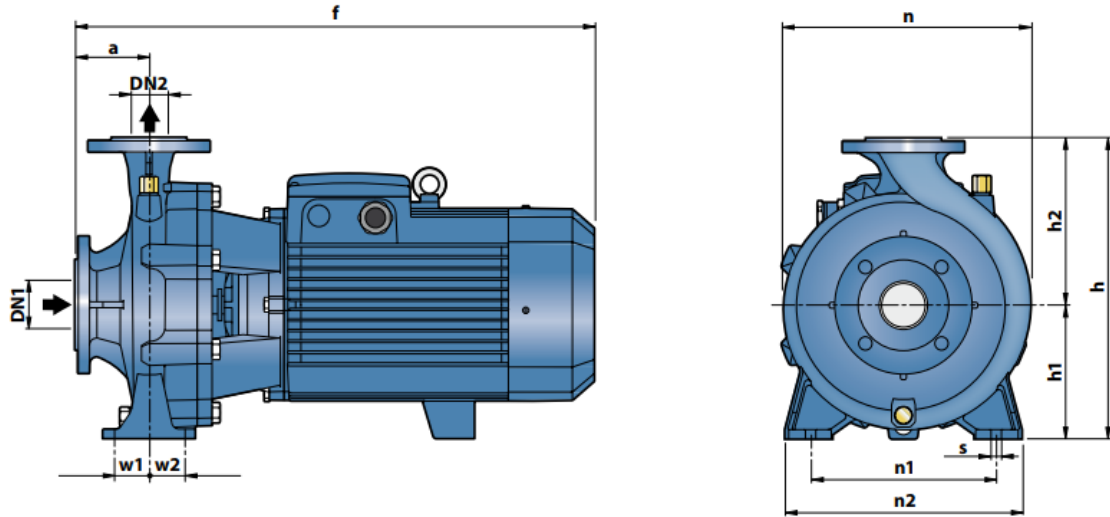
194. Milgram, J., Cheriet, M., and Sabourin, R. "'One against one' or 'one against all': Which one is better for handwriting recognition with SVMs?". in Tenth International Workshop on Frontiers in Handwriting Recognition. 2006. Suvisoft.
195. Awad, M. and Khanna, R., "Efficient learning machines: theories, concepts, and applications for engineers and system designers." 2015: Apress.
196. Rahbar, M., Amirkhani, S., Chaibakhsh, A., and Rahbar, F. "Unbalance fault localization in rotating machinery disks using EEMD and optimized multi-class SVM." in Instrumentation and Measurement Technology Conference (I2MTC). 2017. IEEE.
197. Platt, J.C., Cristianini, N., and Shawe-Taylor, J. "Large margin DAGs for multiclass classification." in Advances in neural information processing systems. 2000.
198. Campbell, C. and Ying, Y., "Learning with support vector machines." Synthesis lectures on artificial intelligence and machine learning, 2011. **5**(1): p. 1-95.
199. Qu, J. and Zuo, M.J., "Support vector machine based data processing algorithm for wear degree classification of slurry pump systems." Measurement, 2010. **43**(6): p. 781-791.
200. Zhong, J.-H., Liang, J., Yang, Z.-X., Wong, P.K., and Wang, X.-B., "An effective fault feature extraction method for gas turbine generator system diagnosis." Shock and Vibration, 2016. **2016**.
201. Wang, X., Zheng, Y., Zhao, Z., and Wang, J., "Bearing Fault Diagnosis Based on Statistical Locally Linear Embedding." Sensors, 2015. **15**(7): p. 16225.
202. Hui, K.H., Ooi, C.S., Lim, M.H., Leong, M.S., and Al-Obaidi, S.M., "An improved wrapper-based feature selection method for machinery fault diagnosis." PloS one, 2017. **12**(12): p. e0189143.
203. Romero-Troncoso, R.J., Saucedo-Gallaga, R., Cabal-Yepez, E., Garcia-Perez, A., Osornio-Rios, R.A., Alvarez-Salas, R., Miranda-Vidales, H., and Huber, N., "FPGA-based online detection of multiple combined faults in induction motors through information entropy and fuzzy inference." IEEE Transactions on Industrial Electronics, 2011. **58**(11): p. 5263-5270.

204. Al-Hashmi, S.A., "Detection and diagnosis of cavitation in centrifugal pumps." 2005, University of Manchester.
205. Karel, S., Petr, N., Jan, B., and Jiff, L., "Detection of Mechanical Failures in Induction Motors by Current Spectrum Analysis." *IEEE Transactions on Industrial Electronics*, 1997: p. 547.
206. Randall, R.B. and Antoni, J., "Rolling element bearing diagnostics—A tutorial." *Mechanical systems and signal processing* 2011. **25**(2): p. 485-520.
207. An, X. and Jiang, D., "Bearing fault diagnosis of wind turbine based on intrinsic time-scale decomposition frequency spectrum." *Proceedings of the Institution of Mechanical Engineers, Part O: Journal of Risk and Reliability*, 2014. **228**(6): p. 558-566.
208. Tian, X., Feng, G., Chen, Z., Albraik, A., Gu, F., and Ball, A., "The investigation of motor current signals from a centrifugal pump for fault diagnosis." 2014.
209. Hidayat, A.Y., Widodo, A., and Haryadi, G.D. "Fault Diagnostic System Bearing Centrifugal Pump Using K-Means Method For Thermography Image And Signal Analysis Vibrations." in *MATEC Web of Conferences*. 2018. EDP Sciences.
210. Luo, Y., Yuan, S., Yuan, J., and Sun, H., "Induction motor current signature for centrifugal pump load." *Proceedings of the Institution of Mechanical Engineers, Part C: Journal of Mechanical Engineering Science*, 2016. **230**(11): p. 1890-1901.
211. Ortaç-Kabaoğlu, R., Eksin, İ., Yeşil, E., and Güzelkaya, M., "Fault Detection and Diagnosis for Nonlinear Systems: A Support Vector Machine Approach." *IFAC Proceedings Volumes*, 2009. **42**(19): p. 355-360.
212. Wuest, T., Weimer, D., Irgens, C., and Thoben, K.-D., "Machine learning in manufacturing: advantages, challenges, and applications." *Production & Manufacturing Research*, 2016. **4**(1): p. 23-45.
213. Yin, Z. and Hou, J., "Recent advances on SVM based fault diagnosis and process monitoring in complicated industrial processes." *Neurocomputing*, 2016. **174**: p. 643-650.

214. Ameid, T., Menacer, A., Talhaoui, H., and Azzoug, Y., "Discrete wavelet transform and energy eigen value for rotor bars fault detection in variable speed field-oriented control of induction motor drive." *ISA transactions*, 2018. **79**: p. 217-231.
215. Chebil, J., Noel, G., Mesbah, M., and Deriche, M., "Wavelet decomposition for the detection and diagnosis of faults in rolling element bearings." *Jordan Journal of Mechanical and Industrial Engineering*, 2009. **3**(4): p. 260-267.
216. Kumar, A. and Kumar, R.J.M., "Time-frequency analysis and support vector machine in automatic detection of defect from vibration signal of centrifugal pump." 2017. **108**: p. 119-133.
217. Yuvaraj, M.M., Elzhiloon, M.P., Thiruvaran, T., Aravinthan, V., and Thanatheepan, M.B. "Bearing Fault Prediction Using Current Signature Analysis in Electric Water Pump." in 2018 IEEE International Conference on Information and Automation for Sustainability (ICIAfS). 2018. IEEE.
218. Jami, A. and Heyns, P.S., "Impeller fault detection under variable flow conditions based on three feature extraction methods and artificial neural networks." *Journal of Mechanical Science and Technology*, 2018. **32**(9): p. 4079-4087.
219. Ebrahimi, E. and Javidan, M., "Vibration-based classification of centrifugal pumps using support vector machine and discrete wavelet transform." *Journal of Vibroengineering*, 2017. **19**(4): p. 2586-2597.
220. Wang, Y., Lu, C., Liu, H., and Wang, Y. "Fault diagnosis for centrifugal pumps based on complementary ensemble empirical mode decomposition, sample entropy and random forest." in 2016 12th world congress on intelligent control and automation (WCICA). 2016. IEEE.

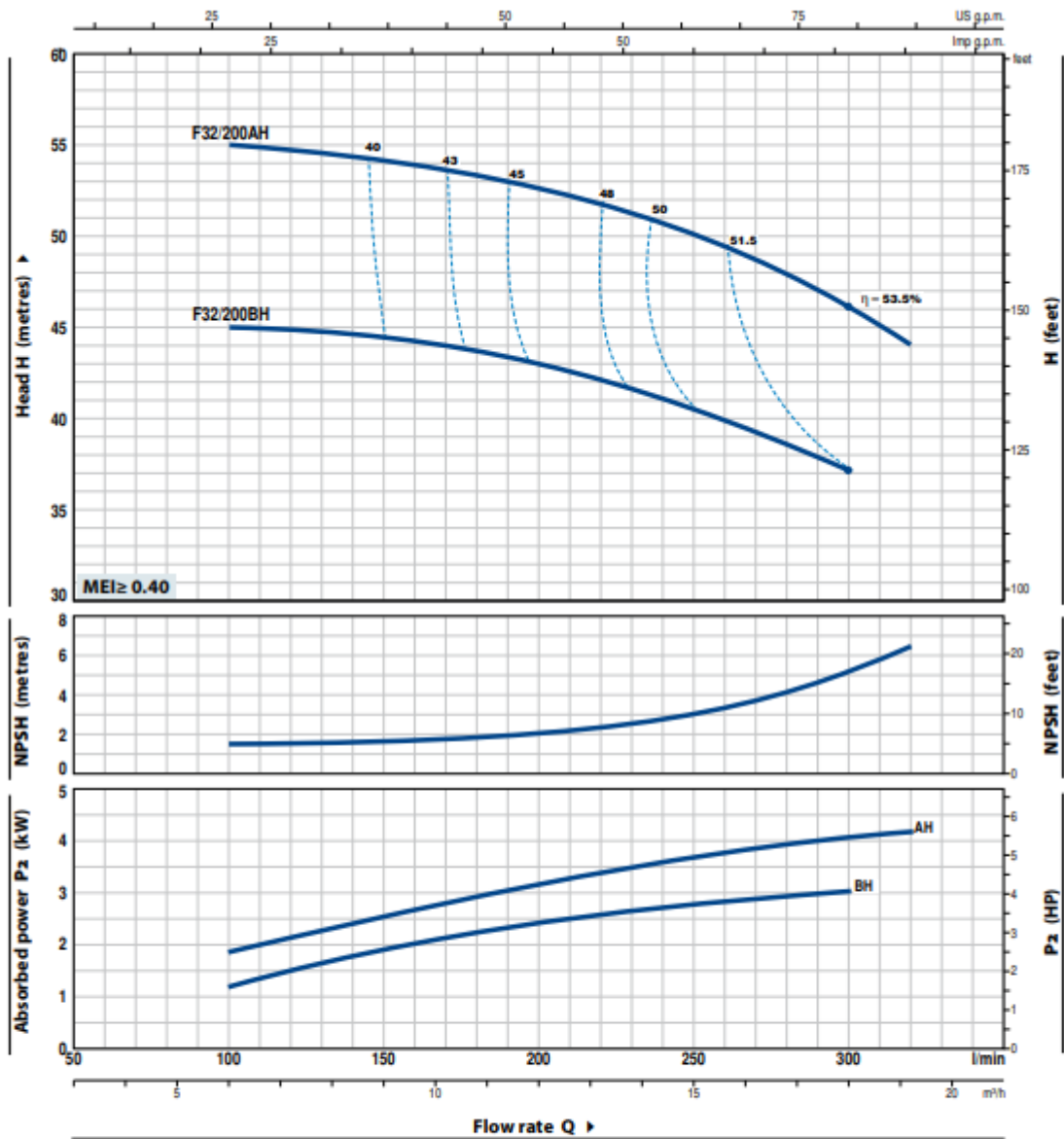
# Appendix A

## A.1 Centrifugal Pump Dimensions and Specifications



Model	Dimensions mm												
	DN1	DN2	a	f	h	h1	h2	n	n1	n2	w1	w2	s
F 32/200AH	50	32	80	469	340	160	180	270	190	240	35	35	14

## A.2 Pump Performance Curves



MODEL	POWER ( $P_2$ )		Q	0	6	9	12	15	18	19.2
	kW	HP		0	100	150	200	250	300	320
F 32/200BH	3	4	H metres	47	45	44.5	43	40.5	37	
F 32/200AH	4	5.5	H metres	57	55	54	52.5	50	46	44

Q = Flow rate H = Total manometric head HS = Suction height

Tolerance of characteristic curves in compliance with EN ISO 9906 Grade 3B.